Enhanced intensity difference squeezing with a low gain off-resonant Four-Wave Mixing in potassium vapor

M.M. Ćurčić [a,b,*], B.M. Jelenković [a]

[a] *Institute of Physics Belgrade, University of Belgrade, Pregrevica 118, Belgrade, 11080, Serbia*
[b] *School of Electrical Engineering, University of Belgrade, Bulevar kralja Aleksandra 73, Belgrade, 11120, Serbia*

A R T I C L E   I N F O

A B S T R A C T

Although potassium stands out among alkalies by its smallest ground state hyperfine splitting, smaller than Doppler broadening, investigations of its four-wave mixing (FWM) quantum properties, like squeezing and entanglement, were neglected. Here we present measurements of quantum correlations in potassium vapor using far-detuned double Λ scheme for FWM. We obtained the relative intensity difference squeezing (IDS) of -6.1 dB, with the squeezing bandwidth between 0.9 to 4.5 MHz on the noise spectra. The squeezing maximum in potassium compares well with the best results obtained in Rb and Cs, and has larger value than previously reported IDS in potassium. This result agrees qualitatively well with the squeezing calculated using analytical expressions from the model of operators when with chosen parameters FWM generates both squeezing and probe at their maximums. The ultimate squeezing level in potassium, predicted by the model, when conjugate absorption in the cell and optical losses behind the cell are neglected, is -10.29 dB. This is among the largest predicting squeezing obtained by FWM in alkalies.

1. Introduction

Squeezed states of light are of great interest because quantum noise reduction below the standard quantum limit (SQL) allows applications to metrology with sub-shot noise precision [1], quantum enhanced sensing [2] and imaging [3,4], quantum interferometry (for gravitational wave interferometry) [5], atomic magnetometry [6] and quantum-enhanced spectroscopy [7].

Spontaneous parametric down conversion (SPDC) and FWM are common methods to generate squeezed light. FWM occurs when a strong pump, through the third order nonlinearity, produces two new frequency components. The frequency and polarization of new photons are governed by the energy conservation law and the phase matching. FWM itself has been extensively studied in both atomic [8–11] and solid-state mediums [12,13]. Of special interest in our research is FWM generated in atomic vapor utilizing double Λ atomic scheme. It was already used in demonstrations of slowing [14,15] and storing [16,17] light pulses, entanglement [18,19] and study of optical nonreciprocity [20]. In addition to above mentioned application associated to this quantum effect, FWM also produces two-mode quantum correlated photon pairs of the same polarization, with multi-spatial-mode squeezing. The amplitude difference (and phase sum) of the two modes have reduced noise at the expense of increased noise in the sum of their amplitudes (and difference in their phases). Due to strong nonlinearity of FWM media, intense parametric amplification of twin photons and

large squeezing are obtained in a single pass of the pump beam through atomic vapor. Quantum correlated and entangled photon pairs have made strong impact on several areas of research and in industry. Applications include quantum metrology [21], microscopy [22] and imaging [23,24], quantum teleportation [25,26] and information [27, 28].

FWM as a means for generating squeezing was first proposed by Yuen and Shapiro [29]. The first experimental observation of squeezed light by FWM was by Slusher et al. [30] in 1985, who used intra-cavity sodium vapor beam and two-level atomic scheme. McCormick et al. [31] used FWM in Rb vapor to generate two-mode squeezing in a joint quadrature of correlated probe and conjugate fields, or intensity difference squeezing (IDS). Large intensity squeezing obtained by phase-insensitive FWM in Rb of -9.2 dB [32] is close to the highest level of squeezing produced by any method for generating squeezed light [33]. This result made FWM in hot alkali vapors widespread method for testing limits of FWM with different gases, and different atomic schemes [34–39]. Several groups tried different approaches to enhance IDS, by modulating internal energy level with additional laser [40], or by conical pump beam [41]. With FWM based two-beam phase sensitive amplifier, IDS above 10 dB was obtained in Rb vapor [42]. The strongest IDS obtained in hot Cs vapor was -6.5 dB [38]. The difficulty in getting higher quantum correlation in Cs is believed to be due to larger hyperfine splitting (hfs) of the ground state in
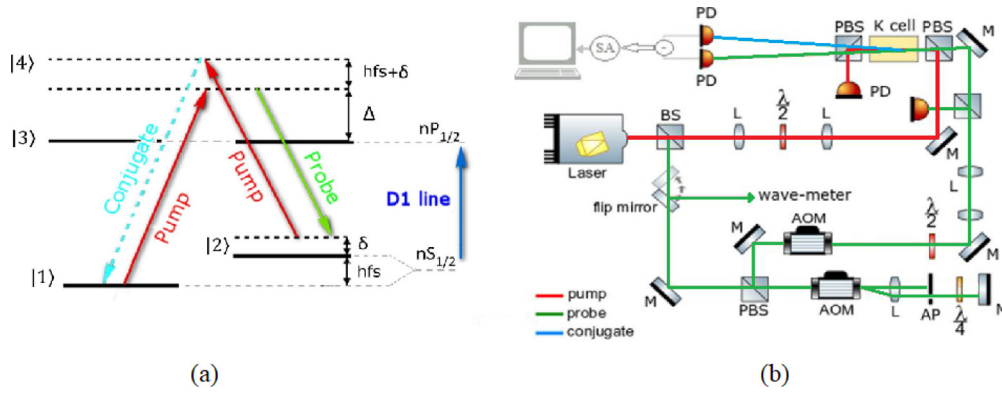

Fig. 1. (a) Double Λ scheme for D_1 line in potassium. Pump beam — thick line (red for online version), probe beam — thin line (green for online version), conjugate beam — dashed line (blue for online version), hfs — hyperfine splitting, Δ — one photon detuning, δ — two photon detuning (b) Experimental setup for FWM, M — Mirror, L — Lens, PBS — Polarization beam splitter, AOM — Acousto-Optical Modulator, AP — Aperture, PD — Photodetector, SA — Spectrum Analyzer.

Cs [37]. Recently, study of IDS based on FWM on double Λ scheme was extended with the use of two pump beams [43,44], generating multi-beam quantum correlation and also with integration of FWM system with optical parametric amplifier [45]. These studies could pave the way to expanding the range of the possible applications of IDS based on FWM in atomic vapor.

Here we present measurements of IDS realized by the nondegenerate FWM in hot potassium vapor. So far the only published result for IDS in potassium is given in [39]. Intensity squeezing in [39] was −1.1 dB, but the probe frequencies were close to atomic resonances, as opposed to the off-resonance FWM used in experiments with the largest values of squeezing [31,32,38]. Potassium has smaller ground state splitting and higher Doppler broadening of absorption resonance than other alkalies. Smaller hyper-fine splitting, of 460 MHz, means higher cross-susceptibility [46], large gain of twin beams for usual pump powers [47], and cheaper method for the probe offset from the pump frequency. In the experiment, the twin beams were generated by the off-resonant double Λ scheme on D1 line in ^{39}K (Fig. 1(a)). We investigated effects of FWM parameters on IDS measuring noise power spectrum of the signal difference, and gains of twin beams as a function of pump detuning, two-photon pump-probe detuning and the vapor density. The relative intensity squeezing were calculated by the model of operators [31,48–50] and compared with experimental dependence of IDS as a function of pump and pump-probe detunings, at several vapor densities.

2. Experiment

The double Λ scheme used for the FWM is given in Fig. 1(a). The pump beam at 770 nm couples $4S_{1/2}$, F = 1 to $4P_{1/2}$ with detuning Δ. The probe "seed" beam couples the $4S_{1/2}$, F = 2 to the same excited state, detuned from the pump-probe Raman resonance by δ. The source for the pump and the probe is the Ti:Sa laser (MBR-110, Coherent), as depicted in the schematic of the experiment, Fig. 1(b). For the probe detuning δ, around ~460 MHz, we had to use two available AOMs summing two frequency offsets to the total that is close to hfs. To keep probe spatially stable during fine detuning, the second AOM had to be in a double pass. The pump and the probe, orthogonally polarized, with diameters 0.8 mm and 0.5 mm, respectively, are intersected at the center of the 30 mm long K cell. Conservation of momentum defines the range of phase matching angle for efficient generation of FWM, from which we choose 4 mrad as the intersection angle between the pump and the probe. The cell windows are AR coated on both sides, resulting in the probe transmission of 0.98(5) per cell window. For calculating expected levels of squeezing, we used measured losses at the cell exit window, on optics elements behind the cell (beam splitter, mirrors and lenses), 0.91(5), and the quantum efficiency of balanced photo-detector, 0.83, leading to the total losses in detection of ~0.25. The

cell was heated by the stream of a hot air for a temperatures ranging from 110 °C to 130 °C, corresponding to atomic density from $1.54\cdot10^{12}$ cm^{-3} to $5.51\cdot10^{12}$ cm^{-3} [51].

After the cell, the probe and the conjugate are directed to the photodiodes of the balance detector (Thorlabs PDB450A-AC), while the pump is blocked by the Glan–Taylor beam splitter with 10^5:1 extinction ratio. The difference of the two signals is sent to a spectrum analyzer (RSA607 A Real-Time spectrum Analyzer from Tektronix) with a resolution bandwidth set to 3 kHz and a video bandwidth of 30 Hz. The results for IDS presented below are values of the noise spectral density of the signal difference at the frequency of 1.5 MHz, minus the SQL. SQL is determined by splitting the probe beam with a 50:50 beam splitter and then sending the obtained beams to the balanced detector, Fig. 2(a). In Fig. 2(b) we present the results of the SQL calibration @ 1.5 MHz, as a function of the total power.

3. Model of operators for intensity difference squeezing

The Hamiltonian governing the FWM process of creation of probe and conjugate photons from annihilated two pump photons, assuming no depletion for the strong pump, is defined with $\hat{H} = i\hbar(\gamma_a\hat{a}^\dagger\hat{b}^\dagger - \gamma_b\hat{a}\hat{b})$, where $\hat{a}$ and $\hat{b}$ are annihilation operators for probe and conjugate, and $\gamma_{a,b}$ is constant, proportional to $\chi^{(3)}$. The time evolution of $\hat{a}$ is given by $\frac{d\hat{a}}{dt} = \frac{1}{i\hbar}[\hat{H}, \hat{a}] = -\gamma_a\hat{b}^\dagger$, and by the similar expression for $\hat{b}$. Then, after defining $\xi = \gamma t$, and choosing χ as real, we can write the equations for $\hat{a}$ and $\hat{b}$ after the mixing as:

$$\hat{a} = \hat{a}_0\cosh(\xi) + \hat{b}_0^\dagger\sinh(\xi), \tag{1a}$$

$$\hat{b}^\dagger = \hat{a}_0^\dagger\sinh(\xi) + \hat{b}_0\cosh(\xi). \tag{1b}$$

Here, ξ is the squeezing parameter that depends on the pump power and frequency (detunings), medium length, and can be calculated from the classical pump field, while $\hat{a}_0$ and $\hat{b}_0$ are input field operators for the probe and conjugate field, respectively.

The mean photon number per mode $\hat{a}$ ($\hat{b}$) at the output, with vacuum field at the input for mode $\hat{b}$ is

$$\langle N_a \rangle = \langle \hat{a}^\dagger\hat{a} \rangle = \cosh^2(s)\langle \hat{a}_0^\dagger\hat{a}_0 \rangle + \sinh^2(s) \simeq G\langle \hat{a}_0^\dagger\hat{a}_0 \rangle, \tag{2a}$$

$$\langle N_b \rangle = \langle \hat{b}_0^\dagger\hat{b}_0 \rangle \simeq (G-1)\langle \hat{a}_0^\dagger\hat{a}_0 \rangle, \tag{2b}$$

where $\cosh^2(s) = G$, is the nonlinear gain coefficient. The variance of the difference of the probe and conjugate photon numbers is $Var(\hat{N}_a - \hat{N}_b) = \langle \hat{a}_0^\dagger\hat{a}_0 \rangle$. The noise reduction factor (NRF) given in respect to SQL, $\langle \hat{N}_a + \hat{N}_b \rangle$, is

$$NRF = \frac{Var(\hat{N}_a - \hat{N}_b)}{\langle \hat{N}_a + \hat{N}_b \rangle} = \frac{1}{(2G-1)} \tag{3}$$

In an ideal case, in the absence of probe absorption in the FWM medium, neglecting twin beam losses after the mixing medium, and
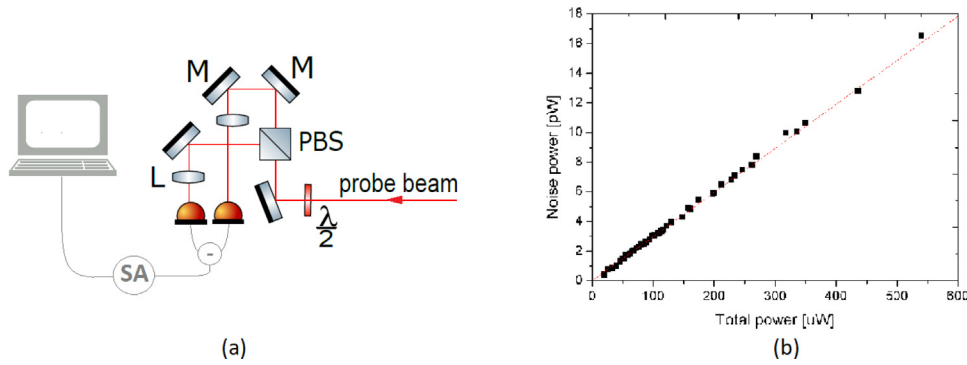
(a)

(b)

Fig. 2. (a) Schematic of the setup used for the balanced beam detection and SQL measurement (b) SQL calibration @1.5 MHz as a function of total power, corrected for the electronic noise.

assuming ideal detection efficiency, squeezing and twin beam intensities are directly associated with the FWM gain. Eq. (3) gives relation between classical (gain) and quantum (squeezing) properties of FWM, showing that for nonclassical behavior, the mixing gain has to be greater than 1. Although noise of probe and conjugate increase with gain, the NRF is decreasing because of correlation in fluctuations imparted on both beams. The IDS in dB below SQL is then given by $IDS = -10\log(2G - 1)$.

The optical losses on the probe (conjugate) are modeled by the action of the beam splitter (BS) as in [48,49]. The heterodyne detection of probe (conjugate) is replaced by an ideal quadrature detection with fictitious BS, with probe (conjugate) on one input port and the empty second input port. The vacuum modes on the empty port contribute to the output of the BS, inducing losses in the transmitted probe (conjugate) beam. The transmitted beams through BS are then $A_t^i = \sqrt{\eta_i}A_{in} + \sqrt{1 - \eta_i}A_{vac}$, Optical losses $\eta_i = \eta_{L,i} \times \eta_{Q,i}$ are product of two terms that quantify transmission losses and efficiency of photodetectors, for $i = a(b)$. If the number operator for the probe (conjugate) at the BS is $\langle \hat{N}_{in} \rangle^{a(b)}$ and transmission through the BS is $\eta_{(a,b)}$, the photon number operator at the exit port of the BS is $\langle \hat{N}_{out} \rangle^{a(b)} = \eta \langle \hat{N}_{in} \rangle^{a(b)}$. After some algebra, assuming equal number of photons for the probe and conjugate at the outputs of BS, the NRF after losses is

$$NRF_{TL} = 1 + \frac{2(G-1)(G(\eta_a - \eta_b)^2 - \eta_b^2)}{G\eta_a + (G-1)\eta_b}, \qquad (4)$$

where with index TL we are referring to the case when transmission losses are included. The Eq. (4) indicates that in addition to the probe mixing gain, the balanced transmissions of the probe and the conjugate, from the cell to the detectors, are important for the noise reduction. When the FWM gains of the probe and conjugate are also similar, we have preferable conditions for optimum squeezing, under given FWM parameters. The imbalance between twin beams at the detectors, due to different gains of the probe and the conjugate, results in lower or no squeezing at all. Note that the results presented below, obtained with BS model, are for equal transmissions of probe and conjugate from the vapor cell and detectors.

Finally, we will compare experimental IDS with the model that includes intrinsic losses of the twin beams in the FWM medium. Absorption and spontaneous emission impose fundamental limit on the maximum squeezing in the vapor cell. Different models, that includes these effects, have been described in [31,49,50]. Eq. (5) for two-mode squeezing is the result of gains and losses due to absorption in the probe introduced through a large number of interleaved stages onto which the medium was divided along paths of twin beams. The losses were introduced through vacuum ports of BS, for the probe and another for the conjugate, in every stage. The model also includes optical losses after the medium, as in Eq. (4).

$$NRF_L = 1 - \eta\frac{2S\sinh^2\zeta}{\zeta\cosh(2\zeta + \chi)} + \eta\sqrt{T_a}\frac{S\log^2 T_a\sinh^4\zeta}{2\zeta^3\cosh(2\zeta + \chi)}. \qquad (5)$$
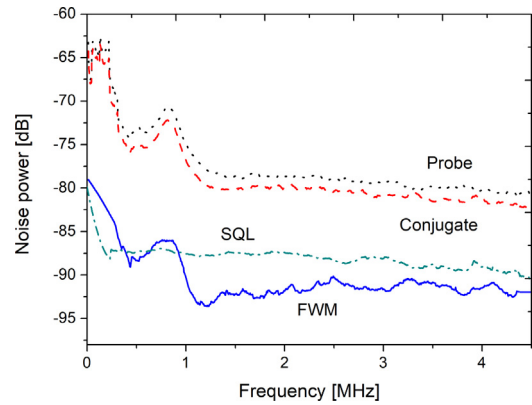

Fig. 3. Measured spectral noise density for the probe-conjugate difference (solid blue line), the SQL (dash–dot green line), the probe (dot black line) and the conjugate (dash red line), corrected for the pump leakage, at 123 °C, for $\Delta = 1.2$ GHz, $\delta = 6$ MHz, $P_{pump} = 750$ mW, $P_{probe} = 6$ μW.

Here, $\zeta = \frac{1}{4}\sqrt{16S^2 + \log^2 T_a}$ and $\tanh\zeta = \frac{\log T_a}{4\zeta}$. The overall squeezing parameter is $S = \cosh^{-1}(G_{in})$, where G_{in} is intrinsic gain. S was calculated by solving Eq. (15) from [49]. T_a is the transmission of the probe in the medium, obtained when the pump power was just below the onset for FWM. The corresponding value for the pump power was determined by the absence of the conjugate beam, monitored by the high sensitivity APD, and by the change of the probe beam profile monitored by the CCD, since at the onset of the FWM the probe beam profile changes from its initial Gaussian profile. Since the pump power at the threshold varies with the cell temperature, the probe transmission was measured for the pump power in the range 200–300 mW, depending on the cell temperature. The absorption of the conjugate is neglected, $T_b = 1$ in Eq. (5). Both absorption and strength of the mixing gain are the characteristics of the alkali atom. Therefore, with the Eq. (5) one can estimate effects of FWM parameters on squeezing and tailor their values for optimization. Assuming no optical losses behind the cell and setting $\eta = \eta_a = \eta_b = 1$, one can estimate the ultimate squeezing expected from the vapor for the particular FWM parameters.

4. Results and discussion

The degree of quantum correlation between the probe and the conjugate is given by the noise power spectral density of the signal from the balanced detector, in Fig. 3. The variance in the photon number of the coherent laser light gives the limit in the corresponding noise in the photodetector signal, that is SQL. SQL in Fig. 3 is from balanced differential homodyne measurements of the laser noise at the same power as the combined optical powers of the probe and the conjugate.
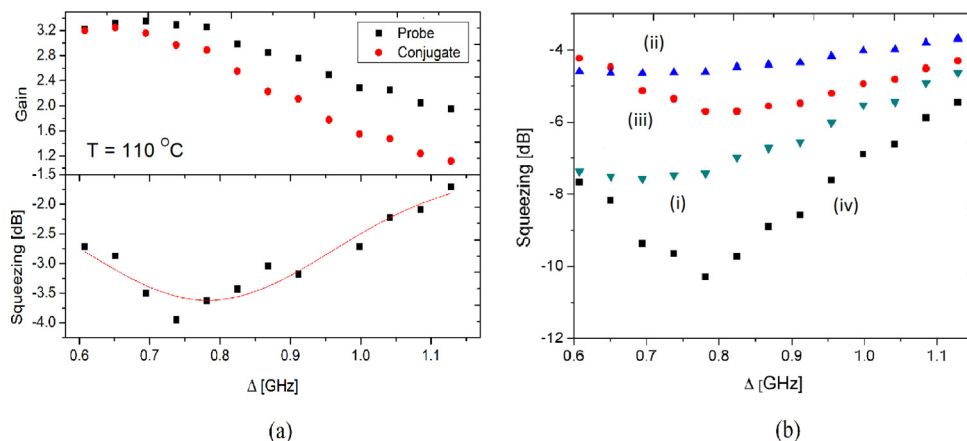
Fig. 4. (a) Gains of the probe (black squares) and the conjugate (red circles) — top plots, and intensity difference squeezing — bottom plots, as a function of Δ; (b) Squeezing vs Δ — calculated results with detection losses, using Eq. (3) ((i) — green inverted triangles), with Eq. (4) ((ii) — blue triangles), and using Eq. (5), with detection losses ((iii) — red circles) and for an ideal detection ((iv) — black squares), at 110 °C, for $\delta = 0$ MHz, $P_{pump} = 700$ mW, $P_{probe} = 6$ µW, at 1.5 MHz.

The spectrum of the SQL is not flat in the whole range of frequency and changes occurring at higher frequency were presented also in [36,37]. Calibration of SQL made in the frequency range 0.5–2.5 MHz confirmed that flat part of spectra is the SQL. The squeezing is observed in the frequency range from 0.9 MHz to 4.5 MHz, limited on the lower side by the technical noise, and on the high side by the detection bandwidth. The maximum of IDS is −6.1 dB at 1.2 MHz. Individual spectra of the probe and the conjugate are also shown. In order to find the optimal set of values of experimental parameters, for every cell temperature we first fixed Δ, and changed δ while observing level of IDS on the SA. Next, we jumped to another Δ, and repeated variation of δ. We performed the same process for the temperatures ranging from 110 °C to 130 °C. The frequency noise spectrum of the signal difference in Fig. 3 is obtained at the cell temperature of 123 °C, for $\Delta = 1.2$ GHz, $\delta = 6$ MHz, and for the pump and the probe powers of 750 mW and 6 µW, respectively. Sufficiently high pump power is needed for the enhanced nonlinearity in our experiment, and 750 mW was the maximal available pump power. Measured gains of the probe and conjugate are 7.12 and 7.64, respectively. For the results presented below, the pump power was lower, at the value that we more routinely obtain. All spectra of the noise fluctuations in Fig. 3 and results presented on Figs. 4–6 are corrected for the electronic noise and the pump leakage. The contribution of the fraction of the pump reaching the detectors to the noise of signal difference was determined by extrapolating SQL and probe-conjugate signal difference to zero power, and subtracting the former from the later. Note, that the amount of leaked pump noise in the measured difference of FWM and SQL signals, is frequency dependent, and therefore it has to be evaluated at the frequency at which the results were reported.

We investigated mechanisms of noise reduction by considering dependence of IDS on several FWM parameters: one-photon detuning Δ, two-photon detuning δ and temperature of potassium vapor. The values for IDS in figures below are obtained from the noise spectra at the analyzing frequency of 1.5 MHz. Objectives we wanted to realize with the results in these figures, are to test dependence of IDS and gains in the widest possible range of the variable parameter. Only if this range is appropriately wide, we can have clearer picture of how this parameter is affecting IDS, and more so, how different models compare with the experiment. In Fig. 4(a) we present gains of the probe and the conjugate and the IDS as a function of the one-photon pump detuning Δ, at the temperature 110 °C. We chose two-photon detuning $\delta = 0$ MHz, since it allowed squeezing in the widest possible range of one-photon detuning, at different temperatures. The pump power

was 700 mW. Gain of the probe (conjugate) is the ratio of the probe (conjugate) behind the cell and the probe before the cell, corrected for the losses on the cell windows. The plotted probe gain includes seed probe that is 6 µW. In Fig. 4(b) we plotted NRF calculated using formulas in Eqs. (3)–(5). The simple relation for NRF by Eq. (3) correctly qualitatively describes experimental IDS dependence on Δ, only when pump detuning is large, near the edges of the Doppler broadened absorption line, but gives larger values of squeezing. Good quantitative agreement between experiment and results for NRF_{TL}, by Eq. (4), indicates that our measurements of the probe gain and twin beam losses, as well as predictions of detectors efficiency are correct within a few percent. This model, however, is not qualitatively in agreement with the experiment. Not surprisingly, because internal losses of the probe and the conjugate, which depend on pump detuning, are not taken into account. For calculating NRF_L, we have used optical and detection losses behind the vapor, and probe transmissions and gains through the potassium cell, measured at each Δ for which IDS was observed. We find two reasons for observed discrepancies between the results of interleaved gain–loss model and experiment. Presented results for NRF_L only takes into account absorption of the probe beam. While this assumption is correct for Rb and Cs, it is not so correct for K because of much lower hfs of potassium, hence much smaller conjugate detuning from the probe. Small, but still present conjugate absorption in the vapor cell, degrades the squeezing, as our measurements show. Another reason for the quantitative discrepancy between theoretical results and experiment is the model assumption that pump and probe fully overlap in the vapor, which is not the case in the experiment, were we had to focus two beams at the cell center. Having this in mind, we expect that for a smaller gas cell, the measured IDS will come closer to the predicted values. Finally, we present NRF_L for intrinsic losses only, neglecting optical losses behind the medium. This gives the estimated value for the intrinsic source squeezing from potassium FWM of −10.29 dB, which is among the highest that this and similar models predicted [31,32,37].

The gains of twin beams and the IDS were also measured at higher temperatures of the potassium vapor, at 114 °C, Fig. 5(a), and at 118 °C, Fig. 5(b). The other FWM parameters are the same as in Fig. 4. As temperature increases, Δ for the maximum of squeezing has to be further from the pump resonance. While the one-photon detuning for the maximum of squeezing, Δ_m, was 0.75 GHz at 110 °C, at 118 °C was shifted to $\Delta_m = 1.2$ GHz. As density of the vapor increases, the Δ_m is detuned further from the resonance in order to reduce probe losses due to, other vise, too high probe absorption. At the same time, as seen
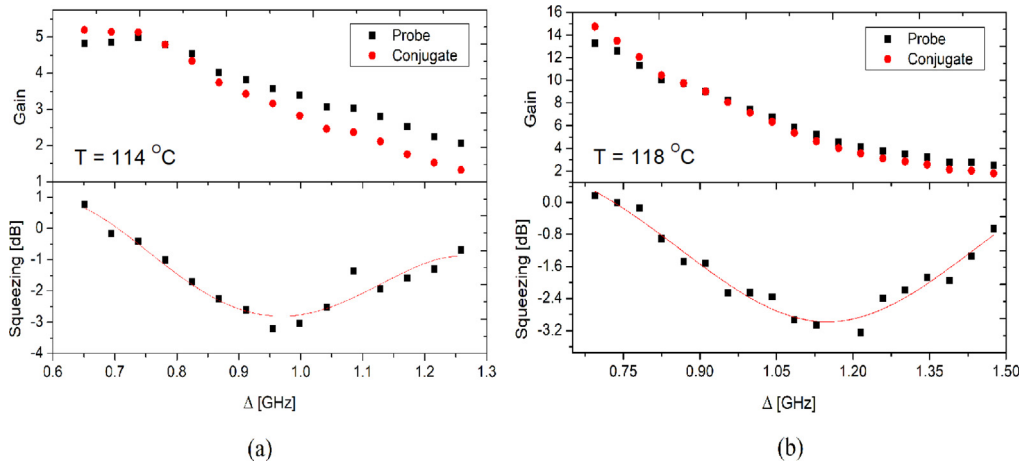
Fig. 5. Measured gains of the probe (black squares) and the conjugate (red circles) — top plots, and intensity difference squeezing — bottom plots, as a function of Δ at different cell temperatures (a) 114 °C, (b) 118 °C, for δ = 0 MHz, P_{pump} = 700 mW, P_{probe} = 6 μW, at 1.5 MHz.

in Figs. 4(a) and 5, at higher densities gain maximum shifts slightly towards lower Δ, resulting in nearly the same gains at Δ_m for all three densities we have in the experiment. The model cannot simulate well the results at higher densities, not even qualitatively, when parameters for the maximums of gains are different from parameters for the maximum of squeezing. For too large Δ, on the other hand, the nonlinearity of medium is vanishing, and gain and squeezing are decreasing, with G below unity and squeezing approaching SQL. The temperature range and the pump detuning in this experiment, although similar in values as in experiments with other alkalis, evidently bring different behavior of squeezing, gains and probe transmission. For instance, in the work with Rb [31] at the temperatures as in this work, the maximums of gain and squeezing are still at the same detuning, while probe transmission spans in different range.

Fig. 6 shows characteristic dependence of IDS and the gain of the probe as a function of two-photon detuning δ for Δ = 1.1 GHz and the cell temperature of 121 °C. Again, This combination of values of Δ and vapor density, allowed the largest range of δ for which the noise of the intensity difference is below SQL. The values of δ for the highest level of squeezing vary, both on the vapor density and on Δ. New temperature requires new detunings, for both δ and Δ, in order to reach maximum of IDS. While keeping the value of δ constant, at lower atom concentration, the optimal conditions for IDS are obtained at smaller pump detuning. At higher cell temperatures it is necessary to detune the pump towards the wings of the Doppler broaden line profile, to keep gains in the range optimal for highest squeezing. Our study shows that value of a single parameter is optimal for IDS only for the specific values of all the other FWM parameters. Change of one FWM parameter requires changes of the others for the new optimal squeezing. Hence, having an adequate theoretical model for description of FWM process and calculation of squeezing level is of great importance when finding the optimal set of experimental parameters.

Presented in the 6 is NRF_L, calculated using known losses behind the cell, from Eq. (5). The calculated NRF behaves similar to experimental results for δ below 8 MHz. Most theoretical models can predict squeezing correctly only when gain is in sync with squeezing, as presented for Rb [31,49] and Cs vapors [37]. An upgrade of existing models is needed for an adequate modeling of squeezing by FWM in hot K. We believe that having microscopic model based on Heisenberg–Langevin formalism, such as described in [8] for cold atoms, with more detailed description of light–atom interaction, but extended to take into account Doppler averaging, transit time of the atoms through the interaction area and frequency detuning due to the motions of atoms, would result in better overall agreement with the experiment.
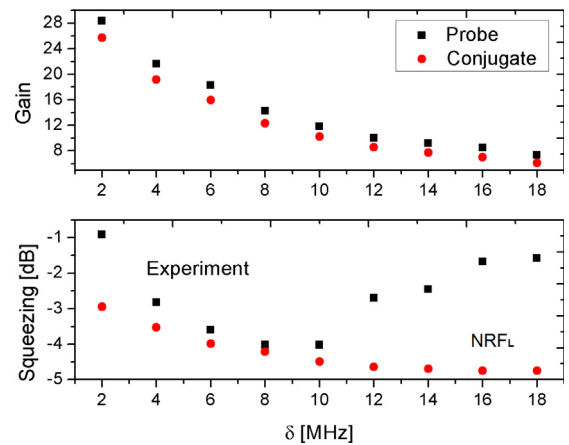

Fig. 6. Gains of the probe (black squares) and the conjugate (red circles) — top plot, and intensity difference squeezing — bottom plot, experimental results (black squares) and calculated (red circles), as a function of δ, at 121 °C, for Δ = 1100 MHz, P_{pump} = 700 mW, P_{probe} = 6 μW, at 1.5 MHz.

5. Conclusion

Intensity difference squeezing of −6.1 dB below SQL was obtained using non-degenerate double Λ atomic scheme for the FWM in potassium vapor, while running the FWM at the large pump detuning of ∼1 GHz, in the far wings of the Doppler broaden line. Obtained level of squeezing is close to the strongest squeezing measured in Cs, and compares well to squeezing obtained in Rb. The large IDS in potassium is of interest for quantum enhanced sensing and imaging, its small hyper-fine splitting means simpler and cheaper methods for controlling pump - probe frequency off-set. By investigating effects of FWM parameters (pump detuning and vapor density) on IDS, we have shown that for the optimum IDS, the single pass gain of the probe remains at the value that ensures optimum balance between squeezing strength and probe absorption. Agreement between calculated noise figures from the model operators and measured IDS is better if the measured gain maximum is obtained at the same FWM parameters as the maximum of squeezing. Better agreement should be obtained after averaging the annihilation and creation operators over atom velocity distribution. Neglecting optical losses behind the mixing source, the model predicts −10.29 dB for the IDS, which is among the highest expected from FWM in alkali vapor.

Data availability

Data will be made available on request.

Acknowledgments

References

[1] M. Taylor, J. Janousek, V. Daria, et al., Nature Photon. 7 (2013) 229—233.
[2] B.J. Lawrie, P.D. Lett, A.M. Marino, R.C. Pooser, ACS Photonics 6 (2019) 1307—1318.
[3] V. Boyer, A.M. Marino, P.D. Lett, Phys. Rev. Lett. 100 (2008) 143601.
[4] G. Brida, M. Genovese, I. Ruo Berchera, Nat. Photonics 4 (2010) 227—230.
[5] J. Aasi, et al., (The LIGO Scientific Collaboration), Nature Photon. 7 (2013) 613.
[6] N. Otterstrom, R.C. Pooser, B.J. Lawrie, Opt. Lett. 39 (2014) 6533–6536.
[7] N. Prajapati, Z. Niu, I. Novikova, Opt. Lett. 46 (2021) 1800–1803.
[8] Q. Glorieux, R. Dubessy, S. Guibal, L. Guidoni, J.P. Likforman, T. Coudreau, E. Arimondo, Phys. Rev. A 82 (2010) 033819.
[9] M.T. Turnbull, P.G. Petrov, C.S. Embrey, A.M. Marino, V. Boyer, Phys. Rev. A 88 (2013) 033845.
[10] J. Qiu, Z. Wang, D. Ding, Z. Huang, B. Yu, Phys. Rev. A 102 (3) (2020) 033516.
[11] M.M. Ćurčić, T. Khalifa, B. Zlatković, I.S. Radojičić, A.J. Krmpot, D. Arsenović, B.M. Jelenković, M. Gharavipour, Phys. Rev. A 97 (2018) 063851.
[12] Z. Wang, Y. Zhang, E. Paspalakis, B. Yu, Phys. Rev. A 102 (6) (2020) 063509.
[13] J. Qiu, Z. Wang, D. Ding, W. Li, B. Yu, Opt. Express 28 (3) (2020) 2975–2986.
[14] V. Boyer, C.F. McCormick, E. Arimondo, P.D. Lett, Phys. Rev. Lett. 99 (2007) 143601.
[15] D. Arsenović, M.M. Ćurčić, T. Khalifa, B. Zlatković, Z. Nikitović, I.S. Radojičić, A.J. Krmpot, B.M. Jelenković, Phys. Rev. A 98 (2018) 023829.
[16] R.M. Camacho, P.K. Vudyasetu, J.C. Howell, Nature Photon. 3 (2009) 103.
[17] N.B. Phillips, A.V. Gorshkov, I. Novikova, Phys. Rev. A 83 (2011) 063823.
[18] X. Pan, S. Yu, Y. Zhou, K. Zhang, K. Zhang, S. Lv, S. Li, W. Wang, J. Jing, Phys. Rev. Lett. 123 (2019) 070506.
[19] K. Zhang, W. Wang, S. Liu, X. Pan, J. Du, Y. Lou, S. Yu, S. Lv, N. Treps, C. Fabre, J. Jing, Phys. Rev. Lett. 124 (2020) 090501.
[20] F. Song, Z. Wang, E. Li, Z. Huang, B. Yu, B. Shi, Appl. Phys. Lett. 119 (2) (2021) 024101.
[21] F. Li, T. Li, M.O. Scully, G.S. Agarwal, Phys. Rev. Appl. 15 (2021) 044030.
[22] T. Li, F. Li, C. Altuzarra, A. Classen, G.S. Agarwal, Appl. Phys. Lett. 116 (2020) 254001.
[23] V. Boyer, A.M. Marino, R.C. Pooser, Science 321 (2008) 544–547.
[24] R.C. Pooser, A.M. Marino, V. Boyer, K.M. Jones, P.D. Lett, Opt. Express 17 (2009) 16722–16730.
[25] S.L. Braunstein, H.J. Kimble, Phys. Rev. Lett. 80 (1998) 869—872.
[26] S.L. Braunstein, C.A. Fuchs, H.J. Kimble, J. Modern Opt. 47 (2000) 267–278.
[27] S.L. Braunstein, P. van Loock, Rev. Modern Phys. 77 (2005) 513.
[28] N. Sangouard, et al., J. Opt. Soc. Amer. B 27 (2010) 137.
[29] H.P. Yuen, J.H. Shapiro, Opt. Lett. 4 (1979) 334.
[30] R.E. Slusher, L.W. Hollberg, B. Yurke, J.C. Mertz, J.F. Valley, Phys. Rev. Lett. 55 (1985) 2409.
[31] C.F. McCormick, A.M. Marino, V. Boyer, P.D. Lett, Phys. Rev. A 78 (2008) 043816.
[32] Q. Glorieux, L. Guidoni, S. Guibal, J.-P. Likforman, T. Coudreau, Proc. SPIE 7727 (2010) 772703.
[33] M. Mehmet, H. Vahlbruch, N. Lastzka, K. Danzmann, R. Schnabel, Phys. Rev. A 81 (2010) 013814.
[34] R.C. Pooser, A.M. Marino, V. Boyer, K.M. Jones, P.D. Lett, Opt. Express 17 (2009) 16722–16730.
[35] S. Kim, A.M. Marino, Opt. Express 26 (2018) 33366–33375.
[36] C. Liu, J. Jing, Z. Zhou, R.C. Pooser, F. Hudelist, L. Zhou, W. Zhang, Opt. Lett. 36 (2011) 2979–2981.
[37] M. Guo, H. Zhou, D. Wang, J. Gao, J. Zhang, S. Zhu, Phys. Rev. A 89 (2014) 033813.
[38] R. Ma, W. Liu, Z. Qin, X. Jia, J. Gao, Phys. Rev. A 96 (2017) 043843.
[39] J.D. Swaim, R.T. Glasser, Phys. Rev. A 96 (2017) 033818.
[40] D. Zhang, C. Li, Z. Zhang, Y. Zhang, Y. Zhang, M. Xiao, Phys. Rev. A 96 (2017) 043847.
[41] L. Cao, J. Du, J. Feng, Z. Qin, A.M. Marino, M.I. Kolobov, J. Jing, Opt. Lett. 42 (2017) 1201–1204.
[42] S. Liu, Y. Lou, J. Jing, Phys. Rev. Lett. 123 (2019) 113602.
[43] S. Liu, H. Wang, J. Jing, Phys. Rev. A 97 (2018) 043846.
[44] H. Wang, C. Fabre, J. Jing, Phys. Rev. A 95 (2017) 051802(R).
[45] X. Pan, H. Chen, T. Wei, J. Zhang, A.M. Marino, N. Treps, R.T. Glasser, J. Jing, Phys. Rev. B 97 (2018) 161115(R).
[46] M.T. Turnbull, P.G. Petrov, C.S. Embrey, A.M. Marino, V. Boyer, Phys. Rev. A 88 (2013) 033845.
[47] M.M. Ćurčić, T. Khalifa, B. Zlatković, I.S. Radojičić, A.J. Krmpot, D. Arsenović, B.M. Jelenković, M. Gharavipour, Phys. Rev. A 97 (2018) 063851.
[48] U. Leonhardt, Phys. Rev. A 48 (1993) 3265.
[49] M. Jasperse, L.D. Turner, R.E. Scholten, Opt. Express 19 (2011) 3765–3774.
[50] Q. Glorieux, R. Dubessy, S. Guibal, L. Guidoni, J.P. Likforman, T. Coudreau, E. Arimondo, Phys. Rev. A 82 (2010) 033819.
[51] D. McKay, Potassium 5p line data, 2009, available online at http://fermionlattice.wdfiles.com/local--files/papers/5P_structure.

Four-wave mixing in potassium vapor with an off-resonant double-Λ system

M. M. Ćurčić[*]

Institute of Physics Belgrade, University of Belgrade, Pregrevica 118, 11080 Belgrade, Serbia
and School of Electrical Engineering, University of Belgrade, Bulevar kralja Aleksandra 73, 11120 Belgrade, Serbia

T. Khalifa, B. Zlatković, I. S. Radojičić, A. J. Krmpot, D. Arsenović, and B. M. Jelenković
Institute of Physics Belgrade, University of Belgrade, Pregrevica 118, 11080 Belgrade, Serbia

M. Gharavipour
Laboratoire Temps-Fréquence (LTF), Institut de physique, Université de Neuchâtel, Neuchâtel CH-2000, Switzerland

We investigate both theoretically and experimentally four-wave mixing (FWM) in hot potassium vapor, generated by a copropagating pump and probe in an off-resonant double-Λ system, and present conditions when this atomic system is (1) a strong phase-insensitive parametric amplifier and (2) a source of large-amplitude squeezing. Theoretically, nonperturbative numerical calculations of optical Bloch-Maxwell equations have been solved for a four-level atomic system of K in order to derive the atomic polarization and then amplitudes of propagating optical waves, pump, probe, and conjugate. For potassium, to our knowledge, there are no such comparisons of theoretical and experimental results of gains of twin beams under the large range of FWM parameters as presented here. Results have shown that one-photon detuning has to be slightly larger than the Doppler broadened transition for large gains and strong squeezing. The gain is particularly large for small red two-photon detuning (-2–$6\,\mathrm{MHz}$) and high K density (5.5–$10 \times 10^{12}\ \mathrm{cm}^{-3}$). Following experimentally and theoretically determined relation between gains, probe transmissions, and squeezing in Rb and Cs, we have found parameters of FWM when maximum squeezing in hot K vapor is expected.

I. INTRODUCTION

Four-wave mixing (FWM) is a nonlinear phenomenon that in alkali-metal vapors can efficiently generate entangled photon pairs, essential for probing quantum properties of light and for quantum information [1–3]. It also enables slowing and storing of light in atomic ensembles [4–9], essential elements for quantum memories.

Different schemes have been used to generate paired photons, such as on-resonant spontaneous FWM [2], the diamond [10], and double ladder scheme FWM [11]. An atomic system that is often used for generation of twin beams is off-resonant FWM in a double-Λ scheme, realized by two input fields, pump and probe, in a three (four) -level atomic system. The lower Λ is made of pump and probe photons, while the pump photon and conjugate photon close the upper Λ (see Fig. 1). This atomic scheme is similar to schemes for electromagnetically induced transparency (EIT) and becomes nonlinear FWM under certain conditions: whether the system will behave like EIT or a parametric amplifier depends on laser detunings, atomic density, and pump power [12,13]. While resonant absorption processes for EIT conditions lead to losses, FWM gains of both probe and conjugate, typically observed for high pump beam, allow for much larger propagation distances [4,14,15].

A nondegenerate, off-resonant double-Λ scheme was found to be a good source for relative amplitude squeezing [16–19] and for simultaneously generated intensity correlations and phase anticorrelations or entanglement of probe and conjugate [20,21]. Large entanglement is an important resource for quantum information [22]. A correlation between the amount of squeezing and entanglement and the gain of the twin beam is established [20].

Theoretically, FWM was studied in degenerate and counterpropagating laser beams [23], as well as in nondegenerate and copropagating beams. In the latter, nonlinear parametric processes in FWM were studied in a double-Λ configuration with either resonant (larger contribution from CPT and EIT phenomena) [24] or off-resonant pump frequency [15], in hot gas vapors or in cold atoms [25]. There are different approaches to model complex processes in FWM. They depend on the intended applications of the system, which can be parametric gain, quantum-correlations of twin beams, squeezing and entanglement, slow and stored light, i.e., whether classical or quantum properties are of interest. For work presented here, the most relevant are models that analyze the continuous wave regime and calculate gains of twin beams. Quantum mechanical theory of multiwave mixing was applied for calculating Rabi sidebands generated by FWM [26]. In most models, the treatment is based on analytical solutions, after perturbation theory and a number of approximations being applied [15]. In the seminal paper [24], pump and probe are resonant with atomic transitions with conditions for EIT, while
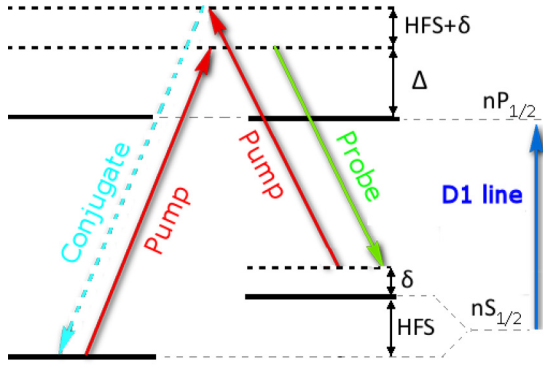
———————
[*]marijac@ipb.ac.rs

FIG. 1. Double Λ scheme at D_1 line of an alkali-metal atom. hfs = hyperfine splitting, Δ = one-photon detuning, δ = two-photon detuning. Levels: $|1\rangle$ and $|2\rangle$ = hyperfine levels of $4S_{1/2}$, $F = 1$ and $S_{1/2}$, $F = 2$ respectively, $|3\rangle = 4P_{1/2}$, $|4\rangle$ = virtual level, degenerate with $|3\rangle$, introduced by the model. Hfs of the level $|3\rangle$ is negligible in comparison with ground state hfs.

cross susceptibilities are enhanced by coherence in the ground hyperfine levels. Heisenberg-Langevin formalism was used to calculate the classical and quantum properties of probe and conjugate beams beyond the linear amplifier approximation [25,27]. A phenomenological approach when the medium is quantum mechanically described by a simple model of distributed FWM gain and probe loss was used in Ref. [16].

FWM in alkali metals has been extensively studded, particularly in Rb and Cs [4,14,16,19,25,28,31], but little work was done on potassium [32–37]. Potassium has hyperfine splitting (hfs) of the ground state of only 460 MHz, by far smaller then for any other alkali metal. For FWM based on two pump photons, small hfs means that detuning of the upper Λ scheme is not far from detuning of the lower Λ scheme. This suggests that large gains and squeezing and other FWM properties are possible at lower laser power.

With this study, we extend our previous work on FWM in K [33] with results of the theoretical model and new experimental results. The model is a semiclassical treatment of FWM processes, and atomic polarization, calculated from optical Bloch equations (written for the system presented schematically in Fig. 1), is applied in the propagation equations to obtain amplitudes of three optical fields at the exit from the K vapor. We compare calculated and measured gains for a wide range of parameters, which is important for efficiency of FWM. This includes the angle between the pump and the probe, atomic density, detuning of the pump from the D_1 transition, Δ, and two-photon detuning in respect to hfs of the ground state, δ.

Performance of FWM for high-level squeezing, quantum information protocols, and quantum cloning machines [3] strongly depends on FWM parameters: vapor density, Δ and δ. The former controls probe absorption, while two detunings control nonlinearity and gain. Measurements and models [16,18] have shown that for stronger squeezing and low noise figures, moderate gains of probe and conjugate are at a maximum, while probe absorption is minimal. We made intensive calculations of gains and probe transmissions for the large range of K density and one- and two-photon detuning,

and present parameters of FWM that we believe will generate the strongest quantum correlations and squeezing in K vapor. In the theoretical analyses for FWM parameters for strong squeezing we have included results that take into account the Doppler average of density matrix elements. These values are compared with values used in a resent experiment [38] to measure squeezing in K vapor. Since for the alkali-metal atoms with higher hyperfine splitting of the ground state, higher powers are required for efficient degree of squeezing [19,29], we believe that potassium, having the smallest hfs of the ground state, could be more convenient, compared to others, for high-level amplitude squeezing.

II. THEORETICAL MODEL

In the model, the three electric field modes, pump (drive), probe, and conjugate, with frequencies ω_d, ω_p, and ω_c, respectively, interact with four levels of the ^{39}K atom. The double-Λ scheme with modes coupling atomic levels of the D_1 transition is given in Fig. 1. Level $|3\rangle$ is $4P_{1/2}$, while levels $|1\rangle$ and $|2\rangle$ are hyperfine levels of $4S_{1/2}$, $F = 1$ and $F = 2$, respectively. The lower Λ scheme consists of the pump photon that couples the level $|1\rangle$ to the level $|3\rangle$ with the one-photon detuning $\Delta_{(13)} = \Delta$. The other "leg" of the first Λ scheme is the probe photon that stimulates the Stokes scattering from level $|3\rangle$ to the level $|2\rangle$, with two-photon detuning $\Delta_{(132)} = \delta$. The pump is sufficiently strong to drive the off-resonant transition $|2\rangle \rightarrow |4\rangle$ in the upper Λ scheme. By the way of stimulating anti-Stokes scattering the conjugate photon closes the upper scheme. The total detuning for the level $|4\rangle$ is $\Delta_{(1324)} = (2\omega_d - \omega_p) - (\omega_4 - \omega_1)$, where $\omega_4 - \omega_1$ is angular frequency of the transition $|1\rangle \rightarrow |4\rangle$. We introduce level $|4\rangle$, which is degenerate to the level $|3\rangle$, and like level $|3\rangle$ is weakly coupled to both level $|1\rangle$ and level $|2\rangle$ because of a large detuning.

Atoms are simultaneously illuminated by the pump, probe, and conjugate and experience a total electric field approximated by the sum of three monochromatic fields:

$$\mathbf{E} = \sum_{i=d,p,c} \mathbf{e}_i E_i^{(+)} e^{-i\omega t + i\mathbf{k}_i \mathbf{r}} + \text{c.c.} \tag{1}$$

Here $E^{(+)}$ is the slowly varying approximation of the fields envelope, at positive frequencies. The Hamiltonian for the atomic system is given by

$$\hat{H} = \hat{H}_0 + \widehat{H_{\text{int}}} = \sum_{i=1}^{4} \hbar\omega_i |i\rangle\langle i| - \hat{\mathbf{d}} \cdot \mathbf{E}(\mathbf{r}, t), \tag{2}$$

where $\hat{H}_0$ is the unperturbed Hamiltonian of the system and $\widehat{H_{\text{int}}}$ is interaction Hamiltonian, $\hbar\omega_i$ is the energy of atom level i, and $\hat{\mathbf{d}}$ is atomic dipole moment.

Atomic dynamics is described by the set of Bloch equations for density matrix elements $\hat{\rho}$:

$$\dot{\hat{\rho}} = -\frac{i}{\hbar}[\hat{H}, \hat{\rho}] + \widehat{SE} + \hat{R}, \tag{3}$$

where $\widehat{SE}$ denotes the spontaneous emission from the excited states, and $\hat{R}$ is the relaxation due to atom transit time-induced losses and collisional dephasing. The full set of Eq. (3) is given in the Appendix. Because of the fast oscillating laser field, as
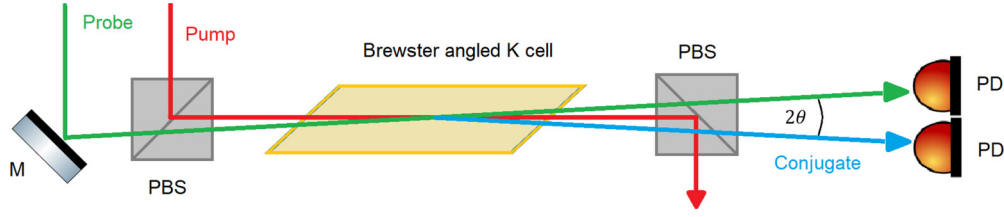
FIG. 2. Experimental setup. M = mirror, PBS = polarization beam splitter, PD = photodetector.

in Eq. (1), substituting H from Eq. (2) into Eq. (3) produces fast oscillating terms in ρ_{ij}. After substitution,

$$\tilde{\rho}_{ij} = e^{-i\omega_{(ij)}t + i\mathbf{k}_{(ij)}\mathbf{r}}\rho_{ij}, \tag{4}$$

where $\omega_{(ij)}$ are different angular frequencies: $\omega_{(13)} = \omega_{(24)} = \omega_d$, $\omega_{(23)} = \omega_p$, $\omega_{(14)} = \omega_c$, $\omega_{(12)} = \omega_{(13)} - \omega_{(23)}$, $\omega_{(34)} = \omega_{(14)} - \omega_{(13)}, \omega_{(ij)} = -\omega_{(ji)}$, and $\mathbf{k}_{(ij)}$ are wave vectors of sums (differences) of wave vectors: $\mathbf{k}_{(13)} = \mathbf{k}_{(24)} = \mathbf{k}_d$, $\mathbf{k}_{(23)} = \mathbf{k}_p$, $\mathbf{k}_{(14)} = \mathbf{k}_c$, $\mathbf{k}_{(12)} = \mathbf{k}_{(13)} - \mathbf{k}_{(23)}$, $\mathbf{k}_{(34)} = \mathbf{k}_{(14)} - \mathbf{k}_{(13)}$, $\mathbf{k}_{(ij)} = -\mathbf{k}_{(ji)}$ with $\mathbf{k}_c = 2\mathbf{k}_d - \mathbf{k}_p - \Delta\mathbf{k}$. Terms that oscillate with the sum of frequencies are neglected in the rotating wave approximation. Left in Eq. (3) are time-independent terms and a few spatially dependent terms with oscillating coefficients $e^{i\Delta kz}$.

Propagation along the z direction and temporal evolution of pump, probe, and conjugate are described by the set of nonlinear equations for the slowly varying envelopes of the three fields:

$$\left(\frac{\partial}{\partial z} + \frac{1}{c}\frac{\partial}{\partial t}\right)E_d^{(+)} = i\frac{kN}{2\varepsilon_0}d(\tilde{\rho}_{(42)} + \tilde{\rho}_{(31)}), \tag{5a}$$

$$\left(\frac{\partial}{\partial z} + \frac{1}{c}\frac{\partial}{\partial t}\right)E_p^{(+)} = i\frac{kN}{2\varepsilon_0}d\tilde{\rho}_{(32)}, \tag{5b}$$

$$\left(\frac{\partial}{\partial z} + \frac{1}{c}\frac{\partial}{\partial t}\right)E_c^{(+)} = i\frac{kN}{2\varepsilon_0}d\tilde{\rho}_{(41)}. \tag{5c}$$

Here N is the atom density.

Since we are also interested in probe absorption, we calculate the above equations by setting the intensity of pump beam to be zero. The probe transmission is then the quotient of the intensities of the outgoing and incoming probe beam. In a hot vapor the Doppler effect is present. The shift of the observed angular frequency is dependent on the z component of the velocity, v_z, for which the Maxwell distribution is given by

$$f(v_z) = \sqrt{\frac{m}{2\pi kT}}e^{\frac{-mv_z^2}{2kT}}, \tag{6}$$

The observed angular frequency is $\omega_0 = \sqrt{\frac{1-\beta}{1+\beta}}w_s$, where ω_s is angular frequency of the source and $\beta = v/c$. The frequency shift alters one photon detuning and detuning of the conjugate pulse, while two-photon detuning stays the same since the pump and probe are almost copropagating. Hence, density matrices depend on v_z. We perform Doppler averaging with the most basic approximation. We calculate the signals, gains of twin beams, and probe transmission for different v_z and then average them over the Maxwell distribution.

The gains of the probe (conjugate) are calculated from the ratio of amplitudes of probe (conjugate) at the exit from the K vapor to the probe amplitude at the entrance to the vapor. The model assumes that the pump and the probe fully overlap. The gas cell used in the experiment is 5 cm long, therefore for a typical angle between the probe and the pump ~3 mrad, beams are overlapped only in the part of the cell. Our theoretical results are for a 1 cm long interaction region. Parameters used in the calculations are as in the experiment, like atom density, one- and two-photon detuning, and angle between pump and probe. Rabi frequencies of the pump and probe are calculated from the laser intensity I using $\Omega = \frac{2dE_0^{(+)}}{\hbar}$, $E = E_0\cos(\omega t) = E_0^{(+)}e^{-i\omega t} + E_0^{(-)}e^{i\omega t}$, $E_0^{(+)} = \frac{E_0}{2} = \sqrt{(\eta I/2)}$. Here $\eta = 376.73$ Ω [39] is the vacuum impedance, and d is the reduced dipole matrix element, which for potassium is $d = 1.74 \times 10^{-29}$ Cm [40]. For total relaxation rates, γ (see the Appendix), we used the value $\gamma \sim 10^5$ Hz.

III. EXPERIMENT

We have measured gains of the probe and the conjugate using the setup described in Ref. [33]; see Fig. 2. Laser beam from the high-power, narrow line laser (Coherent, MBR 110) is split in two by a 90:10 beam splitter. A stronger beam is used as the pump beam, and the weaker fraction is the probe beam. The probe is sent through two AOMs, one in a double pass, for the probe frequency detuning in respect to the pump frequency, and for scanning of this detuning around the hfs of the K ground state. Thus, we vary two-photon detuning δ by changing the probe frequency and vary one-photon detuning Δ by tuning the pump frequency. Diameters of the pump and the probe beams are 1.1 mm, and 0.75 mm, respectively. Two beams are orthogonally polarized and recombined on the polarizing beam cube before entering the K cell. This is the vacuum K cell with natural abundance of isotopes, 5 cm long, 25 mm in diameter. The cell was heated by hot air up to 150 °C. Pump and probe beams enter the cell at the small angle θ. We can adjust this angle by changing the probe direction with the entrance mirror, placed before the combining cube. With the pump beam behind the cell blocked, two beams emerge: probe and the frequency up-shifted beam (conjugate). Both beams are detected with the pair of photodetectors. We get the gains of the probe and the conjugate from the ratios of measured powers of the probe and conjugate beams behind the cell to the probe beam input power. Radius and shape of beams behind the cell are monitored with a CCD beam profiler.
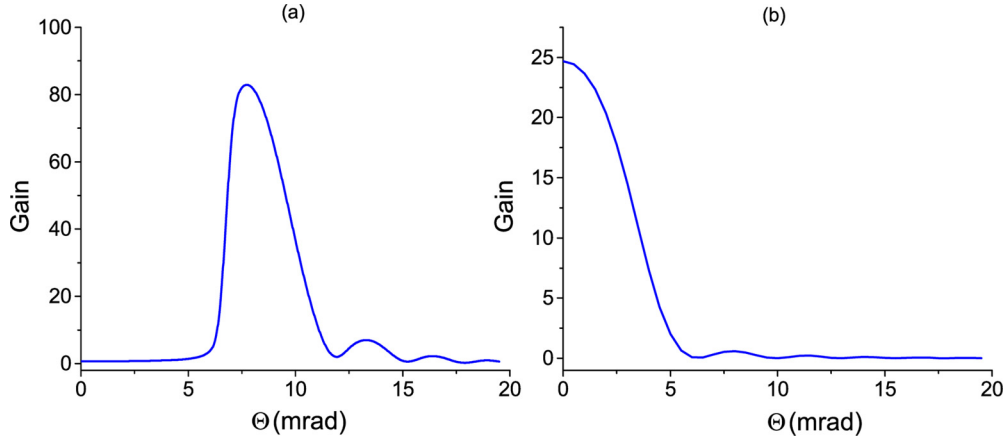
FIG. 3. Calculated gain of the conjugate beam as a function of the angle θ for two pump powers. (a) $\Omega_d = 3.25$ GHz, (b) $\Omega_d = 1.95$ GHz, for $N = 1 \times 10^{12}$ cm^{-3}, $\delta = -9.5$ MHz, $\Delta = 1$ GHz, and $\Omega_p = 22.5$ MHz.

IV. RESULTS AND DISCUSSION

In this section we present results of gains of twin beams as a function of FWM parameters: the angle between the pump and the probe, gas density, one- and two-photon detuning, and the probe power. But, as we will show, dependence on one of the parameters depends on values of the other parameters.

A. Measured and calculated gains of probe and conjugate

1. Dependence of gains on the angle between pump and probe

Probe and conjugate gains as a function of the angle θ between the pump and the probe are results of FWM phase matching. As we see from results in Figs. 3 and 4, the phase matching condition is satisfied at different angles θ, depending on values of other parameters. Behavior of FWM gains versus θ is influenced by the index of refraction at the probe frequency, which is influenced by values of laser powers, densities, and detunings. In Figs. 3 and 4 we present calculated conjugate beam gains as a function of θ. We decided not to show results for the probe because the model gives very similar behavior of gains of the probe and the conjugate.

Results in Fig. 3 are obtained for different pump Rabi frequencies, while results in Fig. 4 are for different density of the K vapor. Results show that FWM gains have different behavior at high and low pump Rabi frequencies Ω_d (Fig. 3)

and at high and low K densities (Fig. 4). In both figures, one- and two-photon detunings, and probe Rabi frequency Ω_p are $\Delta = 1$ GHz, $\delta = -9.5$ MHz, and $\Omega_p = 22.5$ MHz. As we can see, at high Ω_d and higher density, FWM gains are in a narrow range of angles θ and the gain maximum is away from zero values of δ. On the other hand, at lower power and density, FWM phase matching is found at smaller angles. Here gain increases as θ is decreasing. Occurrence of FWM gains at near zero angle means negligible changes of index of refraction at the probe frequency and/or its continuous change along the vapor due to strong pump absorption and therefore variation of pump power along the propagation direction. The possibility of the latter was not supported by the calculated pump absorption. On the other hand, our model shows correlation between how gain depends on angle, and the amount of the phase changes of the probe and conjugate. When the gain versus angle is a narrow peak as in Fig. 3(a), then Δk_z varies for more then 2π over the propagated distance. When gain monotonically changes as the angle increases from zero, Δk_z changes only a little, less then $\pi/4$.

Experimental results for the gains of twin beams as a function of the angle θ for K densities of 5.5×10^{12} cm^{-3} (cell temperature 130 °C) and 1.75×10^{13} cm^{-3} (150 °C) are given in Fig. 5. The smallest value of the angle between pump and probe we needed to separate the probe and conjugate
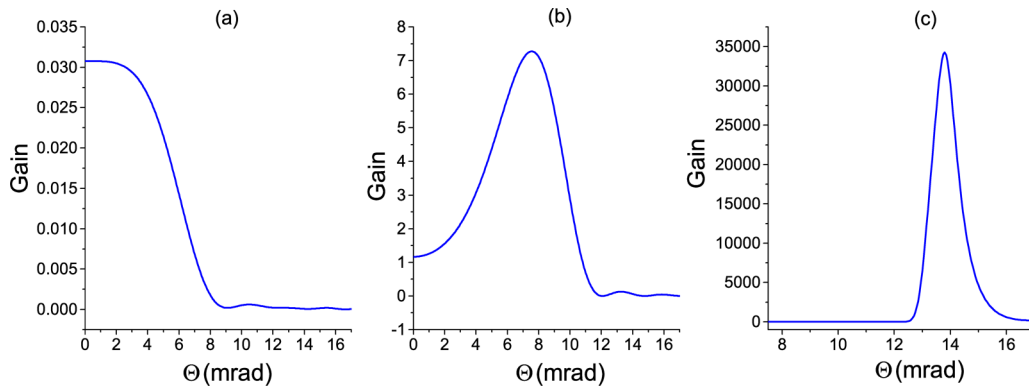

FIG. 4. Calculated gain of the conjugate beam as a function of the angle θ, for three values of the potassium density. (a) $N = 1 \times 10^{13}$ cm^{-3}, (b) $N = 1 \times 10^{12}$ cm^{-3}, and (c) $N = 1 \times 10^{11}$ cm^{-3} for $\Omega_d = 1.95$ GHz, $\Omega_p = 22.5$ MHz, $\delta = -9.5$ MHz, and $\Delta = 1$ GHz.
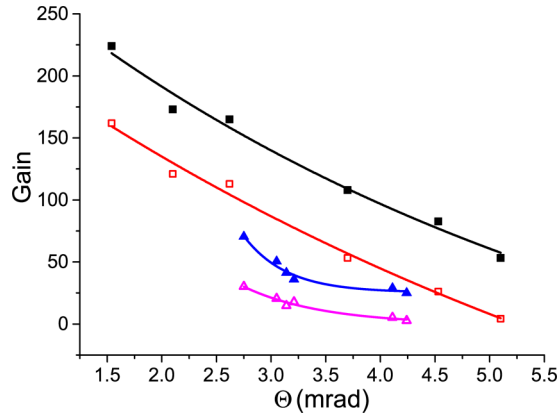
FIG. 5. Experimental results of gains of probe (open symbols) and conjugate (filled symbols) for two K density, 5.5×10^{12} cm^{-3} (squares) and 1.7×10^{13} cm^{-3} (triangles). $\Delta = 1$ GHz (for lower density) and 1.35 GHz (for higher density). $\delta = -3.7$ MHz, $P_d = 370$ mW, and $P_p = 25 \mu$W.

behind the cell was $\theta = 1.5$ mrad. The twin beam gains at the highest vapor density that we had in the experiment are lower and were measured only at high $\Delta = 1.35$ GHz. Experimental results of gains versus angle, as shown in Fig. 5, are typical for copropagating pump and probe with a similar diameter in a rather long gas cell, because beams do not fully overlap in parts of the cell.

2. Dependence of gains on two-photon detuning

Calculated and measured gains of the probe and the conjugate versus two-photon detuning δ, for several values of one-photon detuning, are presented in Fig. 6. Dependence is given for two Δ, 1 GHz and 1.35 GHz, and for $\theta = 5.5$ mrad. Typical widths of calculated gains are between 1.5 and 3 MHz, and of measured gains are 6–13 MHz.

Maximum of gains are, at δ_m, shifted from two-photon resonance ($\delta \approx 0$). This shift is mainly due to differential Stark shift, δ_S, because of different detunings of hyperfine levels from the off-resonant pump. As shown in Fig. 6, δ_m is larger for smaller Δ. Not shown, but when Δ is 670 MHz, $\delta_m = -12$ MHz. The maximum of the gain curve may not coincide with the FWM resonance because of Raman absorption at the resonance. We experimentally investigate how δ_m varies with certain parameters by keeping Δ fixed. For $\Delta = 1$ GHz, $\theta = 3$ mrad, and change of K density from 1.5×10^{12} cm^{-3} to 1.7×10^{13} cm^{-3}, δ_m stayed the same, -3.7 MHz for the probe and -1.7 MHz for the conjugate. On the other hand, changing θ from 5.5 to 2.6 mrad, for the K density of $N = 5.5 \times 10^{12}$ cm^{-3}, moves δ_m from -4 MHz to -2.5 MHz. This slight shift to smaller two-photon detuning when the angle is decreasing is the same behavior of δ_m as found for Rb in Ref. [15].

It appears from Fig. 6 that typical curves representing gains versus δ, both calculated and measured, are not symmetric around the maximum. The asymmetric shape of lines might be because of inhomogeneous differential ac Stark shift, since
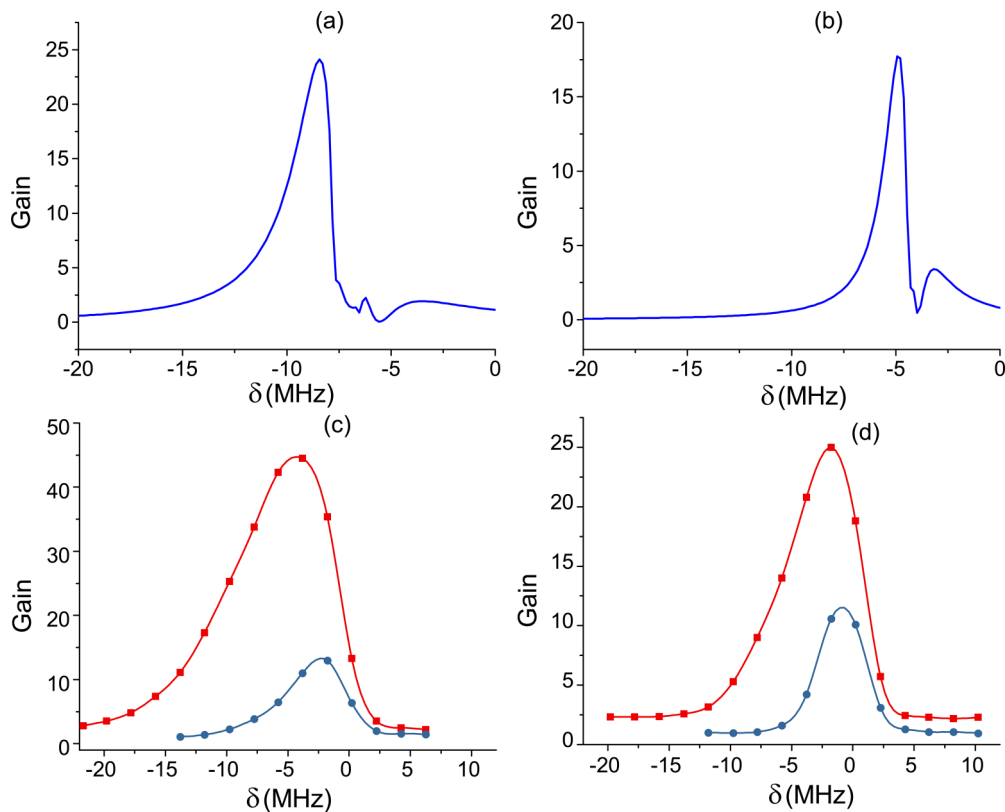

FIG. 6. Gains vs two-photon detuning. (a), (b) Calculations of the conjugate gain. The pump and probe Rabi frequencies are 1.94 GHz and 22.6 MHz, respectively. (c), (d) Experimental results of gains for the probe (solid circles, blue for online version) and the conjugate (solid squares, red for online version). Pump and probe powers are 370 mW and 25~μW, respectively. (a), (c) $\Delta = 1$ GHz, (b), (d) $\Delta = 1.35$ GHz. Density $N = 5.5 \times 10^{12}$ cm^{-3}, $\theta = 5.5$ mrad.
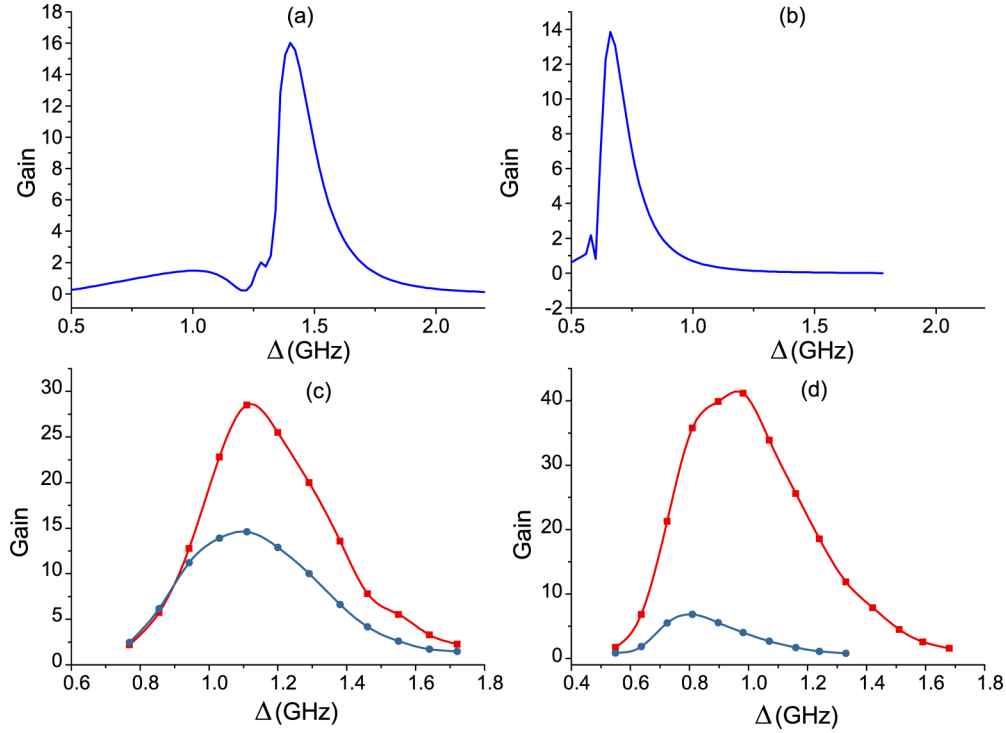
FIG. 7. Gains vs one-photon detuning. (a), (b) calculations of the conjugate gain. (c), (d) experimental results of gains of probe (solid circles, blue for online version) and conjugate (solid squares, red for online version). (a), (c) $\delta = -4$ MHz, (b), (d) $\delta = -8$ MHz. Pump and probe Rabi frequencies, as well as pump and probe powers, K vapor densities, and angle θ are the same as in Fig. 6

atoms in different areas of Gaussian beams experience different laser fields, and thus have different ac shift.

3. Dependence of gains on one-photon detuning

Potassium has larger Doppler broadening than other alkali metals, ~ 850 MHz. Width of Doppler line broadening in hot alkali metal vapors determines the range of Δ for large FWM gains. It is between 0.5 and 1 GHz for large gains and best squeezing for Rb and Cs [17,18,30,31].

We have calculated and measured gains versus Δ, with δ and θ as parameters. Presented results are for K vapor density of $N = 5.5 \times 10^{12}$ cm^{-3} (130°C) (see Fig. 7). Parameters in the calculations are the same as for results in Fig. 6. Results

in Figs. 7(a) and 7(c) are for $\delta = -4$ MHz, while those in Figs. 7(b) and 7(d) are for $\delta = -8$ MHz. Gains versus Δ are broad, asymmetric curves whose width is 200 MHz for calculated and 400 MHz for measured results.

One-photon detuning for the maximum gain, Δ_m, is close to 1 GHz. We found that Δ_m doesn't change when θ changes if we keep δ the same. On the other hand, for the same angle θ (Fig. 7), Δ_m will have a different value when δ is changed: it is at 0.9 GHz for δ at -8 MHz and can go as far as 1.2 GHz for $\delta \sim 0$ MHz. Because of different detuning, gain of the conjugate is larger then the gain of probe. Large detuning of the probe, beyond the Doppler broadening, minimizes the effect of EIT on the probe absorption.
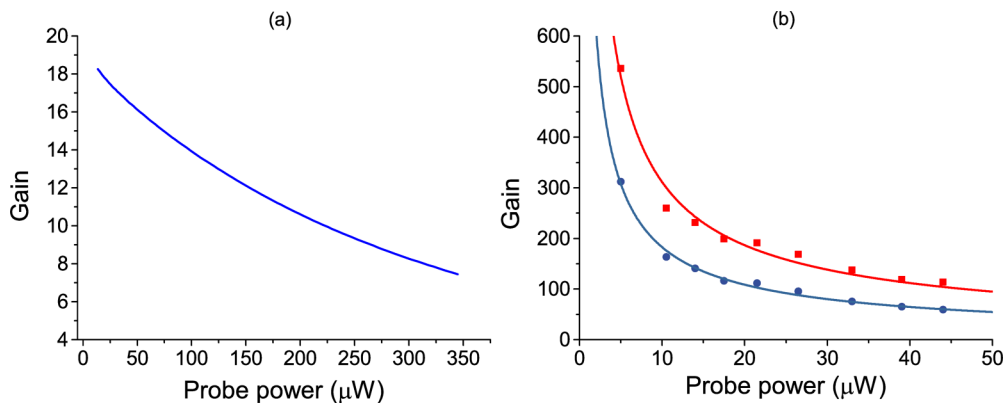

FIG. 8. (a) Calculation of conjugate gain vs probe power. (b) Measurements of probe (solid circles, blue for online version) and conjugate (solid squares, red for online version) gain vs probe power, for $\Delta = 960$ MHz, $\delta = -3.7$ MHz, and cell temperature 130 °C.
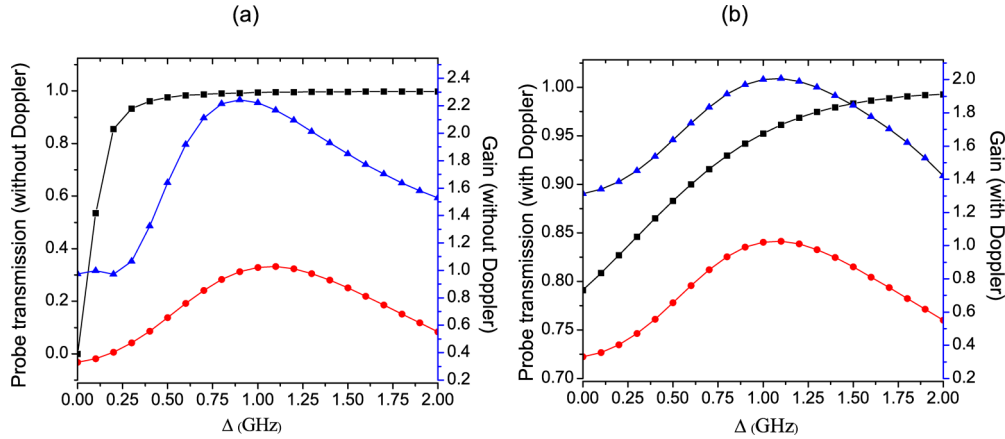
FIG. 9. Calculations of probe transmission (solid squares, black for online version) and gains for probe (solid triangles, blue for online version) and conjugate (solid circles, red for online version): (a) without Doppler averaging; (b) with Doppler averaging.

4. Gain dependence on probe power

Efficiency of FWM in alkali metals depends on the probe power, as presented in Fig. 8, for both calculated and measured values of gains. Evidently the lower the probe power, the higher the gain of both beams. The FWM gain in K vapor can thus be very large. In the experiment, we could not decrease probe below 5 μW because of limited sensitivity of photo diodes. Even without the probe beam at the entrance, with the probe initially in the vacuum state, a strong pump can generate side modes or twin photons [26].

B. Parameters of K vapor for optimum squeezing: Theoretical diagnostics

The numerical model explained above and derived in the Appendix allows us to search for the set of FWM parameters which should provide strong degrees of squeezing in K vapor. It was found, both experimentally and theoretically, in Rb and Cs [16,18,19] that in order to increase the squeezing and noise figure, it is necessary to reduce probe absorption and have modest and similar gains of both probe and conjugate. When plotted as a function of detuning, squeezing is at a maximum when gain is at a maximum. But too large gain results in probe noise that is large due to absorption and losses (fluorescence and nonlinear processes), and depending on gains, one needs FWM parameters that provide optimum probe transmission. Typically, the strongest squeezing is for Δ near the edge of Doppler broadening, when gains are at a maximum and probe transmission at about 90% [16].

We performed thorough analyses of effects of FWM parameters on gains and probe transmission in a search for those that produce maximum gains and large probe transmission at the same time. Results in Fig. 9 show dependence of gains and transmissions on Δ, for K density of 1×10^{12} cm^{-3}, δ -0.5 MHz, and θ 2.8 mrad. Clearly there is the range of Δ near 900 MHz when modest gains are at maximum and probe transmission is high. We recommend this set of parameters for the new measurements of squeezing in K. Results of gains and transmissions are presented with [Fig. 9(a)] and without Doppler averaging [Fig. 9(b)]. Apparently, corrections due

to Doppler broadening are small for gains, as found to be the case also for Rb [15], but are considerable for the probe transmission. Results obtained for squeezing in potassium [38] for Δ of 500 MHz and probe transmission below 50% are below values for Rb [16,29] and Cs [19]. Parameters of FMW in Ref. [38] are outside ranges we believe, based on present results, are optimal for squeezing.

V. CONCLUSION

A nonperturbative numerical model was applied to the double-Λ atomic system in potassium vapor, and gains of probe and conjugate were calculated under the conditions of FWM. Results are in agreement with experimental results and show high gains when Δ is slightly larger than the Doppler width and δ is in the range -10–0 MHz. This system is a strong parametric amplifier with gains of several hundred, larger than observed with other alkali-metal atoms for similar pump laser power. On the other hand, potassium is the only alkali metal whose hfs of the ground state is smaller than the Doppler width, i.e., both pump and probe couple simultaneously both ground hfs levels to the excited level.

The model was also used to find parameters of FWM in K vapor that would be optimal for relative amplitude squeezing. In search for these parameters we included results that take into account Doppler averaging of density matrix elements. We have found that the density of 1×10^{12} cm^{-3}, the angle between the pump and the probe $\theta = 2.8$ mrad, while δ and Δ are -0.5 MHz, and $\sim$900 MHz, respectively, and for the pump and the probe Rabi frequencies 1.938 GHz and 23.72 MHz, respectively, are the set of parameters required for strong squeezing in hot potassium vapor.

APPENDIX

Far-detuned FWM is treated here as an atomic system with two ground and two excited levels. The pump couples two transitions, $|1> \rightarrow |3>$ and $|2> \rightarrow |4>$, while the probe and conjugate couple $|2> \rightarrow |4>$ and $|4> \rightarrow |1>$, respectively. Transitions to $|3>$ are highly detuned, which justifies introducing another far detuned level $|4>$, with a similarly weak coupling strength from the levels $|1>$ and $|2>$.

The explicit form for the spontaneous emission in Eq. (3) is given by

$$\widehat{SE} = \begin{pmatrix} \Gamma_{1,3}\rho_{33} + \Gamma_{1,4}\rho_{44} & 0 & -\frac{\Gamma_{1,3}+\Gamma_{2,3}}{2}\rho_{13} & -\frac{\Gamma_{1,4}+\Gamma_{2,4}}{2}\rho_{14} \\ 0 & \Gamma_{2,3}\rho_{33} + \Gamma_{2,4}\rho_{44} & -\frac{\Gamma_{1,3}+\Gamma_{2,3}}{2}\rho_{23} & -\frac{\Gamma_{1,4}+\Gamma_{2,4}}{2}\rho_{24} \\ -\frac{\Gamma_{1,3}+\Gamma_{2,3}}{2}\rho_{31} & -\frac{\Gamma_{1,3}+\Gamma_{2,3}}{2}\rho_{32} & -\Gamma_{1,3}\rho_{33} + \Gamma_{2,3}\rho_{33} & -\frac{\Gamma_{1,3}+\Gamma_{2,3}+\Gamma_{1,4}+\Gamma_{2,4}}{2}\rho_{34} \\ -\frac{\Gamma_{1,4}+\Gamma_{2,4}}{2}\rho_{41} & -\frac{\Gamma_{1,4}+\Gamma_{2,4}}{2}\rho_{42} & -\frac{\Gamma_{1,3}+\Gamma_{2,3}+\Gamma_{1,4}+\Gamma_{2,4}}{2}\rho_{43} & -\Gamma_{1,4}\rho_{44} - \Gamma_{2,4}\rho_{44} \end{pmatrix}, \tag{A1}$$

and the relaxation term is

$$\hat{R} = -\gamma\left[\hat{\rho} - \text{diag}\left(\frac{1}{2}, \frac{1}{2}, 0, 0\right)\right] - \gamma_{\text{deph}}[\hat{\rho} - \text{diag}(\rho_{11}, \rho_{22}, \rho_{33}, \rho_{44})]. \tag{A2}$$

Optical Bloch equations are

$$\dot{\rho}_{11} = \gamma\left(\frac{1}{2} - \rho_{11}\right) + \Gamma_{1,3}\rho_{33} + \Gamma_{1,4}\rho_{44} + \frac{i}{\hbar}\left(E_d^{(+)*}d\rho_{31} - E_d^{(+)}d\rho_{13} + E_c^{(+)*}d\rho_{41} - E_c^{(+)}d\rho_{14}\right), \tag{A3a}$$

$$\dot{\rho}_{22} = \gamma\left(\frac{1}{2} - \rho_{22}\right) + \Gamma_{2,3}\rho_{33} + \Gamma_{2,4}\rho_{44} + \frac{i}{\hbar}\left(E_p^{(+)*}d\rho_{32} - E_p^{(+)}d\rho_{23} + E_d^{(+)*}d\rho_{42} - E_d^{(+)}d\rho_{24}\right), \tag{A3b}$$

$$\dot{\rho}_{33} = -\rho_{33}\gamma - \Gamma_3\rho_{33} + \frac{i}{\hbar}\left(E_d^{(+)}d\rho_{13} - E_d^{(+)*}d\rho_{31} + E_p^{(+)}d\rho_{23} - E_p^{(+)*}d\rho_{32}\right), \tag{A3c}$$

$$\dot{\rho}_{44} = -\rho_{44}\gamma - \Gamma_4\rho_{44} + \frac{i}{\hbar}\left(E_c^{(+)}d\rho_{14} - E_c^{(+)*}d\rho_{41} + E_d^{(+)}d\rho_{24} - E_d^{(+)*}d\rho_{42}\right), \tag{A3d}$$

$$\dot{\rho}_{12} = -(\gamma + \gamma_{\text{deph}} + i\Delta_{132})\rho_{12} + \frac{i}{\hbar}\left(E_d^{(+)*}d\rho_{32} - e^{iz\Delta k}E_d^{(+)}d\rho_{14} + e^{iz\Delta k}E_c^{(+)*}d\rho_{42} - E_p^{(+)}d\rho_{13}\right), \tag{A3e}$$

$$\dot{\rho}_{13} = -\left(\gamma + \gamma_{\text{deph}} + \frac{\Gamma_3}{2} + i\Delta_{13}\right)\rho_{13} + \frac{i}{\hbar}\left(E_d^{(+)*}d\rho_{33} - E_d^{(+)*}d\rho_{11} + E_c^{(+)*}d\rho_{43} - E_p^{(+)*}d\rho_{12}\right), \tag{A3f}$$

$$\dot{\rho}_{14} = -\left(\gamma + \gamma_{\text{deph}} + \frac{\Gamma_4}{2} + i\Delta_{1324}\right)\rho_{14} + \frac{i}{\hbar}\left(E_d^{(+)*}d\rho_{34} - e^{-iz\Delta k}E_d^{(+)*}d\rho_{12} + E_c^{(+)*}d\rho_{44} - E_c^{(+)*}d\rho_{11}\right), \tag{A3g}$$

$$\dot{\rho}_{23} = -\left(\gamma + \gamma_{\text{deph}} + \frac{\Gamma_3}{2} + i\Delta_{13}\right)\rho_{23} + \frac{i}{\hbar}\left(E_p^{(+)*}d\rho_{33} - E_d^{(+)*}d\rho_{21} + e^{-iz\Delta k}E_d^{(+)*}d\rho_{43} - E_c^{(+)*}d\rho_{22}\right), \tag{A3h}$$

$$\dot{\rho}_{24} = -\left(\gamma + \gamma_{\text{deph}} + \frac{\Gamma_4}{2} + i\Delta_{1324}\right)\rho_{24} + \frac{i}{\hbar}\left(E_d^{(+)*}d\rho_{44} - E_d^{(+)*}d\rho_{22} + e^{iz\Delta k}E_p^{(+)*}d\rho_{34} - e^{iz\Delta k}E_c^{(+)*}d\rho_{21}\right), \tag{A3i}$$

$$\dot{\rho}_{34} = -\left(\gamma + \gamma_{\text{deph}} + \frac{\Gamma_3}{2} + \frac{\Gamma_4}{2} + i\Delta_{1324} - i\Delta_{13}\right)\rho_{34} + \frac{i}{\hbar}\left(E_d^{(+)}d\rho_{14} - e^{-iz\Delta k}E_d^{(+)*}d\rho_{32} + e^{iz\Delta k}E_p^{(+)}d\rho_{24} - E_c^{(+)*}d\rho_{31}\right). \tag{A3j}$$

Here Δk is the phase mismatch defined as $\Delta k = 2k_d - k_p - k_c$, where k_d is the pump wave vector. $\Gamma_{i,j}$ is the decay rate from level j to level i, while $\Gamma_i = \Gamma_{i,1} + \Gamma_{i,2}$. $\gamma = 10^5$ Hz is spontaneous decay from the excited state, and $\gamma_{\text{deph}} = 0$ is the dephasing decay rate.

[1] L. M. Duan, M. D. Lukin, J. I. Cirac, and P. Zoller, Nature (London) **414**, 413 (2001).

[2] C. Shu, P. Chen, T. K. A. Chow, L. Zhu, Y. Xiao, M. Loy, and S. Du, Nat. Commun. **7**, 12783 (2016).

[3] R. C. Pooser, A. M. Marino, V. Boyer, K. M. Jones, and P. D. Lett, Phys. Rev. Lett. **103**, 010501 (2009).

[4] V. Boyer, C. F. McCormick, E. Arimondo, and P. D. Lett, Phys. Rev. Lett. **99**, 143601 (2007).

[5] J. Okuma, N. Hayashi, A. Fujisawa, and M. Mitsunaga, Opt. Lett. **34**, 1654 (2009).

[6] Y. Wu and X. Yang, Phys. Rev. A **70**, 053818 (2004).

[7] J. Wu, Y. Liu, D. S. Ding, Z. Y. Zhou, B.-S. Shi, and G.-C. Guo, Phys. Rev. A **87**, 013845 (2013).

[8] R. M. Camacho, P. K. Vudyasetu, and J. C. Howell, Nat. Photon. **3**, 103 (2009).

[9] A. Eilam, A. D. Wilson-Gordon, and H. Friedmann, Opt. Lett. **33**, 1605 (2008).

[10] D. S. Ding, Z. Y. Zhou, B. S. Shi, X. B. Zou, and G. C. Guo, Opt. Express **20**, 11433 (2012).

[11] A. Leszczyński, M. Parniak, and W. Wasilewski, Opt. Express **25**, 284 (2017).

[12] K. I. Harada, K. Mori, J. Okuma, N. Hayashi, and M. Mitsunaga, Phys. Rev. A **78**, 013809 (2008).

[13] K. I. Harada, T. Kanbashi, M. Mitsunaga, and K. Motomura, Phys. Rev. A **73**, 013807 (2006).

[14] C. F. McCormick, V. Boyer, E. Arimondo, and P. D. Lett, Opt. Lett. **32**, 178 (2007).

[15] M. T. Turnbull, P. G. Petrov, C. S. Embrey, A. M. Marino, and V. Boyer, Phys. Rev. A **88**, 033845 (2013).

[16] C. F. McCormick, A. M. Marino, V. Boyer, and P. D. Lett, Phys. Rev. A **78**, 043816 (2008).

[17] Q. Glorieux, L. Guidoni, S. Guibal, J. P. Likforman, and T. Coudreau, Phys. Rev. A **84**, 053826 (2011).

[18] M. Jasperse, L. D. Turner, and R. E. Scholten, Opt. Express **19**, 3765 (2011).

[19] M. Guo, H. Zhou, D. Wang, J. Gao, J. Zhang, and S. Zhu, Phys. Rev. A **89**, 033813 (2014).

[20] V. Boyer, A. M. Marino, R. C. Pooser, and P. D. Lett, Science **321**, 544 (2008).

[21] A. M. Marino, R. C. Pooser, V. Boyer, and P. D. Lett, Nature (London) **457**, 859 (2009).

[22] S. L. Braunstein and P. van Loock, Rev. Mod. Phys. **77**, 513 (2005).

[23] A. Gaeta, M. Gruneisen, and R. Boyd, IEEE J. Quantum Electron. **22**, 1095 (1986).

[24] M. D. Lukin, P. R. Hemmer, M. Loffler, and M. O. Scully, Phys. Rev. Lett. **81**, 2675 (1998).

[25] Q. Glorieux, R. Dubessy, S. Guibal, L. Guidoni, J. P. Likforman, T. Coudreau, and E. Arimondo, Phys. Rev. A **82**, 033819 (2010).

[26] G. S. Agarwal, Phys. Rev. A **34**, 4055 (1986).

[27] P. Kolchin, Phys. Rev. A **75**, 033814 (2007).

[28] B. Ai, D. S. Glassner, R. J. Knize, and J. P. Partanen, Appl. Phys. Lett. **64**, 951 (1994).

[29] R. C. Pooser, A. M. Marino, V. Boyer, K. M. Jones, and P. D. Lett, Opt. Express **17**, 16722 (2009).

[30] Z. Qin, J. Jing, J. Zhou, C. Liu, R. C. Pooser, Z. Zhou, and W. Zhang, Opt. Lett. **37**, 3141 (2012).

[31] G. Adenier, D. Calonico, S. Micalizio, N. Samantaray, I. Degiovanni, and I. R. Berchera, Int. J. Quantum Inform. **14**, 1640014 (2016).

[32] W. V. Davis, M. Kauranen, E. M. Nagasako, R. J. Gehr, A. L. Gaeta, R. W. Boyd, and G. S. Agarwal, Phys. Rev. A **51**, 4152 (1995).

[33] B. Zlatković, A. J. Krmpot, N. Šibalić, M. Radonjić, and B. M. Jelenković, Laser Phys. Lett. **13**, 015205 (2016).

[34] J. A. Kleinfeld and A. D. Streater, Phys. Rev. A **53**, 1839 (1996).

[35] D. S. Glassner and R. J. Knize, Appl. Phys. Lett. **66**, 1593 (1995).

[36] M. Katharakis, N. Merlemis, A. Serafetinides, and T. Efthimiopoulos, J. Phys. B **35**, 4969 (2002).

[37] M. Y. Lanzerotti, R. W. Schirmer, and A. L. Gaeta, Appl. Phys. Lett. **69**, 1199 (1996).

[38] J. D. Swaim and R. T. Glasser, Phys. Rev. A **96**, 033818 (2017).

[39] D. A. Steck, Quantum and Atom Optics, http://steck.us/teaching (revision 0.12.0, 16 May 2017).

[40] D. McKay, Potassium $5p$ line data, http://fermionlattice.wdfiles.com/local--files/papers/5P_structure, 2009.

Slowing 80-ns light pulses by four-wave mixing in potassium vapor

D. Arsenović, M. M. Ćurčić,[*] T. Khalifa, B. Zlatković, Ž. Nikitović, I. S. Radojičić, A. J. Krmpot, and B. M. Jelenković

Institute of Physics Belgrade, University of Belgrade, Pregrevica 118, 11080 Belgrade, Serbia

We experimentally and theoretically study propagation of 80-ns Gaussian-like probe pulses in hot potassium vapor under conditions of four-wave mixing (FWM). The atomic scheme for FWM is off-resonant, double-Λ atomic scheme, with pump and probe photons, mediated in the K vapor, generating new probe and conjugate photons. We define the subset of FWM parameters, one-photon pump detuning, two-photon pump-probe Raman detuning, vapor density, the pump Rabi frequencies, when slowed pulses exit the vapor are also Gaussian-like. When Gaussian-like pulses exit the cell we are able to compare theoretical and experimental results for fractional delays and broadening for the probe and conjugate. We have obtained fractional delays above 1. Results of the model are compared with the experiment, with and without the model of Doppler averaging, when the atom velocity distribution is divided into different number of groups. We analyze possible causes for pulse broadening and distortion of slowed probe pulses and show that they are the result of quite different behavior of the probe pulse in the FWM vapor. Besides presenting the first results of slowing 80-ns probe pulses, this work is a useful test of the numerical model and values of parameters taken in the model that are not known in experiments.

I. INTRODUCTION

Slow light, or reduced pulse group velocity below the speed of light, was demonstrated in different systems [1–10]. There is a strong interest for slow light because of its applications [11], in particular for all-optical signal processing. Optimizations of different slow light systems are based on results for fractional delays and broadenings of initial pulse waveforms.

There are different protocols and different physical systems for generating slow light and ultimately storage of light. A quantum phenomenon that is widely used for slow light is electromagnetically induced transparency (EIT) [12–15]. Narrow EIT resonance is accompanied by steep dispersion, effectively slowing down wave packets propagating through the medium. EIT for slowing and storing light was applied in many physical systems, very often in alkali-metal vapors [16–18].

Four-wave mixing (FWM), characterized by both quantum and strong nonlinear processes, has been used in the last decade for light slowing [19,20] and storage [21–23]. In a typical FWM scheme, in alkali vapor, pump photons and probe photons couple two sublevels of ground states to the same excited state. The second pump photon simultaneously excites the atom, allowing nonlinear conversion of pump photons into probe and conjugate photons. The process is therefore dominated by a strong photon-photon coupling medicated by the nonlinear medium, and photon conversion. Transmission and gain of twin beams strongly depend on detuning around two-photon Raman resonance. Also, the index of refraction varies strongly around the resonance. The FWM gain compensates optical losses, which is an advantage over the EIT as

a physical system, allowing much longer propagation of probe pulses.

In this work we use the off-resonant double-Λ scheme for FWM in K vapor to theoretically and experimentally investigate propagation of 80-ns probe pulses and generation and propagation of conjugate pulses. This atomic scheme was used before to investigate slow light in Rb [19] and Na [20]. However, there is a growing interest in the behavior of transitions on D lines in potassium vapor [24,25], as well as interest in potassium as an active medium for a study of strong nonlinear processes due to its characteristics [26–30]. Parameters of FWM in [26] simultaneously support two propagation regimes of light pulses, slow and fast light. In our work, we are focused on the FWM regime when this system acts as a slowing and amplifying medium, with obtained fractional delays typically larger than 1. In the model we use Maxwell-Bloch (MB) equations to calculate propagations of pump, probe, and conjugate beams through the K cell. FWM parameters in the study are one-photon detunings of the pump beam Δ, two-photon Raman detaining between pump and probe beams δ, pump and probe Rabi frequencies Ω_d and Ω_p, respectively, pump laser power P_d, and potassium vapor density N_c related to cell temperature T_c. Fixed for all measurements and calculations were phase-matching angle and probe Rabi frequency Ω_p related to the probe power P_p.

Potassium is different from other alkali metals. It has the smallest hyperfine splitting (HFS) of the ground state of all alkali metals [24], smaller than the Doppler width. Comparing theoretical and experimental results, qualitatively in terms of pulse waveforms and quantitatively in terms of fractional delays and broadening, we have tested the model and also values of dephasing and decoherence relaxation rates assumed in the calculations. We have discussed results of
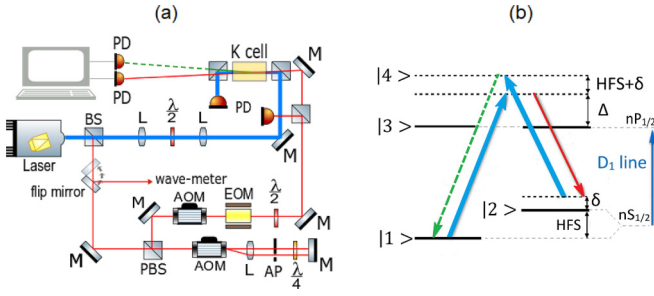
---

*marijac@ipb.ac.rs

023829-1

FIG. 1. (a) Experimental setup. (a) Double-Λ scheme for D_1 line in potassium. Pump beam–thick line (blue for online version), probe beam–thin line (red for online version), conjugate beam–dashed line (green for online version).

the model with and without Doppler averaging of density matrix elements. At the end, we have investigated whether there is a relation between the waveform of the outbound slowed probe pulse, which is either broadened Gaussian-like or distorted, and the pulse behavior as it propagates through the K vapor.

II. EXPERIMENT

The schematic of the experiment is shown in Fig. 1. The output from the CW laser (MBR, Coherent) locked to $4S_{1/2}$-$4P_{1/2}$ D_1 transition in K, at 776 nm, is used for both the pump and the probe beams. A smaller fraction of the probe is sent through two acousto-optic modulators, with the first one in double pass, in order to scan the frequency of the probe beam around Raman resonance with the pump beam frequency. We use the electro-optic modulator to form Gaussian probe pulses. The probe is combined with the pump on the nonpolarizing cube, and both beams are sent to a 4-cm-long vacuum glass cell containing the natural abundance of K vapor. The beams intersect at the center of the cell at the angle of 3 mrad. The pump and the probe beams are linearly and mutually orthogonally polarized with Gaussian radial intensity distribution $1/e^2$ at 1.08 and 0.8 mm, respectively. The K cell was heated by hot air up to 150 °C, or a K density of 1.7×10^{13} cm^{-3}. The probe and the conjugate beams are detected with two photodiodes, and their signals are sent to the storage oscilloscope. Group velocities of the probe and conjugate beams were measured by recording the arrival times of the probe and the conjugate relative to the reference pulse.

The double-Λ scheme was realized on the D_1 line of ^{39}K ($\lambda = 770$ nm [24]), Fig. 1. The pump beam couples the lower hyperfine ground level $4S_{1/2}$, $F = 1$ to the excited $4P_{1/2}$ level with one-photon detuning Δ. Due to the small hyperfine splitting of 55 MHz [24], the hyperfine structure of the $4P_{1/2}$ level is omitted. The probe beam couples the excited $4P_{1/2}$ level to the upper hyperfine ground level $4S_{1/2}$, $F = 2$ and makes a lower Λ scheme with the two-photon Raman detuning δ. Pump photons and new conjugate photons couple $4S_{1/2}$, $F = 2$ to the $4S_{1/2}$, $F = 1$ via an excited state, detuned from the $4P_{1/2}$ levels by $\sim(\Delta + \text{HFS})$, in the upper Λ scheme.

III. THEORETICAL MODEL

Our model describes interaction between ^{39}K atoms in the vapor and electromagnetic (EM) field. The same as in the experiment, four levels of the double-Λ scheme, two ground states $|1\rangle$ and $|2\rangle$, and two excited states $|3\rangle$ and $|4\rangle$, are coupled to produce FWM, Fig. 1. Three components of the total electric field, pump, probe, and conjugate, are denoted by d, p, and c, respectively. The pump couples the $|1\rangle \rightarrow |3\rangle$ and $|2\rangle \rightarrow |4\rangle$ transitions and the probe couples the $|2\rangle \rightarrow |3\rangle$ transition. In the medium, the conjugate beam is generated from optical coherence between levels $|1\rangle$ and $|4\rangle$. Let the energy levels be $E_i = \hbar\omega_i$ with $\omega_3 = \omega_4$, and the angular frequencies of the EM field modes ω_d, ω_p, and ω_c for the pump, probe, and conjugate, respectively. The one-photon detuning is then $\Delta_{(13)} = \omega_d - (\omega_3 - \omega_1)$, and two-photon detuning is $\delta_{(132)} = \omega_d - \omega_p - (\omega_2 - \omega_1)$. Detuning of the conjugate beam is defined as $\Delta_{(1324)} = (2\omega_d - \omega_p) - (\omega_4 - \omega_1)$.

The total electric field

$$\vec{E} = \sum_{i=d,p,c} \vec{e}_i E_i^{(+)} e^{-i\omega_i t + i\vec{k}_i \vec{r}} + \text{c.c.} \tag{1}$$

serves as an interacting potential for ^{39}K atoms. The Hamiltonian is therefore

$$\hat{H} = \hat{H}_0 + \hat{H}_{\text{int}} = \sum_{i=1}^{4} \hbar\omega_i |i\rangle\langle i| - \hat{\vec{d}} \cdot \vec{E}(\vec{r}, t), \tag{2}$$

where $\hat{\vec{d}}$ is the atomic dipole operator.

To obtain the set of Bloch equations, we first start with the equation for the density matrix

$$\dot{\varrho} = -\frac{i}{\hbar}[\hat{H}, \hat{\varrho}] + \widehat{SE} + \hat{R}, \tag{3}$$

with spontaneous emission $\widehat{SE}$ and relaxation $\hat{R}$ included. We have

$$\widehat{SE} = \sum_{i=1}^{4} \Gamma_i(\hat{A}_i\hat{\varrho}\hat{A}_i^\dagger - \hat{A}_i^\dagger\hat{A}_i\hat{\varrho}/2 - \hat{\varrho}\hat{A}_i^\dagger\hat{A}_i/2), \tag{4}$$

with $\hat{A}_1 = |1\rangle\langle 3|$, $\hat{A}_2 = |1\rangle\langle 4|$, $\hat{A}_3 = |2\rangle\langle 3|$, $\hat{A}_4 = |2\rangle\langle 4|$, and Γ_i all equal to half of the spontaneous emission rate. The relaxation term is

$$\hat{R} = -\gamma\left[\hat{\varrho} - \text{diag}\left(\tfrac{1}{2}, \tfrac{1}{2}, 0, 0\right)\right] \\ - \gamma_{\text{deph}}[\hat{\varrho} - \text{diag}(\varrho_{11}, \varrho_{22}, \varrho_{33}, \varrho_{44})], \tag{5}$$

where γ and γ_{deph} are relaxation rates. After the substitution,

$$\tilde{\varrho}_{ij} = e^{-i\omega_{(ij)}t + i\vec{k}_{(ij)}\vec{r}}\varrho_{ij}, \tag{6}$$

where $\omega_{(13)} = \omega_{(24)} = \omega_d$, $\omega_{(23)} = \omega_p$, $\omega_{(14)} = \omega_c$, $\omega_{(12)} = \omega_{(13)} - \omega_{(23)}$, $\omega_{(34)} = \omega_{(14)} - \omega_{(13)}$, $\omega_{(ij)} = -\omega_{(ji)}$, $\vec{k}_{(13)} = \vec{k}_{(24)} = \vec{k}_d$, $\vec{k}_{(23)} = \vec{k}_p$, $\vec{k}_{(14)} = \vec{k}_c$, $\vec{k}_{(12)} = \vec{k}_{(13)} - \vec{k}_{(23)}$, $\vec{k}_{(34)} = \vec{k}_{(14)} - \vec{k}_{(13)}$, $\vec{k}_{(ij)} = -\vec{k}_{(ji)}$, with $\vec{k}_c = 2\vec{k}_d - \vec{k}_p - \Delta\vec{k}$, we apply the rotating wave approximation. The resulting system of differential equations does not have coefficients depending on time. Some coefficients have dependence on $e^{i\Delta kz}$, where $\Delta k = 2k_d(1 - \cos\theta)$, i.e., it is related to the angle θ between the pump and probe beam. Here we set the propagation of the pump in the z direction.
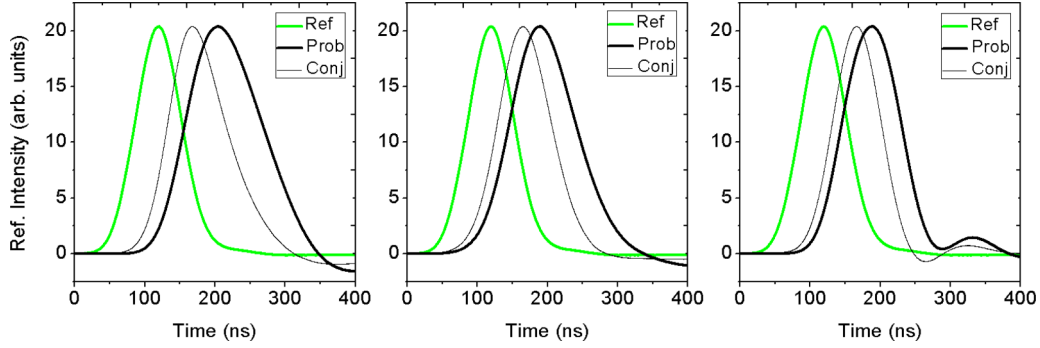
FIG. 2. Experimental observations of slow light, probe (thick black), conjugate (thin black), and reference 80-ns incoming probe beam (green) waveforms for (a) $\delta = -4$ MHz, (b) $\delta = -8$ MHz, and (c) $\delta = -12$ MHz. In all three cases (a), (b), and (c), $\Delta = 0.7$ GHz, $T = 120\,^\circ$C, pump power $P_d = 220$ mW, probe power $P_p = 20\,\mu$W.

With a slowly varying envelope approximation, the propagation equations are

$$\left(\frac{\partial}{\partial z} + \frac{1}{c}\frac{\partial}{\partial t}\right)E_d^{(+)} = i\frac{kN_c}{2\varepsilon_0}d(\tilde{\rho}_{42} + \tilde{\rho}_{31}), \quad (7a)$$

$$\left(\frac{\partial}{\partial z} + \frac{1}{c}\frac{\partial}{\partial t}\right)E_p^{(+)} = i\frac{kN_c}{2\varepsilon_0}d\tilde{\rho}_{32}, \quad (7b)$$

$$\left(\frac{\partial}{\partial z} + \frac{1}{c}\frac{\partial}{\partial t}\right)E_c^{(+)} = i\frac{kN_c}{2\varepsilon_0}d\tilde{\rho}_{41}, \quad (7c)$$

where N_c is the atom density.

In order to take into account the Doppler effect, we divide atoms into M groups, each having different z component of the velocity v_z. Due to the Doppler effect these groups differ by effective detuning. Let us denote with $\Delta_{(13)0}$, $\delta_{(132)0}$, and $\Delta_{(1324)0}$ detunings subject to atoms with velocity $v_z = 0$. For an atom with z component of the velocity v_z different than zero, the observed angular frequency ω_o is $\omega_o = \sqrt{\frac{1-\beta}{1+\beta}}\omega_s$, where ω_s is the angular frequency of the light source and $\beta = v_z/c$. The Doppler shift is $\Delta_D = \omega_o - \omega_s$. The detunings are therefore $\Delta_{(13),m} = \Delta_{(13)0} + \Delta_D$, $\delta_{(132),m} = \delta_{(132)0}$, $\Delta_{(1324),m} = \Delta_{(1324)0} + \Delta_D$, where $m = 1, \ldots, M$ enumerates velocity groups of atoms. In our model, we keep track of density matrices $\varrho_{ij,m}, m = 1, \ldots, M$ for each group of atoms. There are M sets of Bloch equations. Propagation equations are slightly modified. The source term on the right-hand side of Eq. (8) is the sum of contributions of all groups of atoms:

$$\left(\frac{\partial}{\partial z} + \frac{1}{c}\frac{\partial}{\partial t}\right)E_d^{(+)} = \sum_{m=1}^{M} i\frac{kN_{c,m}}{2\varepsilon_0}d(\varrho_{42,m} + \varrho_{31,m}), \quad (8a)$$

$$\left(\frac{\partial}{\partial z} + \frac{1}{c}\frac{\partial}{\partial t}\right)E_p^{(+)} = \sum_{m=1}^{M} i\frac{kN_{c,m}}{2\varepsilon_0}d\varrho_{32,m}, \quad (8b)$$

$$\left(\frac{\partial}{\partial z} + \frac{1}{c}\frac{\partial}{\partial t}\right)E_c^{(+)} = \sum_{m=1}^{M} i\frac{kN_{c,m}}{2\varepsilon_0}d\varrho_{41,m}. \quad (8c)$$

Here $N_{c,m}$ is the atom density of the kth group. We choose $v_{z,m}$ and $N_{c,m}$ to mimic Maxwell distribution $f(v_z) =$ $\sqrt{m/2\pi k_B T}e^{\frac{-mv_z^2}{2k_B T}}$. In the results below, with the Doppler averaging, we have chosen $M = 3$ with Doppler shifts $\Delta_1 = -0.25$ GHz, $\Delta_2 = 0$ GHz, and $\Delta_3 = +0.25$ GHz; the densities are $N_{c,2} = (1.1/3)N_c$ and $N_{c,1} = N_{c,3} = (0.95/3)N_c$.

IV. RESULTS AND DISCUSSION

The probe pulse waveform before the cell is Gaussian with a FWHM of 80 ns; behind the cell the amplified probe and conjugate pulses have different forms. For some FWM parameters they are (broadened) Gaussians, while for others they are distorted. Only when outgoing pulses are Gaussians can we get fractional delays and broadenings. We first present the experimental results, which are compared with the results of numerical simulations, with and without Doppler averaging.

A. Experimental results

We observe propagation of 80-ns probe pulses under conditions of FWM when several parameters are varied. In order to have Gaussian shapes for outgoing probe and conjugate pulses in K vapor, the FWM ought to be realized for densities between 3×10^{12} cm^{-3} and $\sim1.75\times10^{13}$ cm^{-3} (cell temperature 120 °C–150 °C), Δ between 700 MHz and 1.3 GHz, and δ in the range ±10 MHz. Note that not every, or any arbitrary choice of parameter values from the above ranges will produce Gaussian-like pulses at the cell exit. In Fig. 2 we present pulses of reference, probe, and conjugate beams, with their amplitudes normalized to the reference pulse, when $\Delta = 0.7$ GHz for three values of δ, -4, -8, and -12 MHz. The resonant probe scatters much more than the conjugate beam, and is slowed more and amplified less than the conjugate, as shown in Fig. 3. The results presented in Fig. 3 are gains, fractional delays, and broadening versus δ obtained from waveforms of Gaussian-like outbound pulses, like the ones shown in Fig. 2. Gains of twin beams are calculated as the ratio of their outbound intensities to the probe inbound intensity. The maximum of probe gain, around 100, is at negative δ, ~ -4 MHz, a small shift from Raman resonance due to Stark shift of energy levels, induced by the blue detuned pump laser. Delays and broadening also have small maximums at these negative values of δ. Maximum values for probe and
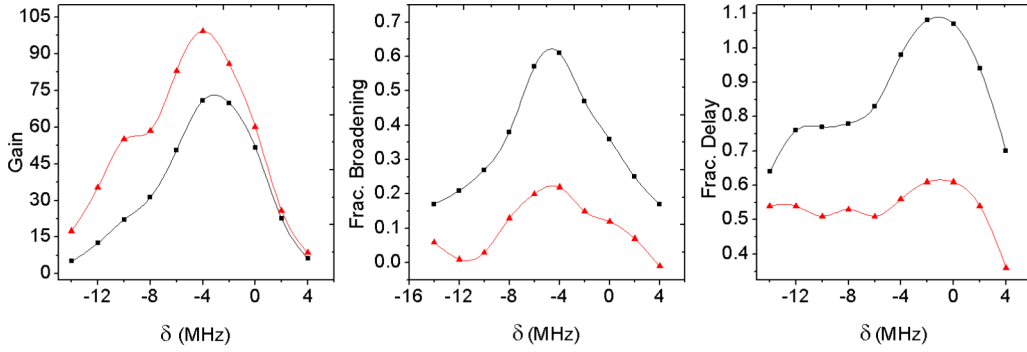
FIG. 3. Probe (solid squares, black for online version) and conjugate (solid triangles, red for online version) (a) gains, (b) fractional broadenings, and (c) fractional delays vs δ, for $\Delta = 0.7$ GHz, $T = 120\,°C$, $P_d = 220$ mW, $P_p = 20\,\mu$W.

conjugate fractional delays are $\sim$1.08 and $\sim$0.6, while their fractional broadenings are 0.35 and 0.15, respectively.

B. Theoretical results

In the model, the probe entering the cell has a Gaussian profile with 80-ns pulse width and the pump has a constant intensity. The pump and probe detunings, and the gas density correspond to their values in the experiment. However, the model uses parameters whose values are not known in the measurements, such as relaxation coefficients. In the calculations the pump is a plane wave, and although the angle between the pump and the probe is the same as in the experiment, there is a different overlap of two beams in the model than in the experiment. Hence, to find the pump and the probe electric field amplitudes adequate to those in the experiment is not straightforward. We obtain better agreement with measurements if electric field amplitudes in the model are a little lower than those implied by the measurements. The presented results are with Doppler averaging of density matrix elements, assuming three velocity groups for atoms, resulting in three Doppler shifts $\Delta_1 = -0.25$ GHz, $\Delta_2 = 0$ GHz, $\Delta_3 = +0.25$ GHz.

Propagation of EM fields through FWM alkali vapors, when all fields are continuous waves, was discussed in [31]. When probe field is in the form of a pulse, the initial condition for

the MB equations is

$$E_p^{(+)} = E_{p0}^{(+)}\left(f_{\text{dc}} + f_{\text{pulse}}e^{\frac{-4\ln 2(t-t_{\text{max}})^2}{FWHM^2}}\right), \tag{9}$$

where FWHM is the pulse full width at half maximum, t_{max} is the time when the pulse reaches peak value, and $f_{\text{dc}} + f_{\text{pulse}} = 1$ and represents dc and pulse components. To improve the stability of numerical simulation, we first solve a stationary system where we set $t = 0$ in Eq. (9) and obtain dependencies of z for all unknown variables. These solutions are initial conditions for $t = 0$ in the time propagation of MB equations. Variable parameters in the numerical simulations are the pump and the probe intensities, atom density, θ, Δ, δ, propagation distance z_{max}, and relaxation coefficients. As a result, we have obtained dependencies of the probe and the conjugate beam pulses on t and z. We have found, like in the experiment, that pulse shapes may be Gaussian-like or deformed by a strong asymmetric broadening or presence of multiple peaks.

Similar to the experiment, FWM parameters giving Gaussian-like outgoing pulses in the calculations are limited to a rather small range. Both measurements and the model show more deviations from Gaussian profiles when atom densities are higher or when the gains are lower. In Fig. 4 we present calculated waveforms of the probe and the conjugate pulses at $z_{\text{max}} = 4$ cm.

If outgoing pulses have Gaussian waveforms, we can extract gains and delays of probe and conjugate pulses by fitting the
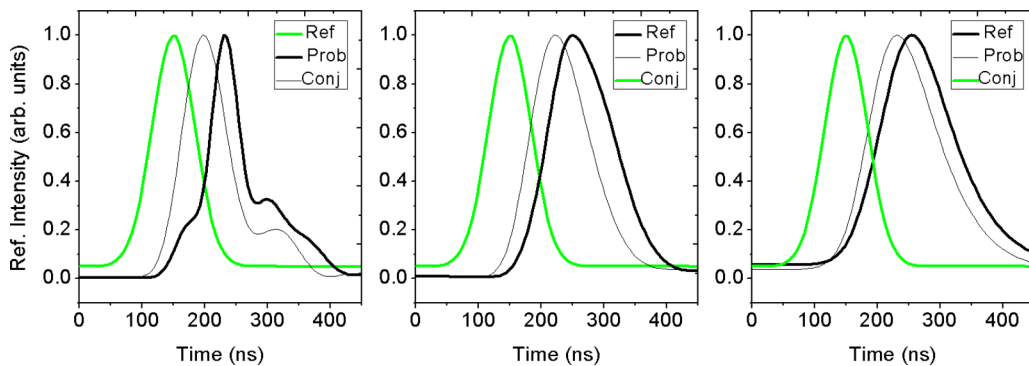
FIG. 4. Calculated waveforms of probe (thick black line) and conjugate (thin black line) for 80-ns incoming probe pulse (green line). (a) $\delta = -4$ MHz, (b) $\delta = -8$ MHz, (c) $\delta = -12$ MHz. Values of other parameters were kept constant, $\Omega_d = 1.38$ GHz, $\Omega_p = 18.9$ MHz, $\gamma = 0.5\times10^7$ Hz, $\gamma_{\text{deph}} = 1.5\times10^7$ Hz, $\Delta = 0.7$ MHz, $N_c = 3\times10^{12}$ cm^{-3} ($T = 120\,°C$), $\theta = 3$ mrad.

FIG. 5. Calculated probe (solid squares, black for online version) and conjugate (solid triangles, red for online version) (a) gains (note that probe gain is multiplied by 10), (b) fractional broadenings, and (c) fractional delays vs δ of 80-ns input Gaussian pulses in K vapor at 3×10^{12} cm^{-3} ($T = 120\,°$C), $\Omega_d = 1.38$ GHz, $\Omega_p = 18.9$ MHz, $\Delta = 0.7$ GHz.

time dependence of both fields to Gaussian profiles. The fit gives three values, $E_i^{(+)\text{out}}$, $t_{i,\text{max}_\text{out}}$, and $FWHM_{i,\text{out}}$, $i = p, c$, for gains, delays, and broadening, respectively. Gains of the probe and the conjugate beams are defined as

$$G_p = \left| \frac{E_p^{(+)\text{out}}}{E_{p0}^{(+)}} \right|^2, \tag{10a}$$

$$G_c = \left| \frac{E_c^{(+)\text{out}}}{E_{p0}^{(+)}} \right|^2. \tag{10b}$$

In Fig. 5 we plot gains, fractional delays, and broadening versus δ for $\Delta = 0.7$ GHz and $N_c = 3 \times 10^{12}$ cm^{-3}. Gain of the conjugate beam in Fig. 5 is larger than that of the probe, but that is not the general property. At the beginning of the propagation, at $z = 0$, there is only a probe beam, $G_p = 1$ and $G_c = 0$, while at $z = z_{\text{max}}$ we have $G_c > G_p$. Therefore G_p/G_c is directly dependent on z, for other parameters fixed. The values of δ for which gains are maximal depends on the pump intensity, a property known already from the CW regime [31]. Gains have maximums at the negative δ, determined by the detuning Δ and the pump Rabi frequency Ω_d.

In the study of slowing light, we are looking for the range of values of δ where the broadening is low and fractional delay is as high as possible. Similar to the experimental results, this turns out to be the case for $\delta \sim -4$ MHz.

Relaxation coefficients are fitting parameters in the model. For $\gamma = 0.5 \times 10^7$ and $\gamma_{\text{deph}} = 1.5 \times 10^7$, we get good agreement with the experiment.

1. Effect of Doppler averaging with different numbers of atom velocity groups

Including the Doppler effect into the model has, for most of the FWM parameters, a strong effect on probe and conjugate waveforms in and behind the vapor. Since Doppler averaging of the density matrix elements can considerably increase computing time, it is also good to know what might be the optimal number of atom velocity groups onto which the velocity distribution is divided. In Fig. 6 we plot the results of the model without taking into account the Doppler effect, top graph (a), with Doppler averaging with three velocity groups, middle graph (b), and with the Doppler averaging using five velocity groups, lower graph (c). Results are for the following parameters: $\Delta = 0.7$ GHz and $\delta = -12$ MHz. Values of other parameters in simulations are: $\Omega_d = 3.08$ GHz, $\Omega_p = 18.9$ MHz, $N = 3 \times 10^{12}$ cm^{-3}, $\gamma = 5 \times 10^7$, $\gamma_{\text{deph}} = 1.5 \times 10^7$. Having no Doppler averaging gives very much different results than obtained in the experiment. Averaging with three velocity groups gives a more compact profile at the end of the propagating distance. It is broadened with the small secondary peaks, features that measurements have also showed. In the presented case, a further increase of the number of velocity groups does not make a big difference in

FIG. 6. Numerical simulations of probe (thick black) and conjugate (thin red) waveforms. a) without Doppler averaging, b) with Doppler averaging using 3 velocity groups, and c) using 5 velocity groups. Results are for 80 ns probe inbound pulse, $\Delta = 1$ GHz, and $\delta = 4$ MHz. Other parameters for simulations: $\Omega_d = 2.31$ GHz, $\Omega_p = 18.9$ Mhz, $N_c = 3 \times 10^{12}$ cm^{-3}, $\gamma = 5 \times 10^7$ Hz, $\gamma_{\text{deph}} = 1.5 \times 10^7$ Hz.
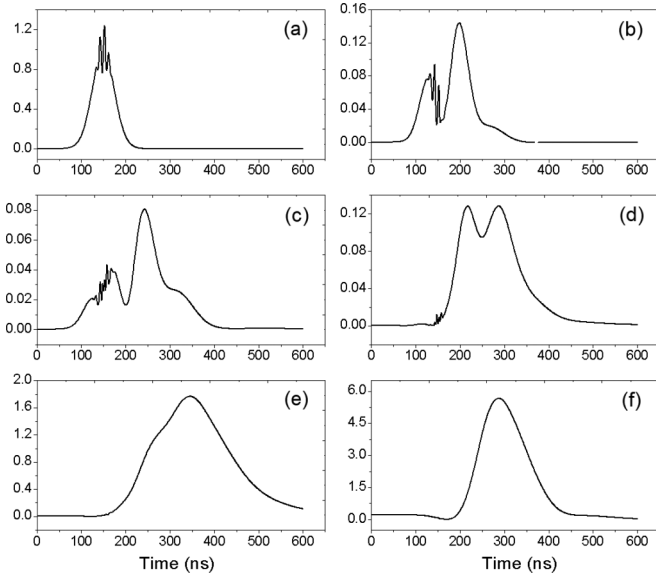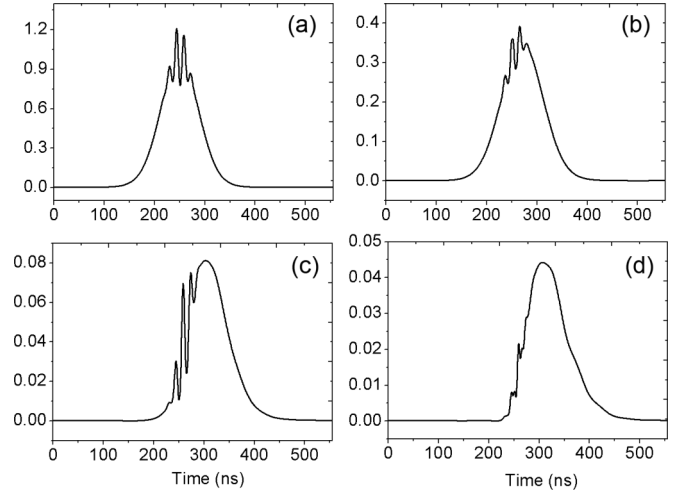
FIG. 7. Dynamics of 80-ns probe pulse propagation through K vapor cell of 4 cm, example of pulse destruction and revival. (a)–(f) Pulse waveforms at 0, 8, 16, 24, 52, and 100% of the total cell length, respectively. Small perturbations at the top of the probe pulse are followed in several figures representing pulse waveform at a later time (distance). Parameters for the simulations: $\Delta = 0.7$ GHz, $\delta = -2$ MHz, $\Omega_d = 3.08$ GHz, $\Omega_p = 18.9$ MHz, $N_c = 3 \times 10^{12}$ cm^{-3}, $\gamma = 0.5 \times 10^7$ Hz, $\gamma_{\text{deph}} = 1.5 \times 10^7$ Hz.

FIG. 8. Dynamics of 80-ns probe pulse propagation through K vapor cell of 4 cm, example of pulse broadening. (a)–(d) Pulse waveforms at different percentages of cell length, 0%, 20%, 60%, 100%, respectively. $\Omega_d = 1.72$ GHz, $N_c = 1 \times 10^{12}$ cm^{-3} ($T = 110\,^{\circ}$C), $\Delta = 0.7$ GHz, and $\delta = 0$ MHz. γ and γ_{deph} are the same as in Fig. 7.

the obtained pulse's waveforms. This is not always the case. For higher pump Rabi frequencies and higher gas temperatures, calculations with five groups of atoms give better agreement with the experiment compared to the ones with three velocity groups. Also, for larger δ, when stronger multiple peaks are observed in the pulse profile, averaging with five velocity groups is a better option. However, one has to be careful with the choice of velocity values.

2. Probe pulse behavior in the hot potassium vapor—Two case studies

Whether the outbound pulse waveform is broadened Gaussian-like or distorted with multiple pulses depends on the pulse behavior from the time it enters the vapor to the time when it exits from the vapor. We have studied probe pulse propagation, while the pulses are at different distances from the (cell) vapor entrance, for two sets of FWM parameters. Both sets of parameters give Gaussian-like outbound pulses, but as we will see below, these pulses exit the vapor after different behaviors while in the vapor. To ease comparison of different and sometimes complex behavioral studies of pulses in the K vapor, we numerically followed propagation of the marker, placed on the top of the probe input pulse, in respect to propagation of the pulse itself. This wavelet is so small that it does not generate an additional effect on the behavior of the pulse, its delay, or broadening. By following the location of the marker versus the pulse peak, we show that the Gaussian pulse at the output may not be directly connected to the input pulse by a time evolution. Instead, another pulses, behind the initial, start to appear, and with enough gain at the end of the

propagation distance, they dominate over the initial pulse. An example is given in Fig. 7 for the following parameters: $\Delta = 0.7$ GHz, $\delta = -2$ MHz, $\Omega_d = 3.08$ GHz, $\Omega_p = 18.9$ MHz, $N_c = 3 \times 10^{12}$ cm^{-3}, $\gamma = 0.5 \times 10^7$, $\gamma_{\text{deph}} = 1.5 \times 10^7$. It is clear from the location of the marker that the pulse entering the cell disappears at about $z = 0.6 \times z_{\text{max}}$ (2.5 cm from the entrance). The choice of parameters for results in Fig. 7 give a broadened and slightly distorted outbound pulse, and we see that the secondary pulses, in the high-gain regime, are responsible for the slowed light pulse and broadening.

In Fig. 8 we give an example of pulse propagation when the initial pulse is preserved, i.e., the same pulse travels from the entrance to the exit of the medium. It is only slowed and broadened, and as seen from the graphs in Fig. 8, the marker is slipping behind the pulse peak as it slowed more than the probe pulse. Observed pulse broadening is the result of the pulse front traveling faster that the back of the pulse.

The different behavior of pulses in Figs. 7 and 8 is at different gas density and pump power. This type of simulation shows that for some parameters, there will be only the primary pulse, while for others, secondary pulses may appear, in the vapor and at the exit. The additional pulses may be small, or dominate, or can completely replace the initial pulse, depending on the length of the vapor cell. For ranges of FWM parameters both theory and measurement give complex waveforms of outbound pulses, which theory describes as the result of a generation of new pulses. The secondary pulse is more delayed and less broadened than the primary, and thus offers new possibilities for slow light applications.

V. CONCLUSION

Gains, frictional delays, and broadening of probe and conjugate pulses after 80-ns probe pulses traverses the 4-cm K vapor cell have been measured and calculated when FWM is generated by the double-Λ scheme. Of the broad range of FWM parameters good for parametric gains in the

medium, only the small subrange is good for slowing Gaussian pulses. Both the experiment and the model have shown that an outbound pulse is a nondistorted Gaussian only when every FWM parameter is in a specific, small subrange: 0.7 GHz $< \Delta < 1.3$ GHz, -16 MHz $< \delta < 4$ MHz, 3×10^{12} cm^{-3} $< N_c < 9.96 \times 10^{12}$ cm^{-3}. Both model and experiment have shown that maximum fractional delays are at the maximum of pulse broadening, and typically at two-photon detuning when gains of the probe and conjugate have the highest values. The maximal fractional delays are 1 in the experiment and 1.4 in the model.

We have shown that without Doppler averaging the model fails to reproduce correct pulse profiles. For more complex waveforms, Doppler averaging over a larger number of atom velocity groups, a minimum of 5, might be needed. Following the time (and distance) propagation of the small wavelet, placed at the top of the probe pulse at the cell entrance, in respect to the propagation of the probe pulse itself, we have shown that, depending on the FWM parameters, the outbound Gaussian-like pulse is the result of quite different pulse propagation dynamics in the vapor. In some cases the initial pulse will disappear and new one can be formed, and for a sufficient gain or length of the vapor, a newly generated pulse will dominate the waveform of the outbound pulse.

ACKNOWLEDGMENTS

[1] M. M. Kash, V. A. Sautenkov, A. S. Zibrov, L. Hollberg, G. R. Welch, M. D. Lukin, Y. Rostovtsev, E. S. Fry, and M. O. Scully, Phys. Rev. Lett. **82**, 5229 (1999).

[2] R. M. Camacho, M. V. Pack, and J. C. Howell, Phys. Rev. A **73**, 063812 (2006)

[3] R. M. Camacho, M. V. Pack, J. C. Howell, A. Schweinsberg, and R. W. Boyd, Phys. Rev. Lett. **98**, 153601 (2007).

[4] J. E. Sharping, Y. Okawachi, and A. L. Gaeta, Opt. Express **13**, 6092 (2005).

[5] Y. Okawachi, M. S. Bigelow, J. E. Sharping, Z. Zhu, A. Schweinsberg, D. J. Gauthier, R. W. Boyd, and A. L. Gaeta, Phys. Rev. Lett. **94**, 153902 (2005).

[6] A. V. Turukhin, V. S. Sudarshanam, M. S. Shahriar, J. A. Musser, B. S. Ham, and P. R. Hemmer, Phys. Rev. Lett. **88**, 023602 (2001).

[7] E. Baldit, K. Bencheikh, P. Monnier, J. A. Levenson, and V. Rouget, Phys. Rev. Lett. **95**, 143601 (2005).

[8] P.-C. Ku, F. Sedgwick, C. J. Chang-Hasnain, P. Palinginis, T. Li, H. Wang, S.-W. Chang, and S.-L. Chuang, Opt. Lett. **29**, 2291 (2004).

[9] H. Su and S. L. Chuang, Opt. Lett. **31**, 271 (2006).

[10] M. S. Bigelow, N. N. Lepeshkin, and R. W. Boyd, Phys. Rev. Lett. **90**, 113903 (2003).

[11] J. B. Khurgin and R. S. Tucker, *Slow Light Science and Applications* (CRC Press, Boca Raton, FL, 2009).

[12] A. Kasapi, M. Jain, G. Y. Yin, and S. E. Harris, Phys. Rev. Lett. **74**, 2447 (1995).

[13] L. V. Hau, S. E. Harris, Z. Dutton, and C. H. Behroozi, Nature (London) **397**, 594 (1999).

[14] J. Zhang, G. Hernandez, and Y. Zhu, Opt. Lett. **31**, 2598 (2006).

[15] J. J. Longdell, E. Fraval, M. J. Sellars, and N. B. Manson, Phys. Rev. Lett. **95**, 063601 (2005).

[16] L. Ma, O. Slattery, P. Kuo, and X. Tang, Proc. SPIE 9615, Quantum Communications and Quantum Imaging XIII **9615**, 96150D (2015).

[17] D. Budker, D. F. Kimball, S. M. Rochester, and V. V. Yashchuk, Phys. Rev. Lett. **83**, 1767 (1999).

[18] D. F. Phillips, A. Fleischhauer, A. Mair, R. L. Walsworth, and M. D. Lukin, Phys. Rev. Lett. **86**, 783 (2001).

[19] V. Boyer, C. F. McCormick, E. Arimondo, and P. D. Lett, Phys. Rev. Lett. **99**, 143601 (2007).

[20] J. Okuma, N. Hayashi, A. Fujisawa, and M. Mitsunaga, Opt. Lett. **34**, 1654 (2009).

[21] Y.-F. Fan, H.-H. Wang, X.-G. Wei, A.-J. Li, Z.-H. Kang, J.-H. Wu, H.-Z. Zhang, H.-L. Xu, and J.-Y. Gao, Phys. Lett. A **376**, 785 (2012).

[22] R. M. Camacho, P. K. Vudyasetu, and J. C. Howell, Nat. Photon. **3**, 103 (2009).

[23] N. B. Phillips, A. V. Gorshkov, and I. Novikova, Phys. Rev. A **83**, 063823 (2011).

[24] R. K. Hanley, P. D. Gregory, I. G. Hughes, and S. L. Cornish, J. Phys. B **48**, 195004 (2015).

[25] A. Sargsyan, A. Tonoyan, J. Keaveney, I. G. Hughes, C. S. Adams, and D. Sarkisyan, J. Exp. Theor. Phys. **126**, 293 (2018).

[26] J. D. Swaim and R. T. Glasser, Opt. Express **25**, 24376 (2017).

[27] A. Lampis, R. Culver, B. Megyeri, and J. Goldwin, Opt. Express **24**, 15494 (2016).

[28] B. Zlatković, A. J. Krmpot, N. Šibalić, M. Radonjić, and B. M. Jelenković, Laser Phys. Lett. **13**, 015205 (2016).

[29] J. D. Swaim and R. T. Glasser, Phys. Rev. A **96**, 033818 (2017).

[30] M. M. Ćurčić, T. Khalifa, B. Zlatković, I. S. Radojičić, A. J. Krmpot, D. Arsenović, B. M. Jelenković, and M. Gharavipour, Phys. Rev. A **97**, 063851 (2018).

[31] M. T. Turnbull, P. G. Petrov, C. S. Embrey, A. M. Marino, and V. Boyer, Phys. Rev. A **88**, 033845 (2013).

Check for updates

Slowing probe and conjugate pulses in potassium vapor using four wave mixing

B. ZLATKOVIĆ,[1,*] M. M. ĆURČIĆ,[1] I. S. RADOJIČIĆ,[1] D. ARSENOVIĆ,[1] A. J. KRMPOT,[1,2] AND B. M. JELENKOVIĆ[1]

[1]*Institute of Physics Belgrade, University of Belgrade, Pregrevica 118, 11080 Belgrade, Serbia*
[2]*krmpot@ipb.ac.rs*
[*]*bojan@ipb.ac.rs*

Abstract: We present an experimental study on ultraslow propagation of matched optical pulses in nondegenerate four wave mixing (FWM) in hot potassium vapor. The main figures of merit, i.e. fractional delay and fractional broadening, are determined to be 1.1 and 1.2, respectively. The latter two are approximately constant for the broad range of the two photon detuning. Input probe pulses between 20 ns and 120 ns can be delayed within broad range of the gain. The results are compared with the preceding works for Rb and Na.

1. Introduction

Low group velocity of light pulses i.e. slow light is of the great importance for many applications, in particular for all-optical signal processing. The applications that utilize slow light effect like optical delay lines [1,2], slow-light buffers [2], Phased Array Radar Beam Steering [2] are among many others. Since the first observation of group velocity reduction [3] a number of different techniques of slow light generation have emerged. All of these techniques are based on exploiting large dispersions which accompany narrow transparency windows. In gases, electromagnetically induced transparency (EIT) [4] has been used in hot [5,6] and cold atomic/molecular gases [1,7], as well as double absorption resonances [8,9]. EIT technique can be also applied in solids [10,11] along with coherent population oscillations [12,13], double dark states [14], and spectral hole burning [15]. In optical fibers techniques based on Brillouin scattering [16] and stimulated Raman scattering [17] were implemented. Although aforementioned techniques and methods were successful in reducing group velocity, all of them suffer from signal attenuation due to absorption.

Any technique used for optical delay lines is expected to provide arbitrary optical delay with minimum of signal distortion. In this sense light amplifying mediums are good candidates [16,18,19]. On the other hand, quantum noise accompanied with the amplifying FWM is a serious issue in quantum information applications and it is studied in details theoretically [20] and experimentally [21]. The mediums suitable for implementation of double-lambda atomic scheme are of particular interest. [22–26]. This scheme is characterized with large nonlinearities of susceptibility based on the coherence between sublevels of ground state which result in high gain of parametric FWM [23]. Obtained gain resonances are spectrally narrow which enables slowing down of optical pulses [26,27].

Since the recent observation of high-gain parametric FWM in hot potassium vapor [28], new interest has aroused for exploration of different quantum optical effects in this media [29,30]. In light of this interest, we were motivated to investigate the slowing of short light pulses in hot potassium vapor based on parametric non degenerate FWM. In particular, we find optimal pulse duration and delay-to-pulse broadening ratio.

2. Experimental realization

The double-lambda scheme was realized on D1 line of ^{39}K ($\lambda = 770$ nm, [31]), Fig. 1(b). Pump beam couples lower hyperfine ground level $4S_{1/2}$, F=1 to the excited $4P_{1/2}$ level with one-photon detuning Δ. Due to small hyperfine splitting 55 MHz [31] the hyperfine structure of the $4P_{1/2}$ level is omitted. Probe beam couples excited $4P_{1/2}$ level to the upper hyperfine ground level $4S_{1/2}$, F=2 and it has two-photon detuning δ. Due to high intensity, pump couples $4S_{1/2}$, F=2 to the excited state having detuning $\Delta + HFS$, where HFS is ground state hyperfine splitting. The double Λ scheme is closed by the newly created conjugate beam that couples the excited state with detuning $HFS + \Delta$ and $4S_{1/2}$, F=1 level. The results for 120ns Gaussian shaped pulse duration are shown in Fig. 2. The magnitudes of probe and conjugate amplification are given by their respective gains which are defined as ratios of probe and conjugate peak intensities and reference peak intensity: $G_p = I_p/I_r$, $G_c = I_c/I_r$. The slowing of optical pulses is described by fractional delay. Fractional delay is defined as the ratio between absolute delay, which is the time difference between probe (conjugate) peak and reference peak, and reference pulse width ('Delay'/'Width R' from Fig 1 (c)). Likewise, fractional broadening is defined as the ratio of probe (conjugate) pulse width to the reference pulse width ('Width P'/'Width R' from Fig 1 (c) for probe). The latter parameter is informative about the broadening of the slowed light pulses and should be as close as possible to one.
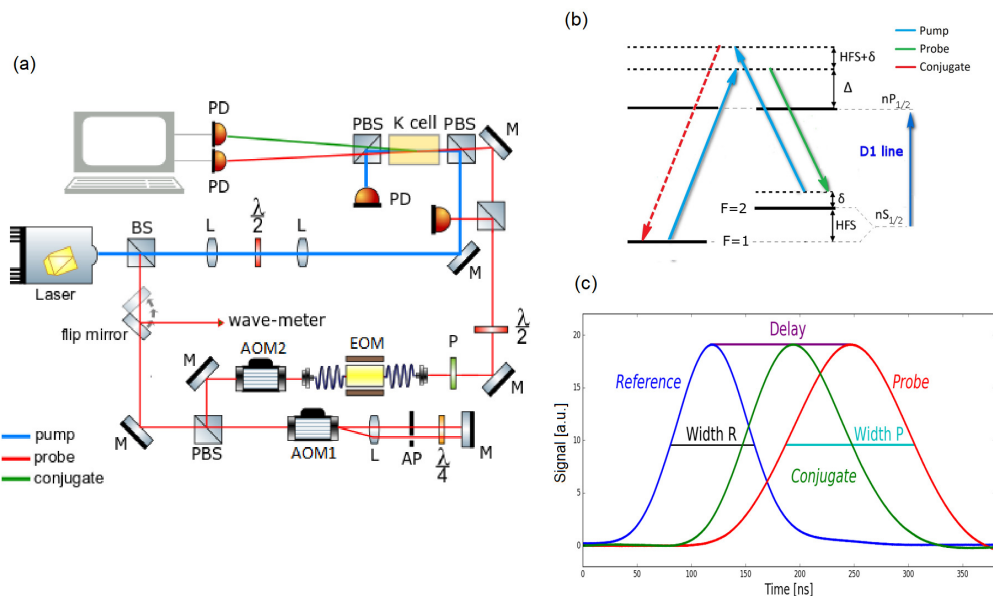
Fig. 1. (a) Experimental setup (BS - beam splitter, PBS - polarizing beam splitter, L - lens, AOM - acousto-optic modulator, EOM - fiber coupled electro optic modulator, P - linear polarizer, M - mirror, PD - photodiode, $\lambda/2$ - lambda-half wave plate, $\lambda/4$ - lambda-quarter wave plate, AP - aperture). (b) Double-lambda scheme at D1 potassium line. (c) The appearance of typical pulses order and basic definitions.

In our experiment (Fig. 1(a)) single mode Ti: Saphire laser was stabilized to the D1 potassium line and it is used for creating pump and probe beams. A small fraction of the beam is picked by a 90:10 beam splitter and sent to the acousto-optic modulator (AOM1) in double pass configuration which operates in vicinity of 190 MHz. By scanning the RF-frequency fed to the AOM1, we were able to scan two-photon detuning δ. The AOM2 with fixed frequency of 80MHz sets

up the final frequency difference between pump and probe close to the HFS of the ^{39}K (462 MHz [31]). After the AOM2 light was fiber coupled to the LiNaO$_3$ amplitude electro optic modulator (EOM)(EO-SPACE, model: AZ-0K5-10-PFU-PFU-780-S) followed by a polarizer. By applying Gaussian voltage signals from the signal generator to the EOM we were able to create Gaussian polarization pulse in the plane of the polarizer. The polarizer transforms this signal to the Gaussian intensity pulse. The pulse peak power was 20 μW. For the reference pulse, a fraction of the probe pulse was picked and detected before the vapor cell. The pump (200 mW) and probe beams have mutually orthogonal polarizations set by two $\lambda/2$ plates and they are combined at a polarizing beam splitter. Pump and probe waists are 1.05 mm and 0.8 mm, respectively. These two beams intersect at the angle of 3 mrad inside 50mm long, heated, evacuated, natural-abundance potassium vapor cell. The cell temperature was 120^oC. After the vapor cell another PBS deflects the pump away.

The three type of pulses; reference, amplified probe and newly generated conjugate were detected by an avalanche and two PIN photo diodes, respectively. For the reference the Si avalanche photo diode (APD) Hamamatsu S12023-10 was used. The Si APD was biased with 160 V which provides the gain of 100 and the bandwidth of 600 MHz. For both, amplified probe and conjugate, two identical Si PIN photodiodes Hamamatsu S5973-02 were used. The Si PIN photodiodes were biased with 9 V providing the bandwidth of 1.4 GHz. Due to very low intensity of the reference pulses, the Si APD had to be used because of its amplification. In all cases the photo current was fed to 50 Ω load and DC coupled to the oscilloscope. Each photodiode has enough bandwidth for detection of pulses in the duration range 20-120 ns that is used in the experiment.

3. Results and discussion

Typical results for delayed amplified probe and conjugate pulses for input pulse duration of 120 ns and 20 ns are shown in Fig. 2(a) and 2(b), respectively. The two pulse duration values are chosen from the edges of the interval in order to illustrate the fastest and the slowest signal changes in the experiment. The waveforms for the other pulses durations (40 ns and 80 ns) and/or for other parameters regardless the pulse duration are not shown, but the relevant parameters are extracted and used later on throughout the paper.

In Fig. 2(a) we present results for 120 ns long pulse with one photon detuning Δ = 1 GHz and two photon detuning δ = 0 MHz. The curves were obtained upon 1000 averaged measurements. We have observed amplified Gaussian probe pulse of gain 16 and delay 124 ns which gives fractional delay of 1.1. The fractional broadening for this case was 1.2. Newly created conjugate pulse was also Gaussian with fractional delay of 0.56 and fractional broadening of 1.05. The emergence of conjugate pulse before the probe pulse observed in references [26,27] was confirmed for the case of potassium as well. In Fig. 2(b) the results for 20 ns long pulse are presented with one photon detuning Δ = 700 MHz and two photon detuning δ = 0 MHz.For this set of parameters we have also observed Gaussian shape of amplified probe and conjugate signals as well as the emergence of the conjugate before the amplified probe. For amplified probe we have measured gain of 14.5, fractional delay of 3.7 and fractional broadening of 3.2. For conjugate we have measured 10, 2.7, 2,7 for gain, fractional delay and fractional broadening respectively. We would like to emphasize that separation between probe and conjugate at the exit of the cell can be tuned by choosing different parameters.

In order to obtain the results presented in this paper we scanned δ from -4 MHz to 10 MHz. For the values of δ out of this range, including the -4 MHz and 10 MHz values, the pulse profile loses its Gaussian shape and becomes distorted, so that the relevant parameters such as pulse width, delay and broadening couldn't been extracted. The latter case is shown in Fig. 2(c) as an illustration. According to the findings in [26] waveform distortion in Fig. 2(c) could be due to complex dynamics that arises from the interplay of parametric amplification and Raman

absorption. Certain balance between losses and gains of probe beam are critical for temporal shapes of twin beams, which means that the range of δ that gives undistorted waveforms will be different at different Δ, and K density. Also, it should be noted that the gain for the amplified probe pulse in Fig. 2(c) is around 0.9, which is considered to be extremely low in potassium. All the peaks of the pulses are normalized to the same value in order to make the pulses comparable. Due to small leakage of the light through the EOM and parasitic differentiation of the signal in the detection and acquisition circuits the false undershoot at the times larger than 320 ns (Fig. 2(c)) becomes pronounced since it is magnified in the normalization procedure.
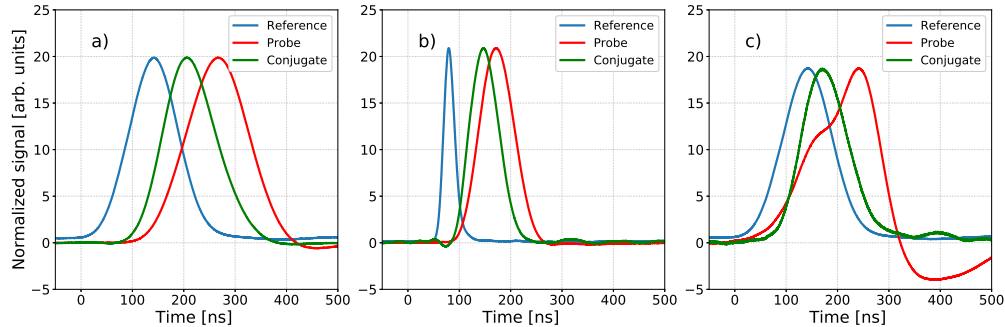
Fig. 2. Slowing the optical pulses by FWM in K vapor. The waveforms are obtained upon 1000 averaged measurements. (a) τ = 120 ns, δ = 0 MHz, Δ = 1 GHz (b) τ = 20 ns, δ = 0 MHz, Δ = 0.7 GHz (c) τ = 120ns, δ = -4 MHz, Δ = 1 GHz (Note: Gaussian shape of the probe is lost). Other parameters were kept constant throughout depicted measurements: T=120°C, Δ=1 GHz, I_{pump}= 200 mW, I_{ref} = 20μW, θ = 3mrad.

In Fig. 3 we have plotted the dependence of fractional broadening, fractional delay and gain for probe and conjugate pulse as a function of δ for Δ = 1 GHz. Fractional delay and broadening of both, probe and conjugate, are either nearly flat or vary slowly with δ in the region where the gain is not negligible. The best result, in terms of the lowest broadening and largest delay, was achieved for the probe gain of 16 which is close to a half of maximum gain of 26 (achieved for δ = 2 MHz). Our results are qualitatively different in comparison with results obtained in Rb [26] and Na [27]. In Rb the delay is highest near the bare state 2-photon resonance and drops down quickly as the δ is increased. Although the dependence of fractional delay and fractional broadening on pump Rabi frequency (i.e. intensity) is depicted in [27] we can conclude that the gain and the delay are in trade-off relation in Na since both gain and delay are monotonic functions of pump Rabi frequency. In other words, for sodium vapor one can say that higher the gain, smaller the delay and and vice versa while in potassium we do not see such strong dependence of delay (or broadening) on gain. This difference might arise from the fact that in potassium the hyperfine splitting is less than the Doppler width and the condition, set in [26], $\Delta + HFS \gg \Delta$ is not fulfilled in this case.
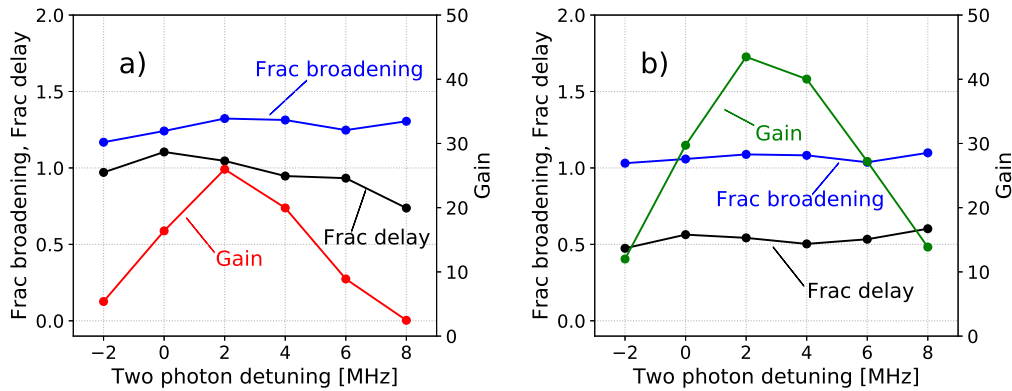
Fig. 3. Fractional delay, fractional broadening and gain dependence on δ for (a) amplified probe (b) conjugate. T=120°C, Δ=1 GHz, $I_{pump} = 200mW$, $I_{ref} = 20\mu W$, $\theta = 3$ mrad.

In Table 1 we have updated the overview of the results given in [27] with values for potassium at zero δ. The obtained (fractional) delays are somewhat larger than those in Rb [26] and comparable to those in Na [27] at the approximately same experimental conditions.

Table 1. **Summary of the results for slowing of short optical pulses via FWM in Rb, Na and K.**

Medium	Rb	Na	K
Reference pulsewidth [ns]	70	109	120
Gain	13	28	16
Fractional delay	0.57	1.03	1.1
Fractional broadening	-	1.12	1.2

For increasing the capacity of information carried by a train of optical pulses, the pulses have to be as short as possible. In order to find the shortest input pulse duration that will have the optimal slowing characteristics, i.e. the longest delay and minimal distortion, we have performed the measurements of fractional delay and fractional broadening with various pulse durations (Fig. 4). All the pulses had the Gaussian temporal shape. By lowering the pulse duration fractional delay and fractional broadening are increased simultaneously. As suggested by [32] the broadening of the pulse is due to the fact that a short pulse is spectrally broad and a larger number of its Fourier components gets slowed differently which manifests as broadening in time domain. An alternative explanation can be given using equations for group velocity and group delay given in [33] characterizing the slow light effect related to the EIT effect. The group delay is linearly proportional to optical depth and inversely proportional to the (EIT) control, in our case probe, intensity. Since the latter two parameters are fixed when the the pulse duration is decreased, the group delay should be fixed and thus the fractional broadening will increase when decreasing input pulse duration.

In order to have optical delay lines capable of producing arbitrary delay the fractional delay should be one or higher. Comparing results from Fig. 4, we found that the 120 ns long input pulse, gives better results in terms of delay and broadening than other input pulse lengths. These results are the best suited for delay lines in potassium, since there is only about 20% of widening
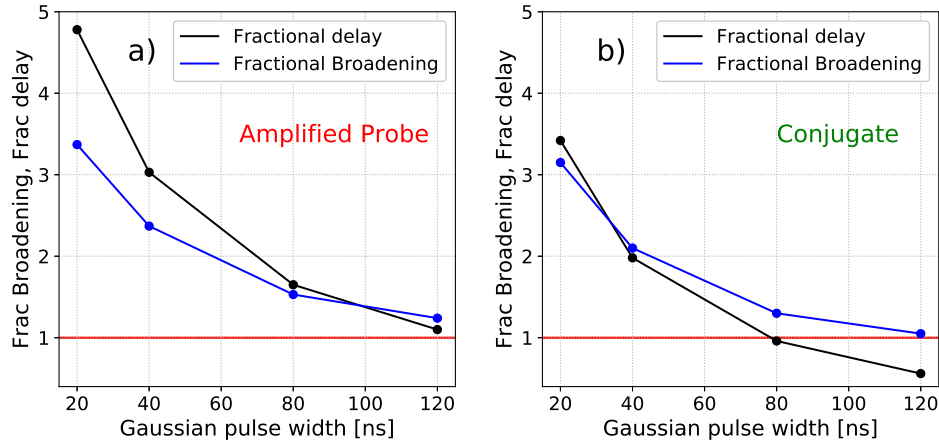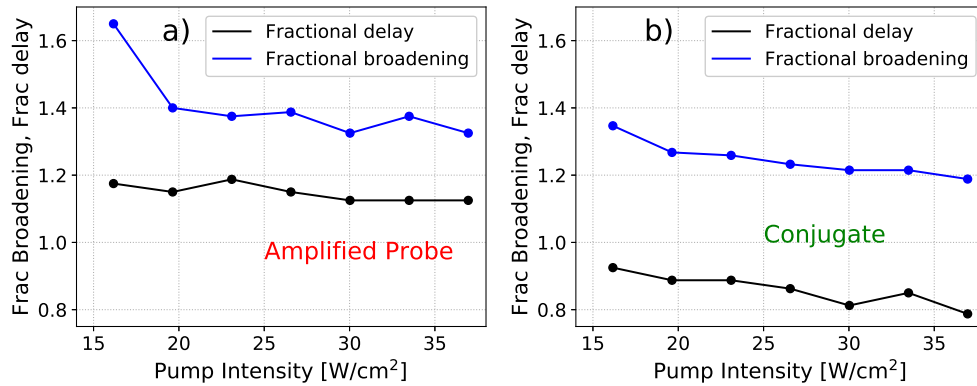
Fig. 4. Dependence of fractional broadening and fractional delay on incident pulse duration in slow light process via FWM in K vapor for (a) amplified probe (b) conjugate pulses. $\delta = 0$ MHz. T = 120^oC, $\Delta = 1$ GHz, $I_{pump} = 200$ mW, $I_{ref} = 20\mu$W, $\theta = 3$ mrad. The red line represents the value with no broadening.

while the fractional delay is above one.

In Fig 5 we show the dependence of fractional delay and fractional broadening on pump intensity. Other parameters were kept constant. One can see that unlike in sodium vapor [27] fractional delay and fractional broadening in our case don't depend strongly on the pump intensity, although they keep the same trend i.e. get lower as the pump intensity increases.

Fig. 5. Dependence of fractional broadening and fractional delay on pump intensity in slow light process via FWM in K vapor for (a) amplified probe (b) conjugate pulses. $\tau = 80$ ns, $\delta = 4$ MHz. T = 120° C, $\Delta = 1.3$ GHz, $I_{ref} = 20\mu W$, $\theta = 3$ mrad.

Comparing the results for fractional delay and fractional broadening dependence on TPD (Fig 3) and on pump intensity (Fig 5) in potassium to the corresponding ones in Rb [26] and in Na [27] one can see that the dependence of these parameters in potassium are rather modest to almost uniform. Since the most conditions are the same (e.g. fine/hyperfine structure quantum numbers, experimental geometry) for all of the alkalies in which this kind of measurements was performed , we could conclude that ground state hyperfine splitting, which is the smallest in K, plays

important role, but possibly associated with rather large Doppler broadening (Doppler broadening in K is as twice as high compared to the ground state hyperfine splitting.). However, for the detailed description of the slow light parameters in potassium one needs to develop throughout theoretical model and to conduct simulations taking into account specific atomic properties such as ground state hyperfine splitting, Doppler broadening and dipole matrix elements. In addition, analytic approximations in the model have to be chosen with care. An approximation may be valid for some alkali atoms but not for others.

4. Conclusion

In this paper we have reported slowed propagation of short optical pulses based on parametric four wave mixing in hot potassium vapor. It is shown that within the range of δ centered around 0 the slow light's figures of merit, i.e. fractional broadening and fractional delay, are approximately constant regardless to the gain. Out of this range, the slowed pulses, amplified probe first, become distorted hindering the determination of the pulse parameters i.e. pulse width and peak. Also, we have shown that fractional delay and fractional broadening are dependent on the input pulse duration. Shortening the input pulse duration may lead to better (fractional) delay, but on the other side, to the larger broadening at the same time. This suggest the trade-off between the latter two when optimal pulse duration is required, for example in delay lines and other applications. The straight forward optical setup, that can be further simplified, doesn't require high coupling (pump) laser intensities achievable even with conventional laser diodes and enables slowing of the pulses within the broad range of gains. It turned out that light slowing systems with gains, including unity, are important in order to manipulate photonics quits [26]. Eventually, the results shown in this study suggest potassium as an medium that is worth to be considered in application of the slow light and FWM effects.

References

1. W. Boyd and D. J. Gauthier, *Slow and fast light*, Progress in Optics **43**, E. Wolf, ed. (Elsevier Science B.V., 2002), Chap. 6.
2. J. B. Khurgin and R. S. Tucker, *Slow Light Science and Applications*, (Chemical Rubber Company, 2009).
3. L. V. Hau, S. E. Harris, Z. Dutton, and C. H. Behroozi,"Light speed reduction to 17 metres per second in an ultracoldatomic gas," Nature **397**, 594–598 (1999).
4. M. M. Kash, V. A. Sautenkov, A. S. Zibrov, L. Hollberg, G.R. Welch, M. D. Lukin, Y. Rostovtsev, E. S. Fry, and M. O.Scully, "Ultraslow group velocity and enhanced nonlinearoptical effects in a coherently driven hot atomic gas," Phys. Rev. Lett. **82**, 5229–5232 (1999).
5. M. Klein, M. Hohensee, Y. Xiao, R. Kalra, D. F. Phillips, andR. L. Walsworth, "Slow-light dynamics from electromagnetically-induced-transparency spectra," Phys.Rev. A **79**, 053833 (2009).
6. J. Zhang, G. Hernandez, and Y. Zhu, "Slow light with cavity electromagnetically induced transparency," Opt. Lett. **33**, 46–48 (2008).
7. R. M. Camacho, M. V. Pack, and J. C. Howell, "Low distortion slow light using two absorption resonances," Phys. Rev. A **73**, 063812 (2006).
8. R. M. Camacho, M. V. Pack, and J. C. Howell, "Wideband width,tunable, multiple-pulse-width optical delays usingslow light in cesium vapor," Phys. Rev. Lett. **98**, 153601 (2002).
9. J. J. Longdell, E. Fraval, M. J. Sellars, and N. B. Manson, "Stopped light with storage times greater than one second using electromagnetically induced transparency in a solid," Phys. Rev. Lett. **95**, 063601 (2005)

10. A. V. Turukhin, V. S. Sudarshanam, M. S. Shahriar, J. A. Musser, B. S. Ham, and P. R. Hemmer, "Observation of ultraslowand stored light pulses in a solid," Phys. Rev. Lett. **88**, 023602 (2001).

11. M. S. Bigelow, N. N. Lepeshkin, R. W. Boyd, "Superluminal and slow light propagation in a room-temperature solid," Science **301**, 200–202 (2003).

12. E. Baldit, K. Bencheikh, P. Monnier, J. A. Levenson, and V.Rouget, "Ultraslow light propagation in an inhomoge-neouslybroadened rare-earth ion-doped crystal," Phys. Rev.Lett. **95**, 143601 (2005).

13. H. H. Wang, Y. F. Fan, R. Wang, L. Wang, D. M. Du, Z. H.Kang, Y. Jiang, J. H. Wu, and J. Y. Gao, "Slowing and storage of double light pulses in a Pr3+:Y2SiO5 crystal," Opt.Lett. **34**, 2596–2598 (2009).

14. B. S. Ham and J. Hahn, "Coherent dynamics of self-inducedultraslow light for all-optical switching," Opt. Lett. **33**, 2880–2882 (2008).

15. Y. Okawachi, M. S. Bigelow, J. E. Sharping, Z. Zhu, A. Schweinsberg, D. J. Gauthier, R. W. Boyd, and A. L. Gaeta, "Tunable all-optical delays via Brillouin slow light in an optical fiber," Phys. Rev. Lett. **94**, 153902 (2005).

16. J. E. Sharping, Y. Okawachi, and A. L. Gaeta, "Wide bandwidth slow light using a Raman fiber amplifier," Opt. Express **13**, 6092–6098 (2005).

17. J. Zhang, G. Hernandez, and Y. Zhu, "Copropagating superluminal and slow light manifested by electromagnetically assisted nonlinear optical processes," Opt. Lett. **31**, 2598–2600 (2006).

18. K. J. Jiang, L. Deng, M.G. Payne, "Ultraslow propagation of an optical pulse in a three-state active Raman gain medium," Phys. Rev. A **74**, 041803(R) (2006).

19. A. Eilam, A. D. Wilson-Gordon, and H. Friedmann, "Slow and stored light in an amplifying double- system," Opt. Lett. **33**, 1605–1607 (2008).

20. N. Lauk, C. O'Brien, M. Fleischhauer, "Fidelity of photon propagation in electromagnetically induced transparency in the presence of four-wave mixing," Phys. Rev. A, **88**, 013823 (2013).

21. Y. F. Hsiao, P. J. Tsai, C. C. Lin, Y. F. Chen, A. Y. Ite, Y. C. Chen, "Coherence properties of amplified slow light by four-wave mixing," Opt. Lett. **39**, 3394–3397 (2014).

22. M. D. Lukin, P. R. Hemmer, M. Lǚffler, and M. O. Scully, "Resonant enhancement of parametric processes via radiative interference and induced coherence," Phys. Rev. Lett. **81**, 2675–2678 (1998).

23. M. D. Lukin, P. R. Hemmer, M. O. Scully, "Resonant Nonlinear Optics in Phase-Coherent Media," Adv. At. Mol. Opt. Phys. **2**, 347–386 (2000).

24. Y. Wu, and X. Yang, "Highly efficient four-wave mixing in double- Λ system in ultraslow propagation regime," Phys. Rev. A **70**, 053818 (2004).

25. Y. Zhang, A. W. Brown, and M. Xiao, "Matched ultraslow propagation of highly efficient four-wave mixing in a closely cycled double-ladder system", Phys. Rev. A **77**, 053813 (2006).

26. V. Boyer, C. F. McCormick, E. Arimondo, and P. D. Lett, "Ultraslow propagation of matched pulses by four-wavemixing in an atomic vapor," Phys. Rev. Lett. **99**, 143601 (2007).

27. J. Okuma, N. Hayashi, A. Fujisawa, and M. Mitsunaga, "Ultraslow matched-pulse propagation in sodium vapor," Opt. Lett. **34**, 1654–1656 (2009).

28. B. Zlatković, A. J. Krmpot, N. Šibalić, M. Radonjić, and B. M. Jelenković, "Efficent parametric non-degenerate four-wave mixing in hot potassium vapor," Laser Phys. Lett. **13**, 015205 (2016).

29. J. D. Swaim, and R. T. Glasser, "Squeezed-twin-beam generation in strongly absorbing media," Phys. Rev. A **96**, 033818 (2017).

30. J. D. Swaim, and R. T. Glasser, "Causality and information transfer in simultaneously slow- and fast-light media," Opt. Express **25**, 24376 (2017)

31. D. A. Steck, "Potassium properties," http://tobiastiecke.nl/archive/PotassiumProperties.pdf

32. M. D. Lukin, and A. Imamoglu, "Controlling photons using electromagnetically induced transparency," Nature **413**, 273–276 (2001).

33. M. Fleischhauer, A. Imamoglu, J. P. Marangos, "Electromagnetically induced transparency: Optics in coherent media," Rev. Mod. Phys. **77**, 633 (2005).

Squeezed States of Light Generated by Four Wave Mixing in Potassium Vapor

M. Ćurčić and B. Jelenković

Institute of Physics, Belgrade, Pregrevica 118, 11080, Belgrade, Serbia

e-mail: marijac@ipb.ac.rs

ABSTRACT

We will present results that demonstrate squeezed light source based on Four Wave Mixing (FWM) in hot Potassium vapor. Squeezed light with the noise level of -6 dB below standard quantum limit is observed in the difference signal between correlated probe and conjugate beams, generated via FWM in potassium vapor. The vapor is contained in the vacuum K cell. For generating FWM we use nearly co-propagating pump and probe beam in a double Λ atomic scheme, which is similar to schemes used to demonstrate sqeezing in Rb and in K. Obtained level of squeezing is improvement from the previous results for squeezing in potassium.

Keywords: lasers, four wave mixing, squeezing, spectral noise power, quantum noise limit.

1. INTRODUCTION

Four Wave Mixing enables amplification of probe photons, and generation of conjugate photons, due to parametric conversion of two pump photons, in a nonlinear process that is mediated by the optical medium. FWM is shown to be an efficient source of quantum correlated, probe and conjugate photons [1]. There is a big interest in entangled photons because of applications in quantum information [2] and imaging [3].

There are different methods for generating squeezed light, but the most often these methods are using non-linear medium. FWM in hot alkali vapours is particularly efficient in generating relative intensity squeezing of probe and conjugate beams, explored in many cases for reduction of signal quantum noise below SQL Relative intensity squeezing of -9.2 dB below QNL was demonstrated in Rb vapor [4]. Squeezing was also demonstrated in other alkali vapors, Cs and K [5,6].

Several experimental and theoretical investigations of FWM in hot alkali vapors have described relations between gains of twin (probe and conjugate) beams and of the probe transitions through the vapor, with the maximum achievable intensity squeezing. According to such results, best relative intensity squeezing is achieved when gains of twin beams are at their maximums, their intensities nearly equal, and the probe transmission through the vapor cell is high.

In this work we experimentally studied relative amplitude squeezing in potassium vapor. The only previous work on squeezing in K [6] has shown low level of squeezing, -1.1 dB. We believe it is worth reinvestigating squeezing in K since their [6] FWM parameters cannot develop conditions for optimal squeezing, as described above. Our previous work with K [7] has shown that K is exceptionally good FWM medium for high gains with relatively low pump powers. We used standard atomic scheme for FWM in alkalis, double Λ scheme, in which pump enables cycling of population from one hyperfine level to the other, and back: the lower Λ is made of the pump and the probe photon, coupling two K ground state hyperfine levels to the excited state (D1 line), while pump photon and the conjugate photon make the upper Λ (Fig. 1a).
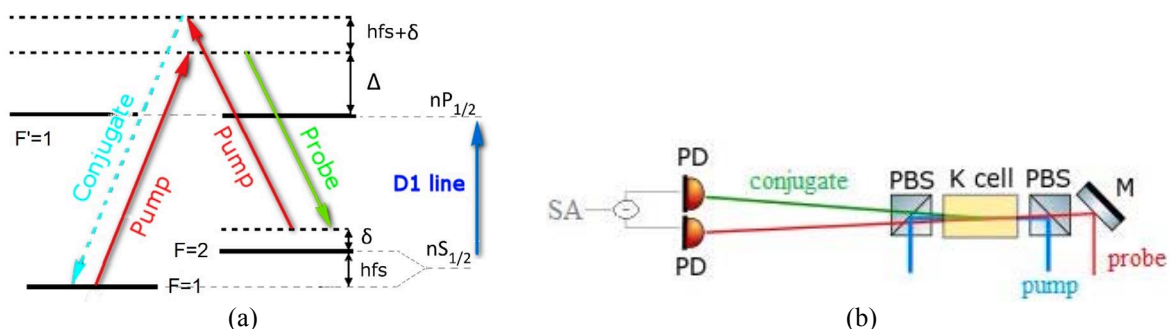

Figure 1: (a) Schematic of atomic levels of ^{39}K, coupled by the pump and probe lasers; (b) Schematic of the experiment, M – mirror, PBS – polarization beam splitter, PD – photodetector, SA – spectrum analyser.

2. EXPERIMENT

The experimental schematic is sketched in Fig. 1b. Pump and probe beams are obtained from the same, MBR 110 (Coherent) laser. Probe is detuned from the pump after passing two AOMs, one in double pass. The difference of this detuning from the hyperfine splitting of $^2S_{1/2}$ state is the two-photon detuning δ. The pump detuning from the F = 1 to F` = 1 level is the one-photon detuning, Δ. Pump and probe beam are linearly and

mutually orthogonally polarized before being overlap at the middle of the heated K cell, intersecting each other at the angle of ~4 mrad. Pump and probe diameters at waists (in the cell) are 800 µm and 650 µm, respectively. The cell is 5 cm long and has dimeter of 25 mm. The pump beam is moved away from the direction of probe and conjugate by the polarization beam splitter. Probe and conjugate beam intensities are measured by the two diodes of the balanced photodetector (PDB450A, Thorlabs)). The difference signal is fed to the spectrum analyser, with the resolution bandwidth of 3 kHz. Throughout the experiment we varied the main FWM parameters in the ranges: 700 MHz $< \Delta <$ 1500 MHz, $-20 < \delta < +10$ MHz. $1 \times 10^{11} < n < 10^{12}$ cm^{-3}.

   The SQL was measured by splitting the laser (beam from the MBR) in two equal parts and recording noise power of the signal difference. Results of the relative intensity squeezing were corrected for the electronic power noise, generated by the balance detector and spectrum analyser.

3. RESULTS AND DISCUSSION

As a result of FWM mixing in alkalis, generated by the double Λ scheme, (Fig. 1a), probe beam is amplified, and conjugate beam, frequency non-degenerate, is generated. Correlation and entanglement of the probe and conjugate photons enables intensity squeezing. Results of measured levels of intensity squeezing in alkali vapors depend on twin beam FWM gains, and probe transmission through the vapor cell. Absorption of probe and subsequent fluorescence brings noisy modes into the squeezed light, degrading the amount of squeezing. The minimum of noise figure of the signal difference between probe and conjugate is, usually, at the maximum of gains, and in an ideal case of no probe losses in the cell, the noise of the difference intensity is related to the noise at cell input by the relation $1/(2G-1)$ [8], where G is the ratio of the probe intensity behind and before the cell. Affecting the results are also losses of light due to imperfect optical elements, reflection on cell's windows, on mirrors used to steer the beams, and on PBS used to divert the pump beam from the direction of probe and conjugate. The final results, noise spectrum on SA, depends on detector efficiency and electronic noise.

   In the experiment we studied effects of all FWM parameters on the amount of squeezing. We varied vapor density, pump and probe powers and pump and probe beam diameters, one and two photon detuning. We have found that larger probe absorption (losses of the order of 30% or more) and non-balanced gains of the probe and the conjugate degrade squeezing so much that it stays above QNL in the measured ranges of noise frequency. For reducing probe losses and balancing gains, we needed very large values of one-photon detuning, $\Delta = 1500$ MHz. We have previously investigated effects of gains of twin beams in FWM in K vapor on slow light of probe and conjugate pulses, and on pulse broadening [7]. There [7] the best slow light results are corelated with the largest gains. Here, for the purpose of best squeezing, we found an indirect role of gains of twin beams, the optimum gain now is a balanced gain, for which probe and conjugate have the same intensities at the photo-detectors. Results presented in Fig. 2 show dependence of gains of both beams as values of δ was changed. Evidently, at $\delta \cong + 6$ MHz, probe and conjugate intensities are well balanced.
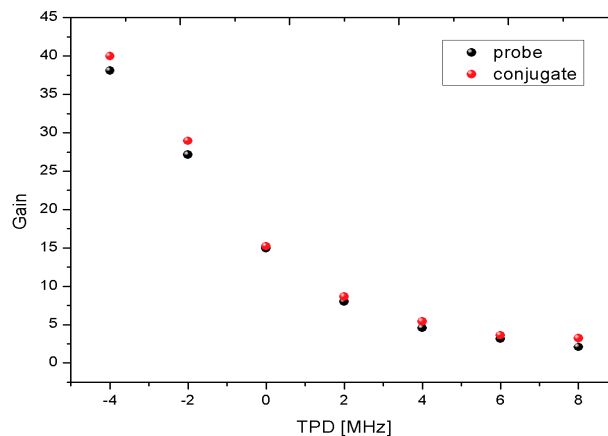

Figure 2. Gains of probe and conjugate as a function of two-photon detuning δ (TPD) for one-photon detuning $\Delta = 1500$ MHz. pump power 250 mW, seed probe power 10 µW, cell temperature 118 ^{0}C (2.6×10^{12} cm^{-3}).

   That balanced gain is most important as demonstrated in Fig. 3, where we plot noise figure of probe and conjugate, at 1 MHz, as a function of δ. At $\delta \geq + 6$ MHz relative intensity squeezing (red circles) falls below SQL. Since noise flour of QNL and squeezed light varies with light power, the laser power used for measuring SQL in Fig. 3 was equal to the combined powers of probe and conjugate.
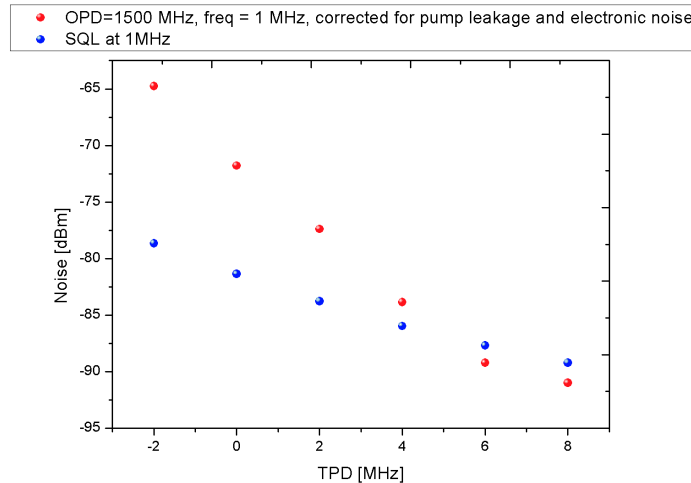
Figure 3. Noise power of difference intensity between probe and conjugate (squeezing, red circles) and of SQL (blue circles0 vs two-photon retuning δ. Values of FWM parameters are the same as in Fig. 2.

   The noise power spectrum of squeezed light and QNL are given in Fig. 4. Two-photon detuning was +8 MHz, while one-photon detuning was 1500 MHz. There is spectral range when noise of squeezed light is below QNL. The modest noise reduction of about -6 dB below QNL is in the frequency range between 750 kHz and 1 MHz. This value is bellow intensity difference squeezing reported also for K in [6]. At their level of probe detuning of few hundred MHz we couldn't obtain squeezing due to high probe absorption and losses.
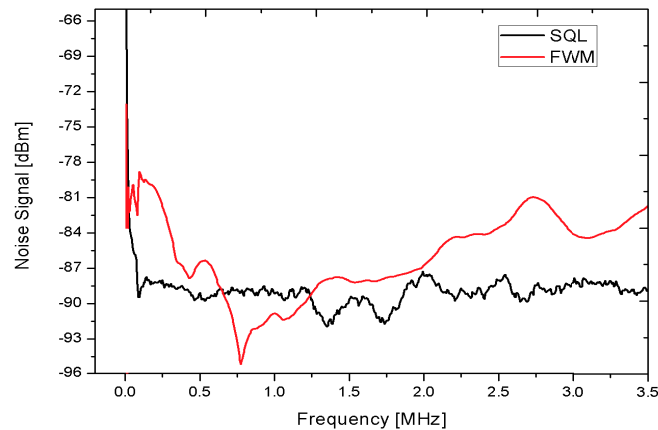
Figure 4. Noise power spectrum of the intensity difference between probe and conjugate (red line) and of SQL (black line). Reduction of noise below SQL of -6 dB is obtained in the range between 760 kHz and 1 MHz.

4. CONCLUSIONS

Using FWM in hot potassium vapor we obtained intensity difference squeezing of -6 dB below SQL in the spectral range of 200 kHz, centred at 850 kHz. This is improvement on squeezing level reported previously for potassium [6]. We found that most critical for squeezing are probe losses in the cell and balanced gains of twin beams. Although correlated, even small unbalanced beams lead to increased noise on the signal difference Balancing intensities of twin beams is challenge, since in general, FWM is not producing balanced beams. We had to carefully tailor FWM parameters to achieve such behaviour of FWM, and the reported squeezing is obtained for high one-photon detuning, $\Delta = 1500$ MHz, and two-photon detuning $\delta = +8$ MHz, while the cell temperature was 118 °C, corresponding to the gas density 2.6×10^{12} cm^{-3}. There is certainly room for further improvements of relative intensity squeezing in K vapor in our experiment. New vapor cell with AR coating on windows will reduce probe and conjugate losses in the cell. Higher quality PBS behind the cell will eliminating more of the pump beam for reaching detectors, and in addition, reduce the probe and conjugate losses.

3

REFERENCES

[1] C. F. McCormick, A. M. Marino, V. Boyer, and P. D. Lett: Strong low-frequency quantum correlations from a four-wave-mixing amplifier, *Phys. Rev. A* 78, 043816 (2008).

[2] S. L. Braustein and P. van Loock: Quantum information with continuous variables, *Rev. Mod. Phys.* 77, 513 (2006).

[3] G. Brida, M. Genovese, and I. Ruo Bechera: Experimental demonstration of sub-shot noise quantum imaging, *Nat. Photon.* 4, 227 (2010).

[4] Q. Glorieux, L. Guidoni, S. Guibal, J. P. Likforman, and T. Coudreau*, Phys. Rev.* A 84, 053826 (2011).

[5] G. Adenier, D. Calonico, S. Micalizio, N. Samantaray, I. Degiovanni, and I. R. Berchera: Realization of a twin beam source based on four-wave mixing in cesium, *Int. J. Quantum Inform.* 14, 1640014 (2016).

[6] J. D. Swaim and R. T. Glasser: Squeezed-twin-beam generation in strongly absorbing media, *Phys. Rev. A* 96, 033818 (2017).

[7] B. Zlatkovic, M. M. Curcic, I. S. Radojicic, D. Arsenovic, A. J. Krmpot, and B. M. Jelenkovic, *Opt. Express* 26, 34266-34273 (2018).

[8] M. Jasperse, L. D. Turner, and R. E. Scholten, *Optics Express* 19, 3765 (2011).

Browse ⌄   My Settings ⌄   Help ⌄   Institutional Sign In

Institutional Sign In

All   ⌄

🔍

ADVANCED SEARCH

Conferences > 2023 23rd International Confe... ❓

Entangled Pairs of Photons for Squeezed Light: Generation and Application

Publisher: IEEE | Cite This | 📄 **PDF**

Marija Ćurčić ; Dušan Arsenović ; Brana Jelenković   **All Authors** •••

43
Full
Text Views

Abstract: We discuss methods of generation of quantum entangled pairs of photons and present results obtained by non-linear process of four way mixing (FWM) in alkali atoms. Two-mo... **View more**

▸ **Metadata**
Abstract:
We discuss methods of generation of quantum entangled pairs of photons and present results obtained by non-linear process of four way mixing (FWM) in alkali atoms. Two-mode squeezing, known also as relative amplitude squeezing, by a pair of photons generated by FWM has been thoroughly investigated because of important applications of such paired photons. We show strong intensity squeezing in potassium vapour and also dependence of IDS on FWM parameters. Experimental results are compared with calculated IDS by the model of operators. Examples of application of twin photons for quantum enhanced sensing and quantum imaging and microscopy will be given.

Abstract

Document Sections

1. INTRODUCTION
2. EXPERIMENT
3. RESULTS AND DISCUSSION
4. SENSING AND IMAGING WITH QUANTUM LIGHT
5. CONCLUSIONS

Authors

Figures

References

Keywords

Metrics

More Like This

Marija Ćurčić
Institute of Physics Belgrade, Belgrade, Serbia

Dušan Arsenović
Institute of Physics Belgrade, Belgrade, Serbia

Brana Jelenković
Institute of Physics Belgrade, Belgrade, Serbia

Contents

1. INTRODUCTION

Squeezed states of light are of great interest because quantum noise reduction below the standard quantum limit (SQL) allows spectroscopy and metrology with sub-shot noise precision, quantum enhanced sensing, and atomic magnetometry. Quantum correlated and entangled pairs of photons generated in these nonlinear processes, enable in addition a two mode amplitude difference squeezing. Quantum correlation of photons from such paired photons, entangled in momentum, energy and numbers, are essential also for applications in quantum imaging and communication. The main sources of such photon pairs are spontaneous parametric down conversion (SPDC), and FWM. In the latter, three photons are mixed with four-level atom to generate correlated probe and conjugate photons. FWM is phase insensitive amplifier, meaning that high gain and therefore high flux of new photons pairs can be generated, a certain advantage of FWM vs SPDC, Also, photons due to FWM have wavelengths close to atomic transitions, allowing transfer of photon to atom entanglement. On the other hand, a large choice of nonlinear crystals available nowadays, provides wide range of frequencies for photons from SPDC.

Authors

Marija Ćurčić
Institute of Physics Belgrade, Belgrade, Serbia

Dušan Arsenović
Institute of Physics Belgrade, Belgrade, Serbia

Brana Jelenković
Institute of Physics Belgrade, Belgrade, Serbia

Figures

References

Keywords

Metrics

More Like This

Monitoring of the optical fiber network by modal interference sensor
Proceedings of 2005 7th International Conference Transparent Optical Networks, 2005.
Published: 2005

al fiber networks for source distribution in parallel THz sensors

Show More

IEEE Personal Account	Purchase Details	Profile Information	Need Help?	Follow
CHANGE USERNAME/PASSWORD	PAYMENT OPTIONS	COMMUNICATIONS PREFERENCES	US & CANADA: +1 800 678 4333	f ⓘ in ▶
	VIEW PURCHASED DOCUMENTS	PROFESSION AND EDUCATION	WORLDWIDE: +1 732 981 0060	
		TECHNICAL INTERESTS	CONTACT & SUPPORT	

About IEEE *Xplore* | Contact Us | Help | Accessibility | Terms of Use | Nondiscrimination Policy | IEEE Ethics Reporting ☒ | Sitemap | IEEE Privacy Policy

A not-for-profit organization, IEEE is the world's largest technical professional organization dedicated to advancing technology for the benefit of humanity.

IEEE Account

» Change Username/Password

» Update Address

Purchase Details

» Payment Options

» Order History

» View Purchased Documents

Profile Information

» Communications Preferences

» Profession and Education

» Technical Interests

Need Help?

» **US & Canada:** +1 800 678 4333

» **Worldwide:** +1 732 981 0060

» Contact & Support

EOSAM 13-17 September 2021
Rome, Italy

TOM9 Optics at Nanoscale (ONS)

Chairs

Vito Mocella
Consiglio
Nazionale
delle Ricerche
(IT)

Concita Sibilia
Sapienza
University
of Rome (IT)

Didier Felbacq
Montpellier
University (FR)

Synopsis

This 5th edition of the international conference wholly dedicated to Optical Nano-Systems covers a spectrum from applied to basic research of this domain providing a forum for all the aspects with the purpose of advancing the state-of-the-art of nanoscale optics.

New properties in nanoscale structures can be dramatically tuned with size and shape of the nanostructures. Completely different optical behaviours are produced compared to the bulk counterparts, such as narrow linewidths for emission, solar energy conversion, etc. Indeed materials and applications require strong effort to develop spectroscopy and microscopy tools allowing visualization and manipulation of optical properties with nanoscale resolution.

Topics

- Emerging Technologies
  - metamaterials,metasurfaces, nonradiating modes, topological insulators

- Nonlinear Optics and Applications
  - chirality and symmetries, plasmonics and SHG, nonlinear materials and THz
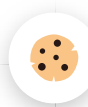
- Quantum Optics and quantum technologies
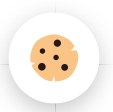
- Optical Sensors
    - novel approaches in optical sensing, optical biosensors, plasmonic sensing

- Materials for photonics
    - quantum dots, perovskite nanostructures, 2D nanomaterials

- Imaging and spectroscopy

- Advanced Theoretical and Numerical Tools for Nanooptics, Photonics and Plasmonics

<u>CALL FOR PAPERS</u>

<u>SUBMIT</u>

➕ Program Committee

➖ Invited Speakers

SPECIAL INVITED

Title: Practical Quantum Communication and Processing

Fabio Antonio Bovino, Sapienza University of Rome (IT)
Title: Ultrafast emission and detection of quantum emitters

Agio, University of Siegen

Title: Ultrafast dynamics in quantum dots

Davide Boschetto, ENSTA Paris Tech (FR)

Title: Expansion(s) of electromagnetic fields on dispersive quasi normal modes

Guillaume Demesy, Institut Fresnel (FR)

Title: Experimenting with optical plasticity in photonic machine learning - towards all-optical Artificial Intelligence

Eugenio Fazio, Sapienza University of Rome (IT)

Title: Monolithic semiconductor light sources for quantum photonic integration on Si

Teemu Hakkarainen, Tampere University (FI)

Title: Intensity squeezed States of lLght from FWM in hot alkali Vapors -Review of Results and ...ations

Brana Jelenkovic, University of Belgrade (RS)

Title: Is practicle perfect optical transmission possible?

Gilles Lerondel, UTT, Troyes (FR)

Title: Generation of nonclassical light in integrated nanophotonic resonators

Marco Liscidini, Universita di Pavia (IT)

Title: Listening to metal nanoparticles super-aggregates by photoacoustics

Roberto Li Voti, Sapienza University of Rome (IT)

Title: Dielectric metasurfaces for emission efficiency control at telecom wavelengths

Giovanni Mattei, University of Padova (IT)

Title: Surface wave photonic crystal biochips for cancer biomarkers detection

Francesco Michelotti, Sapienza University of Rome (IT)
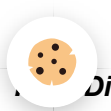
Title: Diagnostic potential of disorder: development of an

innovative nanostructured platform for rapid, label-free and low-cost analysis of genomic DNA

Valentina Mussi, CNR-IMM Roma (IT)

Title: Core-Shell 3D Chiral Metamaterial for Femtomolar Biodetection

Adriana Passaseo, CNR- Nanotec -Lecce (IT)

Title: Plasmonic lattices for controlling light-matter interaction.

Giuseppe Pirruccio, Universidad Nacional Autonoma de Mexico (MX)

Title: Optical properties of porous silicon nanowires at high pressures

Javad Rezvani, Università di Camerino (IT)

Title: On the generalized Snell-Descartes laws for metasurfaces

Emmanuel Rousseau, L2C, University of Montpellier (FR)

Title: New nonlinear chiroptical

***effects: second and third
harmonic scattering from chiral
nanoparticles***

Ventsislav K. Valev, University of
Bath (UK)

*Title: Plasmonic modes in
cylindrical nanoparticles*

Guillaume Weick, IPCMS,
University of Strasbourg (FR)
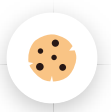
Intensity squeezed states of light from FWM in hot alkali vapors - review of results and applications

Marija Ćurčić, Brana Jelenković
Institute of physics, University of Belgrade, 11080 Belgrade, Serbia

Abstract. We review experimental and theoretical results of quantum properties of twin beams generated by the FWM in hot alkali vapors. Noise spectrum of the intensity difference of twin beams and dependence of squeezing on the range of FWM parameters is presented for the FWM in potassium. Relative intensity squeezing of -5.5 dB below SQL requires that potassium density and detuning of the pump and probe laser beams in the double Λ interaction scheme all fall in the rather narrow range.

1 Introduction

Squeezed states of light can be generated using different techniques in non-linear medium. The non-degenerate far-detuned FWM in hot alkali vapors is recognizes as a simple and efficient way of generating pairs of quantum correlated photons. The highest levels of relative intensity squeezing by the FWM twin beams, produced by this technique [1] are comparable with results obtained using other techniques, like SPDC or OPO [2]. The FWM technique for squeezing has advantages over other methods - frequencies and linewidths of FWM twin beams match transitions in atoms and solid-state systems, and the larger squeezed bandwidth open possibilities for variety of important applications.

Non-classical, sub-noise correlation of twin beams from FWM have shown possibilities in enhanced sensing and imaging [3]. The idea is that random intensity noise in the probe beam that is addressing the sample is subtracted by the measured correlated reference beam. Simultaneous detection of a large number of photons with correlated spatial modes improves sensitivity of CCD and CMOS cameras in their imaging applications. Multi-spatial-mode twin beams produced by certain FWM atomic schemes are of interests for quantum imaging [4].

We review atomic schemes used for FWM, experimental and theoretical results of quantum properties of twin beams and of the noise spectrum of the intensity difference, and the dependence of the results on the range of FWM parameters. We present our resent results of relative intensity squeezing in potassium and show how narrow are ranges of FMW parameters for which we measured highest squeezing level. The previous results in K [5] with the absorptive atomic scheme gave relatively low squeezing level, of -1.1 dB below SQL. We will discuss significance of vapor density, pump and probe powers, and detuning from the atomic transition on the quantum noise reduction.

2 Experiments

Atomic schemes for FWM processes that generate twin beams in alkali vapors can be degenerate in frequency, but the highest intensity squeezing is obtained in non-degenerate schemes [1]. The first experimental demonstration of squeezed light by FWM in alkalis was in Na vapor [6], while the most recent results are in Rb [1, 7] and Cs [8]. The highest degree of intensity squeezing of -9.2 dB was obtained in Rb [1]. There are many factors that can make the difference between experiments with strong and weak squeezing, among them are vapor density, pump and probe beam coherence, detuning of the pump, and two-photon pump-probe Raman detuning,

In the experiment we used rather common interaction scheme, double Λ scheme. In the first Λ the strong pump and the seed probe beam couple potassium hyperfine ground state levels to the same excited state along the D1 transition, while the second Λ is composed by the pump and the generated conjugate. The pump and the probe originate from the same laser and are crossed under a small angle in the heated K cell. The probe and conjugate are detected by the balance photodetector and the difference is converted to output and sent to the spectrum analyser.

3 Effects of FWM parameters on the quantum noise reduction

We have explored the FWM parameter space looking for ranges of their values producing larger squeezing. This includes pump and probe laser powers, potassium density, one-photon pump laser detuning Δ, and pump-probe two photon detuning δ. In the following figures we show results when some of the parameters are varied. Pump power for these results is 800 mW, while cell temperature is varied around $120^0 C$ ($2.9614 * 10^{12}$ cm^{-3}) for the optimal results. Figure 1 presents noise power of the intensity difference signal as a function of measurement frequency obtained for Δ = 1.2 GHz, δ = 6 MHz at 122 ^{0}C. On the same plot we can see noise spectra of the probe and conjugate signal, measured individually.
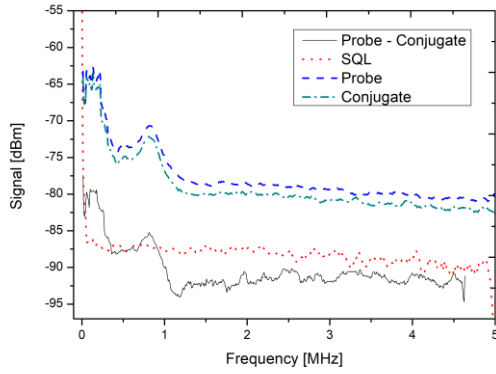

Fig. 1. Intensity difference squeezing of the twin beams (solid black line) and SQL (dot red line) as a function of analyses frequencies. The difference signal falls below SQL for frequencies between 900 kHz and 5 MHz, with the squeezing level of -5 dB between 1 MHz and 2 MHz in the spectral range. Measured probe and conjugate spectra are presented with blue (dashed) and green (dash-dot) line, respectively.

3.1 Dependence on one photon detuning

Figure 2 illustrates strong dependence of squeezing on Δ.
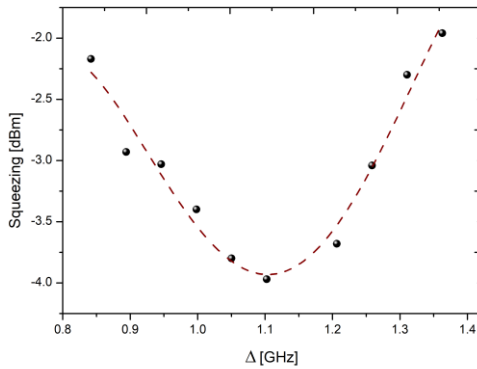
Fig. 2 Level od intensity squeezing as a function as a function of the one-photon pump detuning from D1 line at the 1.5 MHz of noise frequency and for δ = 4 MHz, T = 121º C, and P_{pump} = 800 mW.

One-photon detuning for maximal squeezing has to be of the order or larger than Doppler broadening. Δ for K for optimal squeezing is larger than for Rb and Cs, because this Doppler broadening is larger for K. Detuning Δ ~ 1.1 GHz is compromise between higher absorption and loss of correlation at lower, and fewer collisions and loss of non-linearity at higher detuning.

3.2 Dependence on two photon detuning

There is also strong dependence of relative intensity squeezing on δ as indicated in Fig. 3. The maximum squeezing is away from two-photon resonance and from other non-linear effects like the EIT. At higher δ and lower gains of twin beams quantum correlation is lower.
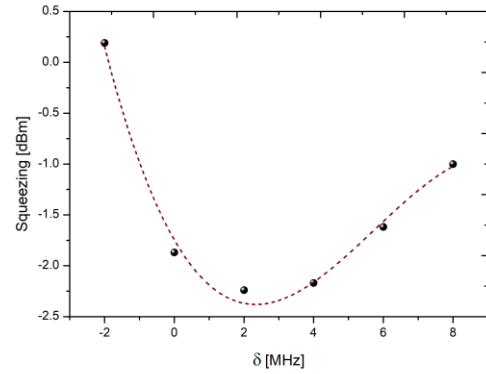

Fig. 3. Dependence of relative intensity squeezing on two-photon detuning for Δ = 1.3 GHz, T = 121º C, and P_{pump} = 800 mW at 1.5 MHz of noise frequency.

References

1. Q. Glorieux, L. Guidoni, S. Guibal, Jean-Pierre Likforman, and T. Coudreau, Phys. Rev. **A 84**, 053826 (2011).

2. J. Laurat, L. Longchambon, C. Fabre, and T. Coudreau, Opt. Lett. **30**, 1177 (2005).

3. I. R. Berchera1 and I. P. Degiovanni, Metrologia **56**, 024001 (2019).

4. Y. Yu, C. Wang, J. Liu, J. Wang, M. Cao, D. Wei, H. Gao, F. Li, Ghost imaging with different frequencies through non-degenerate four-way mixing, Opt. Express **24**, 18290 (2016).

5. Jon D. Swaim and Ryan T. Glasser, Squeezed-twin-beam generation in strongly absorbing media, Phys. Rev. A **96**, 033818 (2017).

6. R. E. Slusher, L. W. Hollberg, B. Yurke, J. C. Mertz, and J. F.Valley, , Phys. Rev. Lett. **55**, 2409 (1985).

7. C. F. McCormick, A. M. Marino, V. Boyer, and P.D. Lett, Strong low-frequency quantum correlations from a four-wave-mixing amplifier, Phys. Rev. A 78, 043816 (2008).

8. R. Ma,W. Liu, Z. Qin, X. Jiaand Ji. Gao. Generating quantum correlated twin beams by four-wave mixing in hot cesium vapor, Phys. Rev. A 96, 043843 (2017).

Slowing light pulses due to four-wave mixing in Potassium vapor

– theory and experiment

M. Ćurčić, B. Zlatković, I. Radojičić, Ž.Nikitović, A. Krmpot, D. Arsenović, and B. Jelenković

Photonic Center, Institute of physics, University of Belgrade, Belgrade, Serbia

Slow light can be obtained using different protocols and different physical systems. Here we investigate slowing of light pulses due to four wave mixing (FWM) in hot Potassium. Slow light is valuable for all signal processing, but in order to be really useful, the system has to produce fractional delays large than one, with the small broadening and absorption. Absorption and distortion are alleviated in the system with the gain, like in FWM, which opens possibilities for stacking many delay lines.

In this work we use off- resonant double Lambda scheme for FWM in K vapor to theoretically and experimentally investigate propagation of 80 ns probe pulse, and generation and propagation of conjugate pulse, which typically separates from the probe pulse at the and of the cell. This atomic scheme was used before to investigate slow light in Rb [1], Na [2]. In the model we first solve optical Bloch equations for all density matrix elements developed in the four level atomic system of K, coupled by three electric fields, pump, probe and conjugate. Calculated optical coherences are then used to calculate amplitudes of these fields as a function of time and distance using Maxwell propagation equation. In the experiment, we tune probe laser to Raman resonance with the pump laser by a pair of AOMs, and generate probe Gasussian 80 ns pulse, by EOM before it is combined with the pump laser and send to the hot K vacuum vapor cell. Group velocities were measured by recording the arrival times of the probe and the conjugate relative to the reference pulse.

Potassium is different from other alkali atoms, with small hyperfine structure, smaller then Doppler width. It wasn't so far used for slowing light pulses. Comparison between theory and experiment provides more insights into the dynamics of pulses propagation through this FWM medium. Agreement between theory and experiment, both qualitative in terms of similar pulse waveforms after the cell, and quantitative in terms of fractional delays and broadening, revels proper values of parameters in calculations, like dephasing and decoherence rates. Moreover, by placing, at the peak of input probe pulse, a small wavelets (amplitude much smaller in comparison with the probe pulse amplitude), and much shorter than the probe pulse, we can follow behavior of the probe pulse in the cell. We show that depending on the FWM parameters, pulses behave quite differently, in some cases showing complete disappearance, and revival of the pulse later in time. Results are given as a function of one photon pump detuning, two Raman pump-probe detuning, gas density, laser power and Rabi frequency.

[1] V. Boyer, C. F. McCormick, E. Arimondo, and P. D. Lett, Phys. Rev. Lett. **99**, 143601 (2007).
[2] J. Okuma, N. Hayashi, A. Fujisawa, and M. Mitsunaga, Opt. Lett. 34, 1654–1656 (2009).

Non-degenerate four wave mixing based slow light in hot potassium vapor

Bojan Zlatković, Marija M. Ćurčić, Ivan S. Radojičić, Dušan Arsenović, Aleksandar J. Krmpot, and Branislav M. Jelenković

Institute of Physics Belgrade, University of Belgrade, Pregrevica 118, 11080 Belgrade, Serbia

We have studied propagation of Gaussian probe pulses of various duration in hot potassium vapor (120°C) under conditions of non-degenerate four wave mixing (FWM). FWM is realized in co-propagating geometry by off-resonant double Lambda scheme at D1 line (770nm) of ^{39}K. Pulse duration was in the range 20 - 120ns, while one and two photon detuning were 700 - 1300MHz and -10 − 10 MHz, respectively. A typical trace of three pulses, reference, amplified probe and conjugate is shown in figure 1 with clearly observable delay of the latter two. The optimal fractional delay and fractinal broadening were measured to be 1.1 and 1.2, respectively and they are comparable to those obtained in Rb (0.57, -) [1] and Na (1.03, 1.12) [2]. Unlike in Rb and Na, fractional delay and broadening of both, probe and conjugate, vary slowly with two photon detuning [3]. In the measurements of fractional delay and fractional broadening with various pulse durations all the pulses had the Gaussian temporal shape. By lowering the pulse duration fractional delay and fractional broadening were increased simultaneously. We found that the 120 ns long input pulse, gives the best results in terms of delay and broadening.
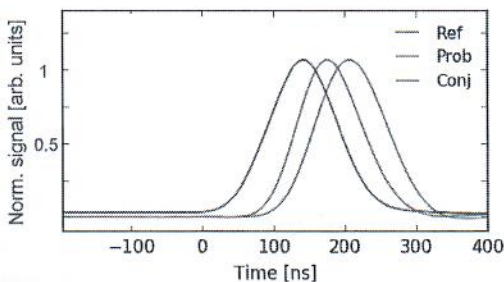
Figure 1. Propagation of the 120 ns optical pulses by the FWM in hot ^{39}K vapor. The curves are obtained upon 1000 averaged measurements. Two photon detuning 0 MHz, one photon detuning 700MHz, T=120°C , I pump = 200mW, I ref = 20μW, angle between probe and pump beams θ = 3mrad.

[1] V.Boyer,C.F.McCormick,E.Arimondo,andP.D.Lett,"Ultraslow propagation of matched pulses by four-wave mixing in an atomic vapor," Phys. Rev. Lett. 99, 143601 (2007).

[2] J. Okuma, N. Hayashi, A. Fujisawa, and M. Mitsunaga, "Ultraslow matched-pulse propagation in sodium vapor," Opt.Lett. 34, 1654–1656 (2009).

[3] B. Zlatković, M. M. Ćurčić, I. S. Radojičić, D. Arsenović, A. J. Krmpot, and B. M. Jelenković, „Slowing probe and conjugate pulses in potassium vapor using four wave mixing", in preparation

Ultraslow propagation of optical pulses in hot potassium vapor

B. Zlatković[1], A. J. Krmpot[1], D. Arsenović[1], I. S. Radojičić[1], M. M. Ćurčić[1], Z. Nikitović[1], and B. M. Jelenković[1]

[1]*Institute of Physics,*
Belgrade, Serbia
e-mail:bojan@ipb.ac.rs

Parametric non-degenerate four wave mixing (4WM) is a nonlinear process in which two pump photons mix in order to create photons with different frequencies. This process is realized via double lambda scheme by stimulating a four-stage cyclical transition resulting in the emission of amplified probe and conjugate photons. Parametric non-degenerate four wave mixing is a promising tool for producing continuous squeezed light [1] and slowed optical pulses [2]. Recent demonstration of this phenomenon in hot potassium vapor [3] has motivated our investigation of slowed optical pulses in the same medium.

In our experiment double lambda scheme is realized on D1 line of potassium isotope ^{39}K. We have studied the influence of the vapor cell temperature i.e. density of potassium atoms, one photon detuning and two photon detuning and the length of the optical pulse on the slowing of optical pulses in 4WM medium.

The laser frequency is locked at various one photon detunings (700 MHz to 1600 MHz) from the 4S1/2Fg=1 -> 4P1/2 transition. The probe is detuned 460 MHz (ground state hyperfine splitting) with respect to the pump beam and scanned around the Raman resonance. The vacuum potassium vapor cell is heated up to 150°C. The pump and probe beam intersect at small angle (3 mrad) set by the phase matching condition. Gaussian shaped probe pulses of length of 80ns were created by electrooptic modulator. and the delay, fractional delay and distortion of probe and conjugate pulses was measured.

We have observed probe delays up to 160 ns and fractional delays up to 2 and slightly less for conjugate. These delays were followed by up to 1.8 times of broadening of probe and conjugate pulses (with respect to width of entering probe pulse). These results motivate further work on this subject that will, as we believe, lead to improvements in slowing of optical pulses.

REFERENCES
[1]V. Boyer, A. M. Marino, R. C. Pooser, P. D. Lett, Science 321, 544–547 (2008).
[2] C. F. McCormick, V. Boyer, E. Arimondo, P. D. Lett, PRL 99, 143601 (2007).
[3] B. Zlatkovic, A. J. Krmpot, N. Sibalić, M. Radonjic, B. M. Jelenkovic, Laser Phys. Lett. 13, 015205 (2016).

Four wave mixing in potassium vapor with off-resonant double lambda system

D. Arsenović, <u>M. M. Ćurčić</u>, B. Zlatković, A. J. Krmpot, I. S. Radojičić, T. Khalifa and B. M. Jelenković
Institute of Physics,
Belgrade, Serbia
e-mail: marijac@ipb.ac.rs

Nowadays, four-wave mixing (FWM) in alkali vapors is a hot topic, essential for exploring new states of light [1] and for quantum information [2]. We studied theoretically and experimentally non-degenerate four-wave mixing (FWM) in potassium vapor. The effect was generated by employing co-propagating pump and probe beams, and using the interaction scheme known as double-lambda scheme. Results obtained by the theoretical model were compared to experimental results obtained using the setup described in [3].

Theoretical model is based on the semi-classical treatment of the FWM processes. We start with solving numerically Bloch equations for density matrix elements of all populations and coherences, relevant for our double-lambda scheme. The coherences are further utilized for calculation of atomic polarization, which is used in the propagation equations for amplitudes of electrical fields of pump, probe and conjugate beams. This kind of approach, with fully numerical calculations and without perturbation theories and approximations, makes our model one of the most detailed among other models of FWM processes.

We have calculated and measured gains of the probe and the conjugate, defined as the ratio of probe and conjugate intensities at the exit from the K vapor cell, and the intensity of the probe beam at the entrance in the cell. Theoretical and experimental profiles of gains for a wide range of relevant parameters were compared and analyzed. Dependences on angle between pump and probe, two photon Raman detuning, one photon detuning from the D1 line, atomic densities and probe power are included in our results. Parameters were chosen for exceptionally high gains of probe and conjugate beams.

Qualitative agreement of experimental results with theoretical predictions was observed. FWM in alkali atoms is a complex process where dependence of efficiency of FWM on one parameter is related to values of other parameters. Strong dependence of the gain profile vs angle on the pump power and atom densities were observed. For a one-photon detuning from D1 transition of the order of 1 GHz, and the vapor density of $\sim 5 \cdot 10^{12}$ cm^{-3}, system acts as a strong phase insensitive amplifier. Gains vs two photon Raman detuning are narrow resonances with the width of the order of 10 MHz, depending on the angle between pump and probe and on one-photon detuning. Resonances are shifted from the zero two photon detuning by a different value, from 0 to -10 MHz, depending on the one photon detuning from D1 line and to a smaller extend on the angle. For the low probe power gain value up to 500 was obtained.

REFERENCES
[1] C. F. McCormick *et al*., Phys Rev A 78, 043816 (2008).
[2] C. Shu *et al*., Nat Comm. 7, 12783(2016).
[3] B. Zlatkovic *et al*., Las Phys Lett 13, 015205 (2015).

Amplitude squeezing by four wave mixing in hot potassium vapor

M. M. Ćurčić and B. M. Jelenković
Institute of Physics, Belgrade, Serbia
e-mail: marijac@ipb.ac.rs

First evidence of squeezed states of light obtained by four wave mixing (FWM) process in alkali vapor was initially presented by Slusher et al. [1] in 1985. Since then squeezing of light in such a medium has occupied interest of many research groups. We experimentally demonstrate relative amplitude squeezing of light (spectral noise power below standard quantum limit) by the use of non-degenerate FWM process in potassium vapor. We use double lambda scheme on D_1 line, with two nearly co-propagating laser beams, pump and probe. Similar schemes were used for experiments in Rb [2] and Cs [3], with the maximal level of squeezing of ~ 9 dB observed in Rb vapor. Potassium has a smaller hyperfine splitting of the ground level compared to other alkali atoms. The research performed so far suggests that this could lead to higher levels of squeezing.

The amplitude difference squeezing can be controlled by the proper choice of the experimental parameters: pump power, one- and two- photon detuning, vapor density, angle between the beams. Their values control nonlinearity, the beam absorption and gain, which are of great importance for the generation of strong quantum correlations. FWM parameters in previous measurements in K [4] are not in agreement with the optimal ones we predicted in our resent work [5]: small probe absorption, similar gains of probe and conjugate, and identical intensities of twin beams at the balanced detectors. Indeed, at FWM parameters quite different than in [4], we obtained higher level of squeezing. Results of measured levels of squeezing at different conditions for FWM will be presented.

REFERENCES
[1] R. Slusher et al., Phys. Rev. Lett. 55, 2409 (1985).
[2] C. F. McCormick et al., Opt. Lett, 32, 178 (2007).
[3] R. Ma et al., Phys. Rev. A 96, 043843 (2017).
[4] J. D. Swaim, R. T. Glasser, Phys. Rev. A 96, 033818 (2017).
[5] M. M. Ćurčić et al., Phys. Rev. A 97, 063851 (2017).

Evolution of laser pulse propagation in
Four Wave Mixing atomic medium

D. Arsenović[1], Ž. Nikitović[1], B. Zlatković[1], I. Radojičić[1],
M. Ćurčić[1], A. J. Krmpot[1] and B. Jelenković[1]
[1]*Institute of physics, Belgrade, Pregrevica 118, 11080 Belgrade, Serbia*
e-mail: ivan.radojicic@ipb.ac.rs

Electromagnetically induced transparency (EIT) and EIT based Four Wave Mixing (FWM), the two effects of quantum coherence and nonlinearity induced in atomic systems, are important because of related phenomena, like slow and storage of light pulses. From the practical point it is important to ensure parameters of EIT and FWM so that pulses propagate through medium without (any) distortion.

In this work we investigate propagation of probe and conjugate pulses through potassium vapor, which is made FWM medium by a double Λ atomic scheme. We are interested in finding conditions when initial Gaussian probe pulse begins to brake, bringing multiple pulses at the exit of the K cell. In our previous works with FWM in potassium we studded slow light and therefore worked with conditions that ensure preservations of Gaussian pulse at the exit of the K cell [1].

We are interested in pulse propagation dynamics that leads to pulse splitting in hot alkali vapor. Understanding mechanism which governs the final shape of the pulse will help to tailor FWM parameters optimal for slowing and storing Gaussian pulses, with minimum distortion and broadening. Theoretically and experimentally we investigate propagations of 80 ns Gaussian probe pulse through double Λ type atomic media, when the second leg of the lower Λ scheme is the strong cw pump laser.

We developed detailed numerical model to describe the FWM in hot potassium vapor, using Maxwell-Bloch equations (MBE). Potassium atoms in vapor cell have large Doppler line broadening, of the order of 800 MHz. The model carefully takes into account pump photon detuning from the D1 line due to Doppler effect, in addition to the detuning set for the pump laser (valid for zero velocity atoms). We select a number of velocity groups of atoms and form separate density matrices for each group and a corresponding set of Bloch equations. At initial time and position (entrance to the cell) for starting point of propagation, for a given pump and probe detuning, we first solve the MBE with all derivatives over time set to zero. Thus, obtained spatial dependence of atomic polarizations is initial condition for the probe pulse at the cell entrance. Comparison with experiment has shown that small steps between two velocity groups are necessary, of the order of 10 MHz. The total number of atom velocity groups, and the type of uneven distribution of groups along the Doppler profile, is the compromise between proximity of results to results of the experiment, and reasonable computer time.

We will present results of the model and of the experiment for ranges of one photon pump laser detuning, two pump-probe laser beams detuning, potassium density, when slowed probe and conjugate pulses start to deform from Gaussian, and begin to split.

REFERENCES
[1] B. Zlatković et al., Opt. Express 26, 34266 (2018).

5 nm diameter and 80 nm length. Single nanorods are individually contacted with electron beam lithography. To increase the measureable current in some cases a small number of rods are contacted in parallel by Cr/Au-contacts.

With the chemical cation exchange Cd can be replaced by Cu in these nanorods [1]. This transforms CdS with a resistivity around 10^{12} Ωcm [2] to CuS which has a 15 orders of magnitude lower resistivity [3]. This method is applied to already contacted nanorods. These rods are electrically measured under ambient conditions. By measuring the same rods before and after the exchange, a drastic decrease in resistance is observed. The resulting resistance is stable for at least 14 days.

[1] B. Sadler et. al., J. AM. CHEM. SOC. 131, (2009)
[2] R. H. Bube, S.M.Thomsen, J. of Chemical Physics 23, (1955)
[3] M. Najdoski et al., J. of Solid State Chemistry 114, (1995)

HL 35.53   Wed 17:30   Poster E
Time-resolved reflectometry measurements on self-assembled quantum dots — •Jakob Penner[1], Kevin Eltrudis[1], Isabel Oppenberg[1], Arne Ludwig[2], Andreas D. Wieck[2], Martin Geller[1], and Axel Lorke[1] — [1]Faculty of Physics and CENIDE, University Duisburg-Essen, Germany — [2]Chair of Applied Solid State Physics, Ruhr-University Bochum, Germany

Time-resolved transconductance measurements on the electron dynamics of self-assembled quantum dots (QDs) [1] can be used to access excited spin- and charge states in an all-electrical measurement [2], an important step towards quantum state manipulation and detection for future quantum information technologies. However, for fast and high-fidelity measurements, the signal-to-noise ratio of the read-out signal is of great importance. Combining transconductance with time-resolved reflectometry in a lock-in measurement scheme promises to significantly increase the signal-to-noise ratio. We use a high-mobility electron transistor (HEMT) with a layer of QDs that are coupled to a two-dimensional electron gas. This allows us to observe the tunneling dynamics between the 2DEG and the QDs in a reflectometry measurement setup. A high-frequency ac driving voltage in combination with a lock-in technique is set to an electrical resonance of an internal LC circuit. The reflected signal depends on the impedance of the sample, where the change in impedance is related the number of electron in the quantum dot layer, hence, to the tunneling dynamics.
[1] B. Marquardt. et al., Nature Commun. 2, 209 (2011).
[2] K. Eltrudis et al., Appl. Phys. Lett. 111, 092103 (2017).

HL 35.54   Wed 17:30   Poster E
Spatiotemporal Dynamics of correlated Carrier Wave Packets in Semiconductors — •Frank Lengers[1], Roberto Rosati[2], Tilmann Kuhn[1], and Doris E. Reiter[1] — [1]Westfälische Wilhelms-Universität Münster, Germany — [2]Chalmers University of Technology, Sweden

Highly focused optical excitation of semiconductors in real space results in strongly localized carrier distributions in the material. Subsequent transport of the excited carrier wave packets occurs on nanometer and picosecond scales and is influenced by the Coulomb interaction. Since the Coulomb interaction in heterostructures of low dimensionality is enhanced with respect to the bulk, we here study a one-dimensional quantum wire as an example system where strongly interacting electrons and holes can be excited. We treat a system of up to two photoexcited electron-hole pairs within a wave function approach and are thereby able to treat the carrier correlations exactly. The wave packet dynamics is analyzed as function of the excited density and excitation energy. We show that high densities can lead to travelling electron-hole wave packets or to enhanced wave packet broadening depending on the excitation conditions.

HL 35.55   Wed 17:30   Poster E
Charging dynamics of self-assembled InAs quantum dots in n-GaAs Schottky diodes — •Lars Kürten[1], Laurin Schnorr[1], Thomas Heinzel[1], Sven Scholz[2], Arne Ludwig[2], and Andreas D. Wieck[2] — [1]Lehrstuhl für Festkörperphysik, Heinrich-Heine-Universität Düsseldorf — [2]Lehrstuhl für Angewandte Festkörperphysik, Ruhr-Universität Bochum

We study the charge transfer dynamics between self-assembled InAs quantum dots (SAQD) embedded in n-GaAs Schottky diodes and the space charge region by Laplace deep level transient spectroscopy (LDLTS). The filling dynamics of the electronic SAQD states are investigated at liquid nitrogen temperature as a function of the applied bias voltage and modeled using band structure calculations. We find

a non-trivial dependence of the apparent total charge transfer on the bias voltage and are able to quantitatively model our data by assuming a competing re-emission of electrons during the filling process via separately measured emission paths.

HL 35.56   Wed 17:30   Poster E
Simulation of mode competition phenomena in (Al,In)GaN laser diodes — •Eduard Kuhn, Lukas Uhlig, Matthias Wachs, Ulrich T. Schwarz, and Angela Thränhardt — Institut für Physik, Technische Universität Chemnitz

Experiments show interesting mode competition phenomena in laser diodes. For example streak camera measurements show cyclic mode hopping, where the currently active mode changes from lower to higher wavelengths. This can be explained by third order effects such as beating vibrations of the carrier density. In this work we describe these mode dynamics using a model based on the semiconductor Bloch equations and discuss the influence of the Hartree-Fock terms and different dephasing terms.

HL 35.57   Wed 17:30   Poster E
Blue InGaAs-VECSELs for Rydberg atom spectroscopy — •Ana Ćutuk[1], Marija Ćurčić[2], Marius Plach[3], Richard Hermann[3], Marius Grossmann[1], Roman Bek[1], Robert Löw[3], Harald Kübler[3], Michael Jetter[1], and Peter Michler[1] — [1]Institut für Halbleiteroptik und Funktionelle Grenzflächen, Center for Integrated Quantum Science and Technology (IQST) and SCoPE, University of Stuttgart, Allmandring 3, 70569 Stuttgart — [2]Photonics Center, Institute of Physics, Belgrade, Serbia — [3]5. Physikalisches Institut and Center for Integrated Quantum Science and Technology IQST, Universität Stuttgart

The Rydberg state of atoms is very attractive for applications in quantum information due to its large dipole moment, lifetime and polarizability. For the excitation of the Rydberg states in rubidium and potassium, laser emission in the blue spectral range is necessary. The vertical external-cavity surface-emitting laser (VECSEL) turns out to be an excellent candidate due to its wavelength versatility and high output power combined with a near diffraction-limited beam profile and the flexibility to add optical components inside the cavity. Our focus is on the development of InGaAs-based VECSELs with the fundamental wavelength in the near-infrared spectral range. By inserting a BBO crystal in a v-shaped cavity, second harmonic generation at around 475 nm and 455 nm can be achieved. Further improvements will be made on reducing the laser linewidth to achieve single mode operation and with analog stabilization according to the Pound-Drever-Hall technique.

HL 35.58   Wed 17:30   Poster E
Characterization of mode competition phenomena in (Al,In)GaN laser diodes — •Lukas Uhlig, Eduard Kuhn, Matthias Wachs, Angela Thränhardt, and Ulrich T. Schwarz — Institute of Physics, Chemnitz University of Technology

(Al,In)GaN laser diodes have various recent applications, such as laser projection systems in augmented/virtual reality glasses, which require a modulation with frequencies ranging from 100 MHz to 1 GHz. Laser diodes show a rich dynamic behavior of the longitudinal modes on a nanosecond to microsecond time scale. We investigate the spectral-temporal dynamics of green InGaN laser diodes in high resolution using a streak camera setup combined with a monochromator. For interpretation we simulate the longitudinal mode dynamics using a multi-mode rate equation model.

The observed effects at pulse onset include the turn-on delay and relaxation oscillations as well as a fast red shift. In longer pulses, we investigate mode competition with mode hopping towards longer wavelengths, which repeats cyclically. Single shot measurements show significant variations between single pulses. Consequently, much of the dynamics cannot be observed in usual averaged / time-integrated characterization.

HL 35.59   Wed 17:30   Poster E
Towards mode locking with a membrane saturable absorber mirror — •Ana Ćutuk, Roman Bek, Michael Jetter, and Peter Michler — Institut für Halbleiteroptik und Funktionelle Grenzflächen, Center for Integrated Quantum Science and Technology (IQST) and SCoPE, University of Stuttgart, Allmandring 3, 70569 Stuttgart

Although providing several superior laser properties, the vertical

Propagation of short twin pulses in four-wave mixing in hot Potassium vapor

I. S. Radojičić[L], M. Ćurčić[1], B. Zlatković[1], Ž.Nikitović[1], A. Krmpot[1], D. Arsenović[1], and B. Jelenković[1]

1. Photonic Center, Institute of physics, University of Belgrade, Belgrade, Pregrevica 118, 11000 Belgrade, Serbia

In this work we investigate, theoretically and experimentally, slowing of light pulses due to four wave mixing (FWM) in hot Potassium. Slow light is valuable for all signal processing, but in order to be really useful, the system has to produce fractional delays large than one, with the small broadening and absorption. Absorption and distortion are alleviated in the system with the gain, like in FWM, which opens possibilities for stacking many delay lines. Special feature of FWM is simultaneously slowing of incident probe pulse and a new beam that emerges from the vapor at quite different frequency, a conjugate beam.

We use off- resonant double Lambda scheme for FWM to investigate propagation of 80 ns probe pulse, and generation and propagation of conjugate pulse, which typically separates from the probe pulse at the end of the cell. This atomic scheme was used before to investigate slow light in Rb [1], Na [2]. The model derives atomic populations, coherences, pulse gains and wave forms solving first optical Bloch equations, and then phenomenological Maxwell equations, taking into account Doppler broadening of transitions. In the experiment, we tune probe laser to Raman resonance with the pump laser by a pair of AOMs, and generate probe Gaussian 80 ns pulse, by EOM before it is combined with the pump laser and send to the hot K vacuum vapor cell. Group velocities were measured by recording the arrival times of the probe and the conjugate relative to the reference pulse.

Potassium has smaller hyperfine structure, smaller than Doppler width then other alkali atoms. It wasn't so far used for slowing light pulses. Comparison between theory and experiment provides more insights into the dynamics of pulses propagation through this FWM medium. Agreement between theory and experiment, both qualitative in terms of similar pulse waveforms after the cell, and quantitative in terms of fractional delays and broadening, revels proper values of fitted parameters, like collisional and transit time dephasing. Moreover, by following location of the small perturbation (placed at the peak of input probe pulse) vs the location of the pulse peak at different distances in the vapor from the entrance, we can follow behavior of the probe pulse in the cell. We show that depending on the FWM parameters, pulses behave quite differently, in some cases showing complete disappearance, and revival of the pulse later in time.

All our results are given as a function of one photon pump detuning, two Raman pump-probe detuning, gas density, laser power and Rabi frequency.

References
[1] V. Boyer, C. F. McCormick, E. Arimondo, and P. D. Lett, Phys. Rev. Lett. **99**, 143601 (2007).
[2] J. Okuma, N. Hayashi, A. Fujisawa, and M. Mitsunaga, Opt. Lett. 34, 1654–1656 (2009).

A – 44

Slowing probe and conjugate pulses in potassium vapor using Four Way Mixing

Bojan Zlatković, Marija Ćurčić, Ivan Radojičić, Aleksandar Krmpot,
Željka Nikitović, Dušan Arsenović and Brana Jelenković
Institute of Physics Belgrade, University of Belgrade, 11079 Belgrade Serbia
email: branaj@ipb.ac.rs

We used four-way mixing (FWM) phenomena to slow light pulses in hot potassium vapor. The atomic scheme for FWM was off-resonant double-Lambda scheme that was previously used to study slow light in Rb [1] and Na vapors [2]. At high atom density and strong pump laser power, this atomic system is a parametric amplifier which generates probe and conjugate photons with gain. The goal of this work was to find how fractional delays and pulse broadenings obtained in K vapor compare with those obtained in other alkali vapors.

We measured and calculated fractional delays and pulse broadening of probe and conjugate for different gas densities, different pump one photon detuning, and two photon Raman detuning. In the experiment phase matching was established at the small angle between probe and pump at the entrance. Probe and conjugate waveforms are detected and placed on the time scale whose zero corresponds to tthe maximum of the reference pulse. Theoretically we calculated waveforms of transmitted probe and conjugate by solving optical Bloch-Maxwell equations for the four-level system.

We present fractional delays and broadening, and gains of probe and conjugate, as a function of two photon detuning for incident probe pulse between 20 and 120 ns, at K densities between 10^{11} and 10^{12} cm^{-3}, for several values of one photon (pump) detuning. Parameters for optimum results will be discussed and will be compared to those reported for Rb and Na.

REFERENCES
[1] V. Boyer, C. F. McCormick, E. Arimondo and P. D. Lett, Phys. Rev. Lett. 99, 143601 (2009).
[2] J. Okuma, N. Hayashi, A. Fujisawa, and M. Mitsunaga, Opt. Lett. 34, 1654 (2009).

Four way mixing in hot potassium vapor –slow light with a gain

Bojan Zlatkovic, Aleksandar Krmpot, Marija Ćurčič and Brana Jelenković

Institute of physics, University of Belgrade, Serbia

Contact: B. Jelenkovic (branaj@ipb.ac.rs)

Abstract. We have investigated reduction of group velocity due to nondegenerate four-wave mixing (FWM) in hot potassium vapor in the presence of gain of both probe and conjugate. Using an amplifying medium toalleviate the absorption and distortion of propagating pulses are important for ideal slow-light propagation, which can happen if (1) probe and conjugate are not be attenuated, (2) fractional delays,defined as the ratio of the delay to the duration of the pulse,for probe and conjugate,are larger than 1, and (3) fractional broadening of probe and conjugateare very small, ideally 1. When these three requirements are met, the probe and conjugate pulses can be delayed by an arbitrary amount, simply stacking the systems.

Figure 1 shows schematic of the experiment and atomic level scheme. Pump and probe are co-linear and orthogonallypolarized. Diagram of atomic levels consists of three hyperfine levels and a double Λ scheme in D1 line in ^{39}K. There are not previous studies of FWM with co-propagating pump and probe. Important feature of this set up and the amplification in the FWM process is the conjugate pulse coupled to the probe and propagating alongside the probe.
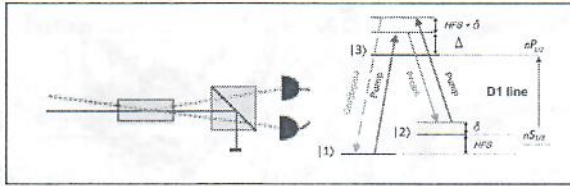
Figure 1. FWM in pottasium vapor.. Schematic of the experiment and atomic level scheme.

We demonstrate [1] high-efficiency of optical phase conjugatin in potassium, with gains of ~ 80 for pump and ~ 60 for congugate, with modest intensities of the pump beam, near ~10 W cm^{-2} for specific atomic denisty, one photon and two photon detuning. Exceptionally high gains in K, in comparisom to other alkaly atoms under similar experimentla conditions, might be due to the smallest ground state hyperfine splitting in potassium among alkalies: cross-susceptibilities between probe and conjugate that give rise to FWM processare higher for smaller hyperfine sppliting [2].

We have observed the ultraslow propagation of Gaussian like probe pulses as short as 20 ns, resulting in a fractional delay of the probe and conjugate of ~ 5. During the propagation a probe pulse is amplified and, depending on the gain, generates a conjugate pulse which is faster and separates from the probe pulse before exiting the K cell at a fixed delay. There is broadening or distortion of pulses resulting in fractional broadening ~1.5..We observed that the gain and the delay are in the trade-off relation, i.e., the higher the gain, the smaller the delay and vice versa. The presence of delay with the gain makes this system very interesting in the context of all-optical information processing.

REFERENCE

[1] B. Zlatković *et al.*, Laser Phys. Lett. **13** (2016), 015205.
[2] M. T. Turnbull *et al.*, Phys. Rev.A **88** (2013), 033845.

Four way mixing in Potassium vapor with large photon amplification

M. Ćurčić, B. Zlatković, I. Radojičić, D. Arsenović, A. Krmpot, B. Jelenković

Institute of Physics, University of Belgrade, Belgrade, Serbia

Contact: B. Jelenković (branaj@ipb.ac.rs)

Abstract. Four-way mixing (FWM) is nonlinear process in which two (pump beam) photons are converted into probe and conjugate photonswhen pump and probe beam co(counter) propagate through specific mediums, like crystals, fibers, cold and hot atomic gases. Two new photons arespecial in a sense that are noise correlated, their intensity difference is below standard quantum limit, they exhibit relative intensity squeezing[1] and can be time-frequency entangled [2].

In this work, we continue [3] to investigate FWM in potassium vapor when strong pump and weak probe co-propagate through K cell, coupling hyperfine levels in the double Λ scheme. We observe that this system is a strong parametric amplifier, producing large gains of probe and conjugate beams for certain values of potassium density (cell temperature), two photon (probe and pump)detuning from Raman resonance, one photon (pump) detuning, and phase matching condition for all four photons in the FWM process.We found thatdependence of amplification on oneparameter is correlated to values of other parameters.

Experimental and theoretical results of dependence of probe and conjugate gains vs density, detuningand angles between pump and probe will be presented.

[1] C. F. McCormick *et al.*, Phys Rev A 78, 043816 (2008).
[2] C. Shu *et al.*, Nat Comm. 7, 12783 (2016) DOI: 10.1038/ncomms12783.
[3] B. Zlatkovic *et al.*, Las Phys Lett 13, 015205 (2015).

Slow propagation of pulses by Four-Way Mixing in Potassium vapor

Bojan Zlatković, Marija Ćurčić, Ivan Radojičić, Aleksandar Krmpot, Željka Nikitović, Dušan Arsenović and Brana Jelenković

Institute of Physics Belgrade, University of Belgrade, 11079 Belgrade Serbia

Contact: branaj@ipb.ac.rs

We used four-way mixing (FWM) phenomena to slow light pulses in hot potassium vapor. The atomic scheme for FWM was off-resonant double-Lambda scheme that was previously used to study slow light in Rb [1] and Na vapors [2]. At high atom density and strong pump laser power, this atomic system is a parametric amplifier for the probe and conjugate photons, frequency up-shifted in respect to the probe frequency. The goal of this work was to find how fractional pulse delays and pulse broadenings of probe and conjugate obtained in K vapor compare with those obtained previously in other alkali vapors. Studdies of slow and storage of light are of interest for applications in all optical switching.

We measured and calculated fractional delays and pulse broadening of probe and conjugate for different gas densities, different one (pump) photon detuning, and two (pump and probe) photon Raman detuning. In the experiment phase matching was established at the small angle between probe and pump at the entrance. Probe and conjugate waveforms are detected and placed on the time scale whose zero corresponds to tthe maximum of the reference pulse. Theoretically we calculated waveforms of transmitted probe and conjugate by solving optical Bloch-Maxwell equations for the four-level atomic system.

We present fractional delays and broadening, and gains of probe and conjugate, as a function of two photon detuning for incident probe pulse between 20 and 120 ns, at K densities between 10^{11} and 10^{12} cm^{-3}, for several values of one photon (pump) detuning. Parameters for optimum results will be discussed and will be compared to those reported for Rb and Na.

REFERENCES
[1] V. Boyer, C. F. McCormick, E. Arimondo and P. D. Lett, Phys. Rev. Lett. 99, 143601 (2009).
[2] J. Okuma, N. Hayashi, A. Fujisawa, and M. Mitsunaga, Opt. Lett. 34, 1654 (2009).

Towards realization of frequency doubled VECSEL for Rydberg spectroscopy in rubidium and potassium

M. M. Ćurčić [1], R. Bek [2], R. Low [3], M. Jetter [2], and B. M. Jelenković[1]

(1) *Institute of Physics, Belgrade, Serbia*

(2) *Institut fur Halbleiteroptik und Funktionelle Grenzflachen, University of Stuttgart, Stuttgart, Germany*

(3) *5. Physikalisches Institut, University of Stuttgart, Stuttgart, Germany*

Contact: M. Ćurčić (marijac@ipb.ac.rs)

Abstract. Optically-pumped vertical external-cavity surface-emitting lasers (VECSELs), also called semiconductor disc lasers, are relatively new type of lasers, first time demonstrated by Kuznetsov [1] in 1990'. They are compact light sources which provide a combination of high output power and good beam quality, with a possibility of tailoring emission wavelength by a proper choice of gain materials. In addition, external cavity makes it possible to utilize intracavity elements, such as birefringent filters and etalons, in order to obtain single mode lasing regime. These characteristics makes the VECSEL a good choice for various range of applications, from spectroscopy and biophotonics to laser projection.

We describe a development of a VECSEL emitting at fundamental wavelength of 948nm (and 920nm), with generation of blue light at 474nm (and 460nm) via nonlinear frequency conversion in BBO crystal. Design process is presented, for which a desired properties for the application in Rydberg spectroscopy [2] in Rb and K are taken into account. We study the design, construction, and optical and thermal properties of the key elements of VECSEL structure. We report our recent progress in obtaining high-quality AlGaAs/GaAsP/InGaAs gain medium. Experimental measurements of the structures realized so far are presented and analyzed. Finally, we give an outlook for the future research consisting of utilizing a new wafer structure in order to improve laser characteristics and reach desired ones.

REFERENCES

[1] M. Kuznetsov, F. Hakimi, R. Sprague, and A. Mooradian, *IEEE Photon. Technol. Lett.*, vol. **9**, pp. 1063–1065 (1997).
[2] R. Low, H. Weimer, J. Nipper, J. B Balewski, B. Butscher, H. P. Buchler, and T. Pfau, *J. Phys. B: At. Mol. Opt. Phys.* **45**, 113001 (2012).

Blue InGaAsP VECSEL for Rydberg spectroscopy in Rb and K

M. M. Ćurčić[1], M. Großmann[2], R. Bek[2], R. Löw[3], M. Jetter[2], B. Jelenković[1]

(1) *Photonics Center, Institute of Physics, 11000 Belgrade, Serbia*

(2) *Institut für Halbleiteroptik und Funktionelle Grenzflächen, Center for Integrated Quantum Science and Technology (IQST) and SCoPE, University of Stuttgart, Allmandring 3, 70569 Stuttgart, Germany*

(3) *5. Physikalisches Institut and Center for Integrated Quantum Science and Technology IQST, Universität Stuttgart, Germany*

Contact: M. M. Ćurčić (marijac@ipb.ac.rs)

Abstract. Due to their characteristics, Rydberg states are becoming very attractive for the applications in the quantum mechanics. For their excitation in Rubidium and Potassium, we are in need of a blue laser source. Conventional GaN-based laser diodes are a cheap solution providing laser emission in the blue spectral range. However, these lasers do not provide the necessary beam quality and divergence that is needed for the applications in spectroscopy. In addition, in order to study nonlinear effects with Rydberg atoms at room temperatures, high laser intensities are required. The vertical external-cavity surface-emitting laser (VECSEL) [1] turns out to be an excellent candidate due to its wavelength versatility and high output power combined with a near-diffraction limited beam profile and the flexibility to add optical components inside the cavity.

Our focus is on the development of InGaAsP-based in-well pumped VECSEL with a fundamental wavelength in the near infrared spectral range. We report our recent progress in obtaining high-quality GaAsP/AlGaAs/InGaAs gain mediums, designed for the purpose of studying nS and nD Rydberg states in Rb and K. The results of the characterizations of different chip structures utilizing linear cavity are presented. We have obtained high intracavity powers, up to 400W. By inserting a BBO crystal in a v-shaped cavity, second harmonic generation at around 475 nm and 455 nm can be achieved. Further improvements will be made on reducing the laser linewidth (well below 1 MHz). By employing Z-shaped cavity together with various intracavity elements (birefringent filter and etalon), laser will be forced into single mode operating regime. We will stabilize the laser frequency to a reference spectroscopy signal from a vapor cell by a piezo-driven mirror.

REFERENCES

[1] M. Kuznetsov, F. Hakimi, R. Sprague, and A. Mooradian, *IEEE Photon. Technol. Lett.* **9** (1997), 1063–1065.

Fast pulse propagation in FWM medium - Conditions for Gaussian pulse preservations (or splitting)

B. Zlatković, M. Ćurčić, Ž. Nikitović, A. Krmpot, D. Arsenović, and B. Jelenković

Institute of physics, Belgrade, Pregrevica 118, 11080, Belgrade, Serbia

Contact: BZ (bojan@ipb.ac.rs)

Abstract. Four Wave Mixing (FWM) in alkali atom vapors exists only under very specific conditions, it is necessary that density of alkali vapor, intensities and frequencies of pump and probe laser beams, have their values within rather narrow ranges. FWM is nonlinear phenomena that can be regarded as scattering of laser beams on nonlinear index grating, generated by the same laser beams. Such scattering results in conversion of two pump photons to additional probe photon, and to conjugate photon at frequency (much) different form the pump and probe frequencies. Interests for FWM comes from applications in all optical storage, and as a source of correlated and entangled photons. Applications of FWM require that pulse shapes are preserved, with small, unavoidable broadening. It is therefore of interest to avoid FWM parameters that can lead to pulses distortion and splitting, due to increased dispersion in FWM medium.

We have investigated probe and conjugate pulse propagation through potassium vapor under conditions of FWM. The initial probe pulse enters K vapor as 80 ns Gaussian. We are defining, experimentally and theoretically, values of FWM parameters, vapor density, pump and probe detuning, that allow pulse propagation without distortion. Theoretical model is helping to understand dynamics of pulse propagation and the cause for their distortion, when FWM parameters take "wrong" values. Model allows us to "peak" inside the K vapor and observe moments of pulse splitting. There are very few (theoretical) papers that have discussed possible causes for pulse splitting in coherent [1] and nonlinear medium [2]. We will discuss their and our views of what is happening in the FWM medium when initial Gaussian probe pulse starts to brake.

REFERENCES

[1] A. P. Spencer, H. Li, S. Cundiff and D. M. Jonas, *J. Phys. Chem. A* **119** (2015), 3936–3960
[2] K. V. Rajitha, N. D. Tarak J. Evers, and M. Kiner, *Phys. Rev. A* **92** (2015), 023840

ATOM.INSTITUTE

Hot Vapor Workshop / Stuttgart 2021

POSTER 2021

Poster 2021, Monday Session:

Name	Title	Abstract
Alexandra Artusio Glimpse	Room temperature Cs-based RF field camera: concept and design	PDF-file
Armen Sargsyan	Two types of circular dichroism of magnetically induced atomic transitions in alkali atoms	PDF-file
Charikleia Troullinou	Quantum enhancement of sub pT/√Hz optically pumped magnetometer with squeezed light	PDF-file
Clare Higgins	Investigation of fine-structure changing collisional transfer in 87Rb vapour in the hyperfine Paschen-Back regime	PDF-file
Dusan Arsenovic	Doppler effect in the slow pulse propagation and distortion through FWM medium	PDF-file
Florian Christaller	Light-induced atomic desorption and single-photon generation in thermalmicro-cells	PDF-file
Jaques Haesler	Wafer-scale fabrication of MEMS atomic vapor cells	PDF-file
Jinwen Wang	Visualization of magnetic fields with cylindrical vector beams in an atomic vapor	PDF-file

Name	Title	Abstract
Julia Amoros-Binefa	Noisy atomic magnetometry in the linear-Gaussian regime	PDF-file
Michal Parniak	Hybrid entanglement between hot atoms and a cryogenic membrane oscillator	PDF-file
Nafia Rahaman	Laser-like spiking emission from continuous-wave excited alkali vapors	PDF-file
Sven Bodenstedt	Fast-field-cycling, ultralow-field nuclear magnetic relaxation dispersion	PDF-file
Valerio Biancalana	Tuning-Dressing exploitation in magnetometric measurements	PDF-file
Victor Lebedev	Optically pumped magnetometers for ultra-low field relaxometry of polarized nuclear spins	PDF-file
Gianvito Lucivero	Femtotesla direct magnetic gradiometer using a single multipass cell	PDF-file

Poster 2021, Tuesday Session:

Name	Title	Abstract
Andrew Daffurn	Gouy phase-matched angular and radial mode conversion in four-wave mixing	PDF-file
Elizabeth Robertson	A scheme for optical reservoir computers with atomic memory	PDF-file
Fraser Logue	Polarimetry of thermal Rb vapour: Magnetic field gradients and cascaded cells	PDF-file

Name	Title	Abstract
Gianni Buser	A broadband Rb vapor cell quantum memory for single photons	PDF-file
James Camparo	Nonlinear Collision Shifts of Alkali 0-0 Hyperfine Transitions Due to Van der Waals Molecule Formation	PDF-file
Janik Wolters	Optical information processing with hot atoms - From classical to quantum	PDF-file
Laurence Pruvost	Hot rubidium atoms for optical vortex conversion	PDF-file
Matteo Fadel	Monitoring the nuclear spin in helium-3 by Faraday interaction	PDF-file
Michal Lipka	How a broadband single-photon interacts with resonant atomic gas?	PDF-file
Michele Gozzelino	Kr-N2: a low-shift buffer-gas mixture for Rb vapor-cell clocks	PDF-file
Quentin Glorieux	Analogue cosmological particle creation in a quantum fluid of light	PDF-file
Ran Finkelstein	Super-extended nanofiber-guided field for coherent coupling to hot atoms	PDF-file

Doppler effect in the slow pulse propagation and distortion through FWM medium

Dušan Arsenović, Željka Nikitović, Bojan Zlatković, Aleksandar Krmpot, Marija Ćurčić, Branislav Jelenković

Institute of Physics, National Institute of the Republic of Serbia, Serbia

Most of the work on pulse propagation in alkali vapors is for FWM parameters that ensure preservation of Gaussian-like pulse at the exit from the vapor. Here we extended the range of parameters to include conditions when twin pulses in FWM medium begin to depart from Gaussian, to distort and split. Calculated pulse waveforms were compared with the experimental results for the propagation of 80 ns probe pulse through the potassium vapor contained in 4 cm K cell. The FWM was established using non-degenerate, non-resonant double Λ configuration.

We used Maxwell-Bloch equations to model FWM. For its atomic part we formed several Optical Bloch equations. Equations governing the electrical fields of beams are derived from Maxwell equations in slowly varying envelope approximation for plane waves.

Calculated waveforms of twin beams agree with the experimental results for the large range of FWM parameters that include cases when pulses are distorted and split, only with a proper Doppler averaging on density matrix elements. Since the extra-large number of velocity classes for Doppler averaging present a big computational burden, we have a good agreement with a relatively small number of velocity classes with nonuniform widths, the narrowest are around the pump detuning or around the maximum gains of probe and conjugate, depending on one-photon detuning.

Results of twin beam propagation through the K vapor in off-resonant FWM, will be given for one-photon detuning in the range of 0.7 to 1.5 GHz, two-photon detuning in the range od ± 20 MHz, and vapor temperatures between 120 C and 150 C. The possible causes for pulse distortion at certain FWM parameters will be discussed.

Experimental and theoretical study of two-mode squeezing by FWM in potassium vapor and its applications

Marija M. Ćurčić[1], Branislav M. Jelenković[1]

(1) *Photonic Center, Institute of Physics Pregrevica 118, 11080 Belgrade, Serbia*

Contact: M. Ćurčić (marijac@ipb.ac.rs)

Abstract. We present experimental results that show intensity difference squeezing (IDS) from a pair of quantum correlated (twin) beams generated by the four-wave mixing (FWM) process in dense potassium vapor. Quantum squeezing was observed by measuring noise power spectrum of the signal difference of twin beams. We search for the highest IDS by the analyzes of effects of important FWM parameters that can be changed in the experiment – one-photon pump and two-photon probe detuning, pump and probe powers, matching angle between the pump and probe, potassium density, and size and shape of potassium cells.

The experimental results are compared to theoretical ones. In our calculations, we use two different models – analytical distributed gain-loss model and microscopic model based on Heisenberg-Langevin formalism. We emphasis the importance of using an adequate model in the study of intensity difference squeezing in potassium vapor. The agreement between results of the models and of the experiment will be discussed. Our results are among of only a few that investigated the IDS in potassium, and will be compared to squeezing obtained in other alkali vapors, notably Rb and Cs.

We will also discuss the changes in the set-up in order to improve the level of squeezing, and do experimental studies in multi-spatial-mode regime. At the end, we present possible applications of twin beams generated in out experiment for quantum enhanced imaging and sensing.

DC Transverse Magnetic Field Scan in True Scalar Cs Magnetometers

Andrej B. Bunjac[1], Zoran D. Grujić[1], M. M. Ćurčić[1], S. Topić[1], Theo Scholtes[2], Jonas Hinkel[2]

(1) *Institute of Physics Belgrade, Pregrevica 118a, 11000 Belgrade, Serbia*
(2) *Leibniz Institute of Photonic Technology, Albert-Einstein-Straße 9, 07745 Jena, Germany*

Contact: Andrej B. Bunjac (bunjac@ipb.ac.srs)

Abstract. We present a true scalar magnetometer (TSM) consisting of a paraffin-coated glass cell filled with Cs vapor with the $\overrightarrow{B_{rf}} \parallel \vec{k}$ geometry where $\vec{k}$ is the light propagation direction for the optical pumping and $\overrightarrow{B_{rf}}$ is a magnetic field oscillating at Larmor frequency [1]. Spin dynamics of this system are described by the Bloch equations in Cartesian spin components:

$$\frac{d\vec{S}}{dt} = \vec{S} \times \vec{\omega} - \gamma\vec{S} + \gamma_p \vec{k}.$$

The measurement of a DC magnetic field transverse to the main magnetic field in the system produced unexpected signal shapes in different transverse directions. Specifically, with the RF field in the YZ plane, the DC field in the x-direction produces unfavorable signal when modulated at sufficiently high frequencies. This difference in the dynamic RF projection phase is investigated by solving the above equation both analytically and numerically with different transverse field geometries. The theoretical calculations produce results that are in good agreement with the observed systematic effects during measurement.

We will present the measurements in both described geometries and discuss the differences between the obtained signals. We will also present the details of both calculation processes and discuss how the results compare to the measurements.
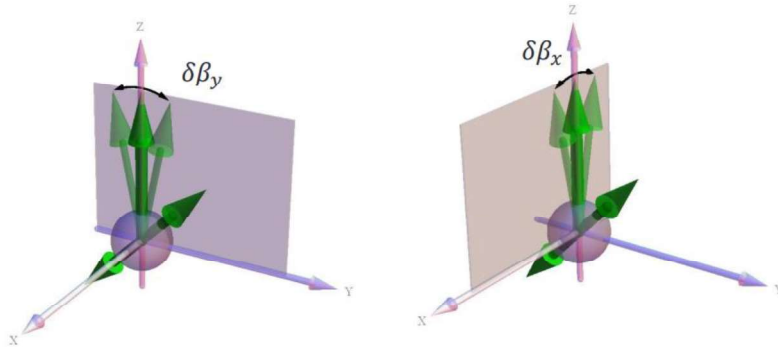
Figure 1. Two different field geometries considered for the DC transverse magnetic field scans. The additional magnetic DC field manifests as a small "rotation" of the main field in the appropriate direction.

REFERENCES

[1] Weis A., Bison G., Grujić Z.D. (2017) Magnetic Resonance Based Atomic Magnetometers. In: Grosz A., Haji-Sheikh M., Mukhopadhyay S. (eds) High Sensitivity Magnetometers. Smart Sensors, Measurement and Instrumentation, vol 19. Springer, Cham.

Why do we need accurate magnetometers and how to realize them

Zoran D. Grujić[1], Andrej Bunjac[1], Saša Topić[1], Marija M. Ćurčić[1],
Jonas Hinkel[2], Theo Scholtes[2]

(1) *Institute of Physics, Pregrevica 118, 11080 Belgrade, Serbia*

(2) *Leibniz Institute of Photonic Technology, Albert-Einstein-Straße 9, 07745 Jena, Germany*

Contact: Z. Grujić (zoran.grujic@ipb.ac.rs)

Abstract. In most cases magnetometers have been developed with accent on sensitivity in order to detect very small changes of magnetic fields like brain waves, magnetic field of beating hart or variations of geomagnetic field. For such applications exist wide range of devices like fluxgates, GMR, SQUID, OPM (Optically Pumped Magnetometer), etc. [1]. Our goal is to improve accuracy or precision of OPMs based on vapors of alkali metals while retaining most of their sensitivity. Alkali metals are very well studied, their properties are measured and theoretically calculated to high precision. It is to expect that a sensor, based on, for example cesium, should be easy to deploy and understand in various schemes. It turned out this is not the case and future research is required in order to overcome heading errors of cesium based OPMs.

Accurate OPMs would have broad range of applications like precision experiments in fundamental research (like measurement of nEDM – neutron Electrical Dipole Moment), metrology, space explorations and for mapping of geomagnetic fields. The latter would benefit in archaeology, mining operations and from improved quality in tracking changes in global distribution and intensity of the Earth's magnetic field.

In my talk I will present the old nEDM experiment at PSI [2] and its improvements towards its next generation – n2EDM [3]. The last part of the talk will be dedicated to accurate magnetometry with Free Spin Precession (FSP) [4] and Free Alignment Precession (FAP) magnetometers. If time permits, prospects of a ^{4}He magnetometer will be discussed.

REFERENCES

[1] A. Grosz, M. J. Haji-Sheikh and S. C. Mukhopadhyay (eds), *High Sensitivity Magnetometers*, Springer International Publishing, Cham (2017)
[2] C Abel, … Z.D. Grujić,… et. al., Phys. Rev. Lett. **124** (2020), 081803
[3] NJ Ayres, … Z.D. Grujić,… et. al., The European Physical Journal C **81** (2021), 1-32
[4] Z.D. Grujić, P.A. Koss, G. Bison, A. Weis, The European Physical Journal D **69** (2015), 135

All-optical Cs magnetometer based on free alignment precession

Marija M. Ćurčić[1], Andrej Bunjac[1], Saša Topić[1], Jonas Hinkel[2], Theo Scholtes[2], Zoran. D. Grujić[1]

(1) *Institute of Physics, Pregrevica 118, 11080 Belgrade, Serbia*

(2) *Leibniz Institute of Photonic Technology, Albert-Einstein-Strasse 9, 07745 Jena, Germany*

Contact: M. M. Ćurčić (marijac@ipb.ac.rs)

Abstract. Since their first demonstration, in 1960s [1], optically pumped atomic-based magnetometers (OPM) [2] have been in the focus of many scientific studies. Recently, they have been of special interest due to their wide range of application, including measurements of magnetic fields in bio-medical science, environmental and geo-science.

Our focus is on the development of a compact, portable magnetometer for geophysical field measurements. We present the design and operating principle of a novel kind of OPMs, optically-pumped Cs magnetometer based on a free alignment precession (FAP). This type of magnetometer is free of some limitations of conventional OPMs, such as frequency shifts and systematic displacements. We use a paraffin-coated Cs vapor cell. Magnetometer operates at room temperature. The atomic medium is pumped with linearly polarized amplitude-modulated light at a double Larmor frequency, $2\omega_L$. This process generates spin alignment. After the optical pumping, the decay of the spin polarization can be detected in the weaker probe beam passing through the cell. The information on the magnetic field and Larmor frequency can be gathered via further signal processing.

We will discuss the influence of various parameters on the performance of our magnetometer – state of polarization of the probe and pump beam, angle between the probe and the external magnetic field, probe and pump powers and lengths. We will present our set-up and first test measurements. Finally, we will give an outlook for the further work.

REFERENCES

[1] A. L. Bloom, *Principles of operation of the rubidium vapor magnetometer*, Appl. Opt. **1**, 61 (1962).
[2] A. Weis, G. Bison, Z. D. Grujić, *High Sensitivity Magnetometers* - Magnetic Resonance Based Atomic Magnetometers, pp 361-424 (2016).

Intensity squeezed states of light by four wave mixing in potassium vapor

M. Curcic, B. Jelenkovic
Institute of Physics, Belgrade, Serbia
e-mail:marijac@ipb.ac.rs

We will present our recent results of intensity difference squeezing generated by four wave mixing (FWM) in high density potassium vapor. Squeezed light with the noise level of several dB below standard quantum limit is observed in the difference signal between correlated probe and conjugate beams. Previous studies of the squeezing in alkalis were done mainly for Rb and Cs [1, 2].

For the FWM process we used non-degenerate double Λ scheme, with nearly co-propagating pump and probe beams. The source for the pump and the probe was the high power MBR (Coherent) laser. The vapor is contained in the vacuum K cell. For the difference of the probe and conjugate beam's intensities after the cell we used balanced detectors with a gain of 10^5 V/A. The signal difference was analysed using the spectrum analyzer.

We have vaired number of parameters: pump one photon detuning (OPD), two pump-probe detuning (TPD), temperature, pump and probe powers, angle between the beams and the lenght of the cell. The best squeezing, we obtained so far, is about – 5.5 dBm, before the correction for losses on the cell window, optics used behind the cell and the detection efficiency. This level of squeezing was obtained at pump and probe powers of 800 mW and 6 μW, OPD and TPD of 1.2 GHz and 6 MHz, at the cell temperature of 122 ºC. We analysed effects of all mentioned parameters on the relative intensity squeezing and on the gains of the twin beams, and compare them with the behavior of squeezing found in Rb and Cs.

REFERENCES
[1] C. F. McCormick, A. M. Marino, V. Boyer, and P.D. Lett, , Phys. Rev. A 78, 043816 (2008).
[2] R. Ma,W. Liu, Z. Qin, X. Jiaand Ji. Gao, Phys. Rev. A 96, 043843 (2017).

On the propagation of twin beam pulses in four-way-mixing medium – cause for asymmetric broadening and splitting

D. Arsenovic, Ž. Nikitović, B. Zlatković, A. Krmpot, M. Ćurčić, B. Jelenković
Institute of Physics, National Institute of the Republic of Serbia, Belgrade, Serbia
e-mail:arsenovic@ipb.ac.rs

Weak probe pulse that propagates a four-way-mixing (FWM) medium is amplified and new conjugate beam is generated as a result of a two pump photon conversion in the nonlinear FWM process. During this propagation, group velocities of these pulses are slowed. The pulses are broadened in respect to the probe pulse, due to dispersion effect on the shape of the pulse – different frequencies of the pulse spectral bandwidth have different group velocities.   As the pulses propagate in the medium, asymmetry in pulse broadening, and even strong distortion due to the higher order dispersion, can occur.

Since the applications of the slow light pulses for optical quantum memories and opitcal switches, requires preservation of initial, usually Gaussian, shape, it is of interest to find parameters for the FWM which maximally preserves the initial shape. The FWM parameters governing the pulse propagation are the pump intensity and medium density, and the detunings of the opitcal fields from atomic transitions, the pump single photon detuning, and the pump-probe two photon detuning.

Theoretical results for the probe and conjugate pulses propagating through the Potassium vapor, under the effects of FWM, are compared with experimental results. We calculated and measured twin pulses waveforms at the exit of the 4 cm long vacuum cell for the 80 ns probe seed beam, when K vapor density is $3*10^{12}$ cm-3 (120 0C), and the pump power in the experiment and Ruby frequency in the theoretical model are 220 mW and 1.5 GHz, respectively. Most previous theoretical works on the pulse propagation in the FWM alkali vapor are based on analytical expressions, and therefore on several assumptions in their models [1]. We have done a full numerical calculations of the density matrix elements, and subsequently the atomic polarization that is governing both gains and shapes of initial seed probe and conjugate pulses.

The 80 ns probe pulse has a spectral bandwidth of 550 MHz, and in a dispersive medium, like the K vapor near the two-photon resonance, different spectral components will acquire different phases and different delays. This causes broadening of twin pulses, while different gains associated with different spectral components of the pulse, can distort the pulse, causing even pulse splitting.

We present results od the model and of experiment that show strong dependence of the pulse waveform on the two-photon detuning, for the same pump one photon detuning and vapor density. We also emphasis importance of Doppler line broadening on the results of the model.

REFERENCES
[1] N. B. Phillips, A. V. Gorshkov and Irina Novikova (2009) *Slow light propagation and amplification via electromagnetically induced transparency and four-wave mixing in an optically dense atomic vapor*, Journal of Modern Optics, 56:18-19, 1916-1925

Squeezed light by FWM in alkali vapor – generation and application

Marija Ćurčić and Branislav Jelenković

Institute of Physics Belgrade, Pregrevica 118, 11080 Belgrade, Serbia

Contact: M. Curcic (marijac@ipb.ac.rs)

Abstract. We present the method for generating amplitude squeezed light (ASL) from twin photon pairs obtained using four way mixing (FWM) in alkali vapors [1], The dependence of ASL on the pump and probe laser detuning, and on the vapor density, obtained in potassium vapor using double-Λ atomic scheme, will be compared with the analytical models. Obtained agreement in certain ranges of FWM parameters, and disagreement in others, will be discussed.

Quantum correlated and entangled photon pairs produced by FWM, or by other methods like SPDC, have been proven in many successful applications. Taking properties of quantum light, quantum sensing and quantum imaging has overcome performances done by classical light, increasing measuring sensitivity by lowering noise below standard quantum limit, SQL. One way of sub SQL images exploits time and mode correlation between twin beams in a differential scheme for noise reduction. We present method of using two-correlated photons microscopy, such as shown in [2], and explain when it will be advantageous over classical two-photon spectroscopy.

REFERENCES

[1] M, Ćurčić and B. Jelenković, Enhanced intensity difference squeezing with a low gain off-resonant Four-Wave-Mixing in potassium vapor, Opt. Communications 533, 129301 (2023),

[2] T. Li, et al., Squeezed light induced two-photon absorption fluorescence biomarkers, Appl. Phys. Lett. 116, 254001 (2020).

Response of a scalar M_x magnetometer to modulation the of transverse magnetic field

Marija M. Ćurčić[1], Aleksandra Milenković[1], Jonas Hinkel[2], Theo Scholtes[2], Zoran D. Grujić[1]

(1) Institute of Physics Belgrade, Pregrevica 118, 11080, Serbia
(2) Leibniz Institute of Photonics Technology, Albert-Einstein-Strasse 9, 07745 Jena, Germany

Contact: M. M. Curcic (marijac@ipb.ac.rs)

Abstract. We present our work on behavior of a M_x variant of OPM (Optically Pumped Magnetometer) [1] under modulation of the transverse magnetic field. Set-up is based on a single beam double-resonance scalar magnetometer with spherical Cs paraffin coated cell, operating in free running mode at room temperature. The medium is pumped at D_1 line at $F_g=4 \rightarrow F_e=3$ transition with circularly polarized light, where direction of light is parallel to the oscillating magnetic field that is driving the magnetic resonance at Larmor frequency, Fig. 1. We have studied the response of our magnetometer to the changes in applied magnetic field, perpendicular to the main offset field. Set of Helmholtz coils is used for the generation of additional modulating filed. Using lock-in detection we obtained in-phase and quadrature components of the transmitted laser power oscillations. Specially, with the main offset field in z-direction, and applied modulation in yz plane, phase of the signal experience unexpected behavior for a scalar magnetometer.

We will present our measurements results and discuss which conditions, with respect to amplitude and frequency of modulating field, so as its orientation, give rise to the before mentioned signal abnormalities.
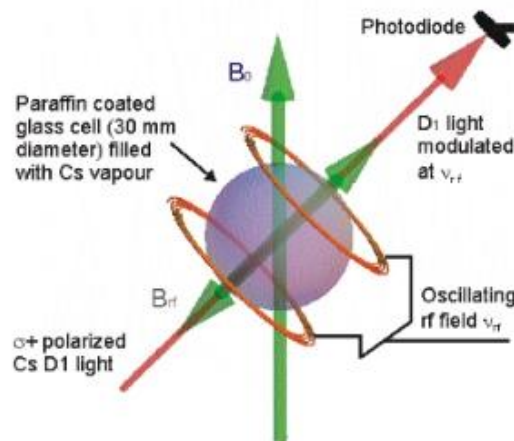
Figure 1. Schematic of the scalar M_x optically pumped magnetometer.

REFERENCES

(1) Weis, G. Bison, Z.D. Grujic, *High Sensitivity Magnetometers* – Magnetic Resonance Based Atomic Magnetometers, Springer, pp 361-424 (2016).

Commercially available vertical cavity surface emitting laser affordable VCSEL diode laser for low noise spectroscopy of cesium D_1 line

Aleksandra Milenkovic[1], Marija Ćurčić[1], Jonas Hinkel[2], Zoran D. Grujić[1], Theo Scholtes[2]

(1) *Institute of Physics Belgrade, Pregrevica 118, 11080, Serbia*
(2) *Leibniz Institute of Photonics Technology, Albert-Einstein-Strasse 9, 07745 Jena, Germany*

 Contact: Aleksandra Milenkovic (aleksandra.milenkovic@ipb.ac.rs)

Abstract. This study tests the applicability of the commercially available VCSEL Laser diodes from Throlabs (part number L895VH1) for laser spectroscopy of cesium D1 line. This 895 nm, 0.2 mW AlGaAs VCSEL diode is a compact light source suited for a variety of applications. It comes in a TO-46 package with an H pin configuration. It outputs a circular Gaussian beam, which is linearly polarized. Its spectral profile is single mode and it is suitable for single frequency applications [1]. It also has such a property that may provide a simple way of making a fast-swept source by temperature tuning [2].

The laser diode in experiments is mounted inside a high thermal mass aluminum block with an NTC temperature sensor in close proximity to the laser diode and a Peltier element below the aluminum mount connecting it with a larger aluminum plate. A self-made laser driver controls the laser current via a potentiometer allowing currents from 0 mA up to 2 mA. The temperature of the diode is controlled by a NTC connected to a PID which controls a Peltier element. The laser characterization produced the following results: lasing threshold: approximately 0.6 mA and weakly divergent beam. To access the performance of the Thorlabs diode two experiments were performed and compared: with Thorlabs diode and Toptica ECDL laser system. Interestingly the PLL signal of the Toptica measurement looks nosier that the signal of the Thorlabs diode. Above 500 Hz the VECSEL diode showed a better performance than the ECDL. Measurements also show that it is possible to use the diode for FSP measurements in a two-beam approach. For this measurement, the pumping diode has not been frequency locked; meanwhile the probing diode has to be on resonance during the probing phase. Running in continuous-wave mode, the second laser could be replaced by a simple laser diode with frequency stabilization.

The mentioned laser diode is affordable, and in addition offers the possibility of conducting experiments in in the frame of the Free Alignment Precession optically pumped magnetometer project (FRAPOPM). F=4 → F'=3

REFERENCES

[1] Thorlabs, *Product Specification Sheet,* https://www.thorlabs.com/thorproduct.cfm?partnumber=L895VH1*, (accessed: 10.02.2023.).*
[2] Sucbei Moon, and Eun Seo Choi, *VCSEL-based swept source for low-cost optical coherence tomography.* Biomedical optics express 8.2 (2017), 1110-1121

Heading error of Free Alignment Precession optically pumped magnetometer

Zoran D. Grujić[1], Marija Ćurčić[1], Aleksandra Milenkovic[1], Jonas Hinkel[2], Theo Scholtes[2]

(1) *Institute of Physics Belgrade, Pregrevica 118, 11080, Serbia*
(2) *Leibniz Institute of Photonics Technology, Albert-Einstein-Strasse 9, 07745 Jena, Germany*

Contact: Zoran D. Grujić (zoran.grujic@ipb.ac.rs)

Abstract. While optically pumped magnetometers (OPMs) have demonstrated competitive sensitivities and low cost with respect to competition, their performance for high accuracy applications is not well studied. Our first attempt [1] to optimize an all optical free spin precession (FSP) magnetometer was success. In unpublished investigations that followed that work it was discovered that FSP magnetometer suffers from a heading error two orders of magnitude larger than its sensitivity. In order to improve the performance a method that uses linearly polarized light Free Alignment Precession (FAP) was proposed.

In this study we measure the Larmor frequency, in a spherical cesium cell with antirelaxation coating, simultaneously with two linearly polarized beams. The experimental setup allows arbitrary mutual orientations of magnetic field $B_0 \approx 1.58\ \mu T$ and directions of polarizations of light beams.
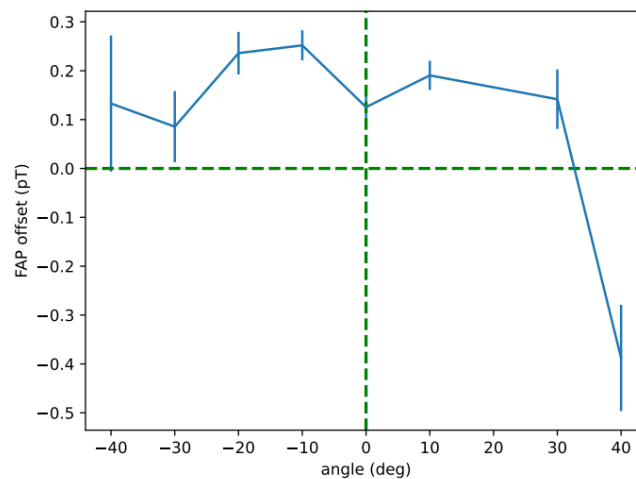
Figure 1. Preliminary measurement of the heading error of a FAP magnetometer. Direction of the B_0 and polarization direction of one of probe beams was fixed while we varied the polarization direction of the second probe beam.

From Fig. 1. we learn that, in this particular case, the heading error is below 1 pT, thus at least six orders of magnitude below B_0. Further investigation is under way.

REFERENCES

[1] ZD Grujić, PA Koss, G Bison, A Weis, *Eur. Phys. J. D* **69** (2015), 135

Analysis of the dynamic RF projection phase in True Scalar Cs Magnetometers

Andrej B. Bunjac[1], Zoran D. Grujić[1], M. M. Ćurčić[1], Theo Scholtes[2], Jonas Hinkel[2]

(1) *Institute of Physics Belgrade, Pregrevica 118a, 11000 Belgrade, Serbia*
(2) *Leibniz Institute of Photonic Technology, Albert-Einstein-Straße 9, 07745 Jena, Germany*

Contact: Andrej B. Bunjac (bunjac@ipb.ac.srs)

Abstract. A true scalar magnetometer (TSM) is one where the phase is independent of the magnetic field orientation and instead depends on the modulus only. We analyzed a magnetometer consisting of a paraffin-coated glass cell filled with CS vapor where the RF field is parallel to the light propagation direction while oscillating at Larmor frequency [1]

The magnetometer was applied in the measurement of small magnetic field components orthogonal to the main field direction. Experimental measurements of the RF projection phase show significantly different behavior in cases where the transversal field component is perpendicular to the RF field and when it is in the plane formed by the main magnetic and the RF fields. For the "in-plane" case the RF projection phase doesn't show any perturbation on changing the intensity or field direction, while the "perpendicular" case shows significant peaks and slow relaxations under the same circumstances.

This phenomenon was initially explored through numerical simulations with a model that shows good agreement with experimental results and later backed with analytical calculations of the Bloch equation for this case in Cartesian spin components. The equations were solved analytically by moving into a rotating frame of reference and applying the Rotating Wave Approximation (RWA) and the disambiguation of the remaining solution terms by the significance of their contribution. The results show a simplified picture of the described problem but capture the qualitative behavior well. The measurements, numerical solution and the analytical approach will all be presented in a wholesome description and analysis of the described phenomenon.
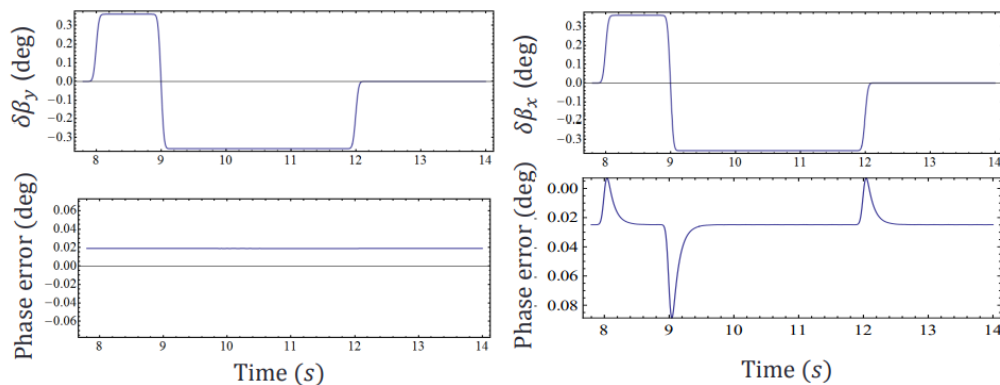
Figure 1. Two different field geometries considered for the DC transverse magnetic field scans. Left: The "in-plane" case with constant phase error, Right: The "perpendicular" case with phase error perturbations.

REFERENCES

[1] Weis A., Bison G., Grujić Z.D. (2017) Magnetic Resonance Based Atomic Magnetometers. In: Grosz A., Haji-Sheikh M., Mukhopadhyay S. (eds) High Sensitivity Magnetometers. Smart Sensors, Measurement and Instrumentation, vol 19. Springer, Cham.

Author Index

Correlated photon pairs by Four Wave Mixing in alkali vapor for imaging application

M.M. Ćurčić, D. Arsenović and B. Jelenković
Institute of Physics Belgrade, University of Belgrade, Serbia
e-mail: marijac@ipb.ac.rs

We will present our results on the generation of relative intensity difference squeezing (IDS) by Four Wave Mixing (FWM) in alkali vapors [1]. Motivated by a specific energy structure of potassium atoms and previously performed studies with different alkali atoms, Rb and Cs, we study both experimentally and theoretically generation of twin pairs – probe and conjugate by means of FWM on double-lambda scheme on D1 line in K, and their correlations. We have demonstrated and measured the squeezing level of – 6.1 dB, and investigated the dependence of gain and squeezing levels on different system parameters such as one-photon pump detuning, two-photon probe detuning, vapor temperature, cell length. We will discuss the obtained dependences and the optimal choice of parameters values, so as the advantages of K over the other alkali elements.

Having a proper theoretical model would ease the search for the optimal system parameters, especially when some specific requirements are desired by the possible application of described system. In addition to our experimental work, we have done a theoretical study and developed a quantum model for hot vapor systems based on Heisenberg-Langevin formalism, including Doppler averaging and transit time of the atoms through the interaction area. We will present the comparison of the obtained results, experimental and theoretical ones.

Finally, we will discuss the application of our quantum light source for the imaging, especially for two photon absorption (TPA), one of the most commonly used technique in bioimaging. During the last decade, taking advantages of quantum light in sensing and imaging has become a way of overcoming the limits of classical techniques, and hence method of improving sensitivity and resolution of the measurements. Entangled two-photon source by spontaneous down conversion (SPDC) in nonlinear crystal has already been shown to be a solution for overcoming photo- and thermal damaging with the common use of strong pulsed laser, and used in performing an enhanced imaging of the cells [2]. We will also comment on the advantages of FWM source of correlated photons over the SPDC.

REFERENCES
[1] M.M. Ćurčić, B.M. Jelenković, Opt. Commun. 533, 129301 (2023).
[2] O. Varnavski *et al.*, J. Phys. Chem. Lett. 13, 2772 (2022).

Experimental and theoretical study of the phase response of M_x magnetometer to modulating transversal magnetic field

<u>M.M. Ćurčić</u>[1], A. Milenković[1], A. Bunjac[1], T. Scholtes[2] and Z. Grujić[1]
[1]Institute of Physics Belgrade, University of Belgrade, Serbia
[2]Leibniz Institute of Photonic Technology, Jena, Germany
e-mail: zoran.grujic@ipb.ac.rs

We will present our results on the study of a scalar optically pumped magnetometer (OPM) [1]. More precisely, we investigate the phase response of a true scalar M_x magnetometer to the sudden changes of transversal magnetic field. As a sensing element we employ paraffin coated cell filled with Cs. A single light source is used for both pumping (polarizing) the medium and probing i.e. reading out a variation in the intensity of the resonant light due to the applied magnetic field. Pump light is circularly polarized. The wave vector and RF magnetic field that drives the spin precession are at 45° with the respect to the main static magnetic field B_0 as presented on Fig. 1. Magnetometer operates at room temperature. Set of Helmholtz coils is used for the generation of additional modulating filed. The sensor head is placed inside a three layer mu-metal shielding. Changes of the magnetometer response are detected with a lock-in amplifier, which enables us to obtain in-phase and quadrature components of the transmitted probe signal.

In addition to experimental study, we did both numerical and analytical modeling of a described system. Theoretical study is based on the transient Bloch equation. Analytically, the equation is solved in rotating frame after applying a rotating wave approximation (RWA). In this manner, we were able to obtain set of simple equations describing detected signal, decomposed into in-phase and quadrature components, for comparison with experimental results and tracking of the phase evolution.

The model results show good agreement with the experiment. Being a scalar magnetometer, our sensor should not experience any changes in the measured phase depending on the orientation of the applied modulating field. However, both experimental measurements and model predictions have demonstrated this is not the case. With the main offset field in z-direction, and applied modulation in yz plane, phase of the signal shows an unexpected behavior for a scalar magnetometer. We will present obtained results, and discuss which conditions lead to the before mentioned signal abnormalities.
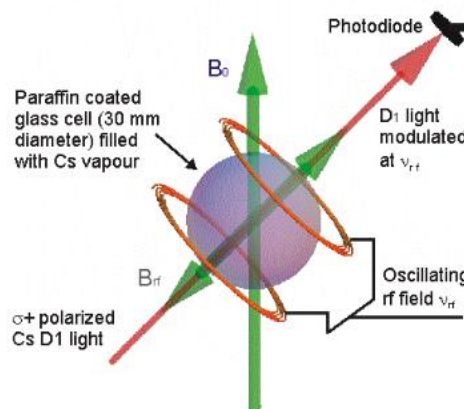

Figure 1. Schematic of the scalar M_x optically pumped magnetometer.

REFERENCES

[1] A. Weis *et al.*, High Sensitivity Magnetometers – Magnetic Resonance Based Atomic Magnetometers, Springer, pp 361-424 (2016).

Measurement of the heading error of a free alignment precession magnetometer

Z.D. Grujić[1], M. Ćurčić[1], A. Milenkovic[1], J. Hinkel[2] and T. Scholtes[2]
[1]Institute of Physics Belgrade, Serbia
[2]Leibniz Institute of Photonic Technology, Jena, Germany
e-mail: zoran.grujic@ipb.ac.rs

Optically pumped magnetometers (OPMs) have proved competitive sensitivities, robustness, and low cost with respect to competition, but their performance for high accuracy applications is not well studied. Optimization of an all optical free spin precession (FSP) magnetometer [1] has shown possible high accuracy of a such device. But, in unpublished investigations that followed that work it emerged that FSP magnetometer suffers from a heading error two orders of magnitude larger than its sensitivity. Then an investigation on applicability of Free Alignment Precession (FAP) produced by linearly polarized light was started.

We studied Larmor frequency measured simultaneously by two linearly polarized beams, in a spherical cesium cell with antirelaxation coating. If frequencies measured by those beams are different and function of the angle between their polarizations a heading error is detected. The experimental setup allows arbitrary mutual orientations of magnetic field $B_0 \approx 1.58$ µT and directions of polarizations of light beams.
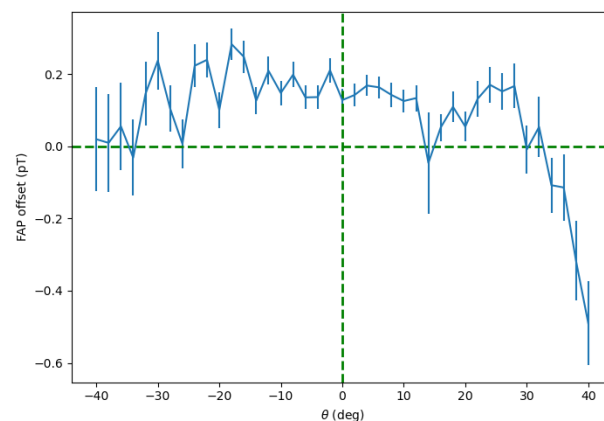

Figure 1. Measurement of the heading error of a FAP magnetometer. Direction of the B_0 and polarization direction of one of probe beams was fixed while we varied the polarization direction of the second probe beam.

In this particular case (see Fig. 1), the heading error is below 1 pT, thus at least six orders of magnitude below B_0. Further investigation is under way.

REFERENCES
[1] Z.D. Grujić *et al.*, Eur. Phys. J. D 69, 135 (2015).